

Inhomogeneous Superconductivity in Condensed Matter and QCD

Roberto Casalbuoni ^y

TH-Division, CERN, CH-1211 Geneva 23, Switzerland

Giuseppe Nardulli^z

Department of Physics, University of Bari, I-70124 Bari, Italy and
INFN, Bari, Italy

(Dated: March 24, 2024)

Inhomogeneous superconductivity arises when the species participating in the pairing phenomenon have different Fermi surfaces with a large enough separation. In these conditions it could be more favorable for each of the pairing fermions to stay close to its Fermi surface and, differently from the usual BCS state, for the Cooper pair to have a non zero total momentum. For this reason in this state the gap varies in space, the ground state is inhomogeneous and a crystalline structure might be formed. This situation was considered for the first time by Fulde, Ferrell, Larkin and Ovchinnikov, and the corresponding state is called LOFF. The spontaneous breaking of the space symmetries in the vacuum state is a characteristic feature of this phase and is associated to the presence of long wave-length excitations of zero mass. The situation described here is of interest both in solid state and in elementary particle physics, in particular in Quantum Chromodynamics at high density and small temperature. In this review we present the theoretical approach to the LOFF state and its phenomenological applications using the language of the effective field theories.

PACS numbers: 12.38.-t, 26.60.+c, 74.20.-z, 74.20.Fg, 97.60.Gb

Contents

I. Introduction	2
II. The general setting	4
A. Nambu-Gorkov equations	4
B. Homogeneous superconductors	7
1. Phase diagram of homogeneous superconductors	11
C. Gap equation for anisotropic superconductor: One plane wave (FF state)	15
1. Second Order phase transition point	18
III. Ginzburg-Landau approximation	19
A. Gap equation in the Ginzburg-Landau approach	19
B. Grand potential	21
C. Crystalline structures	22
1. One plane wave	23
2. Generic crystals	23
3. Two plane waves	23
4. Other structures	26
D. LOFF around the tricritical point	27
1. The LO subspace	28
IV. Superconductivity in Quantum Chromodynamics	33
A. High Density Effective Theory	35
B. CFL phase	37
C. 2SC phase	38
D. LOFF phase in QCD	39
E. One-gluon exchange approximation	44
F. Mass effects	46

^yOn leave from the Department of Physics of the University of Florence, 50019, Florence, Italy

^yElectronic address: casalbunio@ba.infn.it

^zElectronic address: giuseppe.nardulli@ba.infn.it

V . Phonon and gluon effective lagrangians	47
A . Effective lagrangian for the LOFF phase	47
B . One plane wave structure	48
C . Parameters of the phonon effective lagrangian: one plane wave	51
D . Cubic structure	56
E . Parameters of the phonon effective lagrangian: cubic crystal	58
F . Gluon dynamics in the LOFF phase	60
1. One plane wave structure	60
2. Cubic structure	63
V I. Inhomogeneous superconductivity in condensed matter, nuclear physics and astrophysics	63
A . Type I superconductors	64
B . "Clean" and strongly type II superconductors	65
C . Heavy fermion superconductors	66
D . Two-dimensional, quasi-two-dimensional and organic superconductors	67
E . Future developments	68
F . LOFF phase in nuclear physics	69
G . Why color LOFF superconductivity could exist in pulsars	69
H . Astrophysical implications of the QCD LOFF phase	73
V II. Conclusions	77
Acknowledgments	77
A . Calculation of J and K	78
B . Expansion of χ around the tricritical point	79
References	79

I. INTRODUCTION

Superconductivity is one of the most fascinating chapters of modern physics. It has been a continuous source of inspiration for different realms of physics and has shown a tremendous capacity of cross-fertilization, to say nothing of its numerous technological applications. This review is devoted to a less known chapter of its history, i.e. inhomogeneous superconductivity, which arises when the main property of the superconductor is not uniform in space. Before giving a more accurate definition of this phenomenon let us however briefly sketch the historical path leading to it. Two were the main steps in the discovery of superconductivity. The former was due to Kam erlingh Onnes (Kam erlingh Onnes, 1911) who discovered that the electrical resistance of various metals, e. g. mercury, lead, tin and many others, disappeared when the temperature was lowered below some critical value T_c . The actual values of T_c varied with the metal, but they were all of the order of a few K, or at most of the order of tenths of a K. Subsequently perfect diamagnetism in superconductors was discovered (Meissner and Ochsenfeld, 1933). This property not only implies that magnetic fields are excluded from superconductors, but also that any field originally present in the metal is expelled from it when lowering the temperature below its critical value. These two features were captured in the equations proposed by the brothers F. and H. London (London and London, 1935) who first realized the quantum character of the phenomenon. The decade starting in 1950 was the stage of two major theoretical breakthroughs. First, Ginzburg and Landau (GL) created a theory describing the transition between the superconducting and the normal phases (Ginzburg and Landau, 1950). It can be noted that, when it appeared, the GL theory looked rather phenomenological and was not really appreciated in the western literature. Seven years later Bardeen, Cooper and Schrieffer (BCS) created the microscopic theory that bears their name (Bardeen et al., 1957). Their theory was based on the fundamental theorem (Cooper, 1956), which states that, for a system of many electrons at small T , any weak attraction, no matter how small it is, can bind two electrons together, forming the so called Cooper pair. Subsequently in (Gor'kov, 1959) it was realized that the GL theory was equivalent to the BCS theory around the critical point, and this result vindicated the GL theory as a masterpiece in physics. Furthermore Gor'kov proved that the fundamental quantities of the two theories, i.e. the BCS parameter gap and the GL wavefunction, were related by a proportionality constant and can be thought of as the Cooper pair wavefunction in the center-of-mass frame. In a sense, the GL theory was the prototype of the modern effective theories; in spite of its limitation to the phase transition it has a larger field of application, as shown for example by its use in the inhomogeneous cases, when the gap is not uniform in space. Another remarkable advance in these years was the Abrikosov's theory of the type II superconductors (Abrikosov, 1957), a class of superconductors allowing a penetration of the magnetic field, within certain critical values.

The inspiring power of superconductivity became soon evident in the field of elementary particle physics. Two pioneering papers (Nambu and Jona-Lasinio, 1961a,b) introduced the idea of generating elementary particle masses

through the mechanism of dynamical symmetry breaking suggested by superconductivity. This idea was so fruitful that it eventually was a crucial ingredient of the Standard Model (SM) of the elementary particles, where the masses are generated by the formation of the Higgs condensate much in the same way as superconductivity originates from the presence of a gap. Furthermore, the Meissner effect, which is characterized by a penetration length, is the origin, in the elementary particle physics language, of the masses of the gauge vector bosons. These masses are nothing but the inverse of the penetration length.

With the advent of QCD it was early realized that at high density, due to the asymptotic freedom property (Gross and Wilczek, 1973; Politzer, 1973) and to the existence of an attractive channel in the color interaction, diquark condensates might be formed (Bailin and Love, 1984; Barrois, 1977; Collins and Perry, 1975; Frautschi, 1978). Since these condensates break the color gauge symmetry, the subject took the name of color superconductivity. However, only in the last few years this has become a very active field of research; these developments are reviewed in (Alford, 2001; Hong, 2001; Hsu, 2000; Nardulli, 2002a; Rajagopal and Wilczek, 2001). It should also be noted that color superconductivity might have implications in astrophysics because for some compact stars, e.g. pulsars, the baryon densities necessary for color superconductivity can probably be reached.

Superconductivity in metals was the stage of another breakthrough in the 1980s with the discovery of high T_c superconductors. As we anticipated, however, the main subject of this review is a different and separate development of superconductivity, which took place in 1964. It originates in high- T_c superconductors where a strong magnetic field, coupled to the spins of the conduction electrons, gives rise to a separation of the Fermi surfaces corresponding to electrons with opposite spins. If the separation is too high the pairing is destroyed and there is a transition (first-order at small temperature) from the superconducting state to the normal one. In two separate and contemporary papers, (Larkin and Ovchinnikov, 1964) and (Fulde and Ferrell, 1964), it was shown that a new state could be formed, close to the transition line. This state that hereafter will be called LOFF¹ has the feature of exhibiting an order parameter, or a gap, which is not a constant, but has a space variation whose typical wavelength is of the order of the inverse of the difference in the Fermi energies of the pairing electrons. The space modulation of the gap arises because the electron pair has non zero total momentum and it is a rather peculiar phenomenon that leads to the possibility of a non uniform or anisotropic ground state, breaking translational and rotational symmetries. It has been also conjectured that the typical inhomogeneous ground state might have a periodic or, in other words, a crystalline structure. For this reason other names of this phenomenon are inhomogeneous or anisotropic or crystalline superconductivity.

Inhomogeneous superconductivity in metals has been the object of intense experimental investigations especially in the last decade; for reasons to be discussed below the experimental research has aimed to rather unconventional superconductors, such as heavy fermion superconductors, quasi-two dimensional layered organic superconductors or high T_c superconductors. While different from the original LOFF proposal, these investigations still aim to a superconducting state characterized by non zero total momentum of the Cooper pair and space modulation of its wavefunction. At the moment they represent the main possibility to discover the LOFF state in condensed matter physics.

Quite recently it has been also realized that at moderate density the mass difference between the strange and the up and down quarks at the weak equilibrium and/or color and electric neutrality lead to a difference in the Fermi momenta, which renders in principle the LOFF state possible in color superconductivity (Alford et al., 2001b). The same authors have pointed out that this phenomenon might have some relevance in explaining the sudden variations of the rotation period of the pulsars (glitches).

The main aim of this review is to present ideas and methods of the two main roads to inhomogeneous superconductivity, i.e. the condensed matter and the QCD ways. Our approach will be mainly theoretical and the discussion of phenomenological consequences will be limited, first because we lack the necessary skills and second because the theory of the LOFF superconductivity is up to now much more advanced than experiment and its main phenomenological implications belong to the future. For this reason we will give large room to the theoretical foundations of inhomogeneous superconductivity and will present only a summary of experimental researches. Our scope is to show the similarities of different physical situations and to present a formalism as unified as possible. This not only to prove once again the cross-fertilization power of superconductivity, but also to expose experts in the two fields to results that may be easily transferrable from one sector to the other. Moreover, by presenting the LOFF phenomenon in a unified formalism, this review can contribute, we hope, to establish a common language. To this end we discuss the LOFF state both in solid state and in QCD physics starting with Nambu-Gor'kov (NG) equations. For the solid state part they will be derived by the effective theory of the relevant degrees of freedom at the Fermi surface and in the QCD sector by the so called High Density Effective Theory (HDET) that, as we shall see, leads to equations of motion which coincide with the NG equations. In this way one is able to get in touch with a dictionary allowing to

¹ In the literature the LOFF state is also known as the FFLO state.

switch easily from one field to the other.

The plan of this review is as follows. In Section II we start describing the general formalism, based on NG equations (Gor'kov, 1959; Nambu, 1960). As shown by (Polchinski, 1993) using the Renormalization Group approach, the excitations at the Fermi surface can be described by an effective field theory. Its equations of motion are exactly the NG equations of ordinary (homogeneous) superconductivity. We will then apply this formalism to fermions with different Fermi surfaces. The difference can be due to a magnetic field producing an energy splitting between spin up and spin down electrons, or, as in QCD, to a difference in the chemical potential originating from weak equilibrium, or color and electric neutrality, or mass difference between the pairing fermions. We will discuss the circumstances leading, in these cases, to inhomogeneous superconductivity. The Ginzburg Landau expansion can be used, as already mentioned, for the description of the inhomogeneous phase. It will be discussed in Section III, both at zero temperature and close to the tricritical point. The $T = 0$ case is more interesting for QCD applications while the finite temperature case might be relevant in condensed matter. In Section IV we will switch to QCD. We will first give a brief introduction to color superconductivity and then a description of the effective lagrangian for quarks at zero temperature near to the Fermi surface. We will also discuss more specially the LOFF case for QCD with two massless flavors. Since in the LOFF phase both translational and rotational symmetries are spontaneously broken, the Goldstone theorem requires the presence in the physical spectrum of long wave-length, gapless, excitations (phonons). In Section V we discuss the phonon effective lagrangians for two crystalline structures, i.e. the single plane wave and the cubic structure. We will limit our presentation to the QCD case, though the presence of these excitations is obviously general. We will also discuss the gluon propagation inside these two crystalline media. In Section VI we will discuss the possible phenomenological applications of the LOFF phase. This discussion will go from strongly type II superconductor to two-dimensional structures for condensed matter. For hadronic matter we will discuss applications both in nuclear physics and in QCD, with particular emphasis on the physics of glitches in pulsars.

Let us conclude this introduction by apologizing to the many authors whose work is not reviewed here in depth. Space limits forced us to sacrifice a more detailed exposition; the extensive bibliography at the end should help to excuse, we hope, this defect.

II. THE GENERAL SETTING

In this Section we give a pedagogical introduction to inhomogeneous superconductivity. We begin by reviewing homogeneous superconductivity by a field theory with effective Nambu-Gor'kov spin 1/2 fields describing quasi-particles. The effective field theory considers only the relevant degrees of freedom in the limit of small temperatures and high chemical potential; they are the modes in a shell around the Fermi surface. The dominant coupling in this limit is the four fermion interaction as first introduced in the BCS model. The dominance of this coupling can be also proved in a modern language by using the renormalization group approach (Benfatto and Gallavotti, 1990; Polchinski, 1993; Shankar, 1994), which shows that the BCS coupling is marginal and therefore, in absence of relevant couplings, it can dominate over other irrelevant couplings and produce the phenomenon of superconductivity.

After having derived the Nambu-Gor'kov equations and the gap equation in Subsection IIA, we discuss the case of homogeneous superconductor in Section IIB and analyze its phase diagram in Section IIB.1. We assume from the very beginning that the two species participating in the Cooper pairing have different chemical potentials, as this is the necessary situation for the LOFF state. In Section IIC we discuss the case of anisotropic superconductivity. In Section IIC.1 we will show that for appropriate values of the difference in chemical potentials an anisotropic modulated gap $\Delta(r) \sim \exp(iq \cdot r)$ leads to a state that is energetically favored in comparison to both the BCS and the normal non superconducting states. This was the state first discussed in (Fulde and Ferrell, 1964).

A. Nambu-Gor'kov equations

To start with we consider, at $T = 0$, a fermion liquid formed by two species, that we call u and d , having different Fermi energies. In the electron superconductivity, as in the original LOFF papers (Fulde and Ferrell, 1964; Larkin and Ovchinnikov, 1964), the species are the electron spin up and down states, but our formalism is general and will be applied later to the case where the fermion forming the Cooper pair are two quarks with different flavors. In superconducting materials the difference of chemical potentials can be produced by the presence of paramagnetic impurities. All these cases give rise to an effective exchange interaction that can be described by adding the following term to the hamiltonian

$$H_{\text{exch}} = \sum_{\mathbf{r}} \sum_{\mathbf{r}'} \sum_{\alpha\beta} \tau_{\alpha\beta} \psi_{\alpha}^{\dagger}(\mathbf{r}) \psi_{\beta}(\mathbf{r}') \quad (2.1)$$

In the case of electron superconductivity is proportional to the magnetic field and the effect of (2.1) is to change the chemical potentials of the two species:

$$\mu = \mu_0 + \frac{1}{2} \hbar \omega_c; \quad \mu_d = \mu_0 - \frac{1}{2} \hbar \omega_c; \quad (2.2)$$

Adopting a BCS interaction, the action can be written as follows

$$A = A_0 + A_{BCS}; \quad (2.3)$$

$$A_0 = \int dt \frac{d^3p}{(2\pi)^3} \psi^\dagger(p) (i\partial_t - E(p) + \mu + \mu_d) \psi(p); \quad (2.4)$$

$$A_{BCS} = \frac{g}{2} \int dt \sum_{k=1}^Z \frac{d^3p_k}{(2\pi)^3} \psi^\dagger(p_1) \psi(p_4) \psi^\dagger(p_2) \psi(p_3) (2\pi)^3 \delta(p_1 + p_2 - p_3 - p_4); \quad (2.5)$$

Here and below, unless explicitly stated, $\psi(p)$ denotes the 3D Fourier transform of the Pauli spinor $\psi(r;t)$, i.e. $\psi(p) = \int d^3r e^{-ip \cdot r} \psi(r;t)$. For non relativistic particles the functional dependence of the energy would be $E(p) = p^2/2m$, but we prefer to leave it in the more general form (2.4).

The BCS interaction (2.5) can be written as follows

$$A_{BCS} = A_{cond} + A_{int}; \quad (2.6)$$

with

$$\begin{aligned} A_{cond} &= \frac{g}{4} \int dt \sum_{k=1}^Z \frac{d^3p_k}{(2\pi)^3} \frac{1}{i} \tilde{\psi}(p_3; p_4) \psi^\dagger(p_1) C \psi^\dagger(p_2) \\ &\quad \sim \int dt \sum_{k=1}^Z \frac{d^3p_k}{(2\pi)^3} \frac{1}{i} \tilde{\psi}(p_1; p_2) \psi(p_3) C \psi(p_4) (2\pi)^3 \delta(p_1 + p_2 - p_3 - p_4); \\ A_{int} &= \frac{g}{4} \int dt \sum_{k=1}^Z \frac{d^3p_k}{(2\pi)^3} \psi^\dagger(p_1) C \psi^\dagger(p_2) + \frac{1}{i} \tilde{\psi}(p_1; p_2) \\ &\quad \psi(p_3) C \psi(p_4) \sim \int dt \sum_{k=1}^Z \frac{d^3p_k}{(2\pi)^3} \frac{1}{i} \tilde{\psi}(p_3; p_4) (2\pi)^3 \delta(p_1 + p_2 - p_3 - p_4); \end{aligned} \quad (2.7)$$

where $C = i\sigma_2$ and

$$\tilde{\psi}(p; p^0) = \langle \psi(p) C \psi(p^0) \rangle; \quad (2.8)$$

In the mean field approximation the interaction term can be neglected while the gap term A_{cond} is added to A_0 . Note that the spin 0 condensate $\tilde{\psi}(p; p^0)$ is simply related to the condensate wave function

$$\psi(r) = \langle \psi(r;t) C \psi(r;t) \rangle \quad (2.9)$$

by the formula

$$\psi(r) = \int \frac{d^3p}{(2\pi)^3} \frac{d^3p^0}{(2\pi)^3} e^{i(p+p^0) \cdot r} \tilde{\psi}(p; p^0); \quad (2.10)$$

In general the condensate wavefunction can depend on r ; only for homogeneous materials it does not depend on the space coordinates; therefore in this case $\tilde{\psi}(p; p^0)$ is proportional to $\delta(p + p^0)$.

In order to write down the Nambu-Gorkov (NG) equations we define the NG spinor

$$\psi = \frac{1}{\sqrt{2}} \begin{pmatrix} \psi \\ c^\dagger(-p) \end{pmatrix}; \quad (2.11)$$

where we have introduced the charge-conjugate field

$$c = C \psi^\dagger; \quad (2.12)$$

We also define

$$\psi(p; -p^0) = \frac{g}{2} \int \frac{d^3p^0}{(2\pi)^6} \tilde{\psi}(p^0; p + p^0 - p^0); \quad (2.13)$$

The free action can be therefore written as follows:

$$A = \int dt \frac{d\mathbf{p}}{(2\pi)^3} \frac{d\mathbf{p}^0}{(2\pi)^3} \gamma(\mathbf{p}) S^{-1}(\mathbf{p}; \mathbf{p}^0) \gamma(\mathbf{p}^0); \quad (2.14)$$

with

$$S^{-1}(\mathbf{p}; \mathbf{p}^0) = (2\pi)^3 \left(i\partial_t - \mathbf{p} + \frac{3}{2} \frac{(\mathbf{p} \cdot \mathbf{p}^0)}{(\mathbf{p}; \mathbf{p}^0)} \right) \left(i\partial_t + \mathbf{p} + \frac{3}{2} \frac{(\mathbf{p}; \mathbf{p}^0)}{(\mathbf{p} \cdot \mathbf{p}^0)} \right); \quad (2.15)$$

Here

$$\mathbf{p} = E(\mathbf{p}) \mathbf{v}_F(\mathbf{p} = \mathbf{p}_F); \quad (2.16)$$

where

$$\mathbf{v}_F = \frac{\partial E(\mathbf{p})}{\partial \mathbf{p}} \Big|_{\mathbf{p} = \mathbf{p}_F} \quad (2.17)$$

is the Fermi velocity. We have used the fact that we are considering only degrees of freedom near the Fermi surface, i.e.

$$p_F < p < p_F + \Lambda; \quad (2.18)$$

where Λ is the ultraviolet cutoff, of the order of the Debye frequency. In particular in the non relativistic case

$$\mathbf{p} = \frac{p^2}{2m} \frac{\mathbf{p}_F^2}{2m}; \quad \mathbf{v}_F = \frac{\mathbf{p}_F}{m}; \quad (2.19)$$

S^{-1} in (2.15) is the 3D Fourier transform of the inverse propagator. We can make explicit the energy dependence by Fourier transforming the time variable as well. In this way we get for the inverse propagator written as an operator:

$$S^{-1} = (G_0^+)^{-1} (G_0)^{-1}; \quad (2.20)$$

and

$$\begin{aligned} [G_0^+]^{-1} &= E - \mathbf{p} + \frac{3}{2} + i \text{sign} E; \\ [G_0]^{-1} &= E - \mathbf{p} - \frac{3}{2} - i \text{sign} E; \end{aligned} \quad (2.21)$$

with $\partial_t = \partial/\partial t$ and \mathbf{p} the momentum operator. The i prescription is nothing but the usual one for the Feynman propagator, that is forward propagation in time for the energy positive solutions and backward propagation for the negative energy solutions. As for the NG propagator S , one gets

$$S = \begin{pmatrix} G & F \\ F & G \end{pmatrix}; \quad (2.22)$$

S has both spin, $\frac{1}{2}$, and a bNG indices, i.e. $S^{ab_0^2}$. The NG equations in compact form are

$$S^{-1} S = 1; \quad (2.23)$$

or, explicitly,

$$\begin{aligned} [G_0^+]^{-1} G + F &= 1; \\ [G_0]^{-1} F + G &= 0; \end{aligned} \quad (2.24)$$

² We note that the presence of the factor $1 = \frac{p}{2}$ in (2.11) implies an extra factor of 2 in the propagator: $S(\mathbf{x}; \mathbf{x}^0) = 2 \langle T \gamma(\mathbf{x}) \gamma(\mathbf{x}^0) \rangle$, as it can be seen considering e.g. the matrix element $S^{11}: \langle T \gamma(\mathbf{x}) \gamma(\mathbf{x}^0) \rangle = i\partial_t \int d\mathbf{r} \frac{1}{3} \langle \mathbf{x} \cdot \mathbf{x}^0 \rangle$; with $\mathbf{x} = (\mathbf{r}; t)$.

Note that we will use

$$\langle r | j | r^0 \rangle = \frac{g}{2} (r | (r - r^0)) = (r | (r - r^0)) ; \quad (2.25)$$

or

$$\langle p | j | p^0 \rangle = (p | p^0) \quad (2.26)$$

depending on our choice of the coordinate or momenta representation. The formal solution of the system (2.24) is

$$\begin{aligned} F &= G_0 G ; \\ G &= G_0^+ G_0^+ F ; \end{aligned} \quad (2.27)$$

so that F satisfies the equation

$$F = G_0 G_0^+ G_0^+ F \quad (2.28)$$

and is therefore given by

$$F = \frac{1}{[G_0^+]^{-1} []^{-1} [G_0]^{-1} +} : \quad (2.29)$$

In the configuration space the NG Eqs. (2.24) are as follows

$$\begin{aligned} (E - E(r)) + \int_3 G(r; r^0; E) + (r) F(r; r^0; E) &= (r - r^0) ; \\ (E - E(r)) + \int_3 F(r; r^0; E) - (r) G(r; r^0; E) &= 0 : \end{aligned} \quad (2.30)$$

The gap equation at $T = 0$ is the following consistency condition

$$(r) = i \frac{g}{2} \int_0^Z \frac{dE}{2} \text{Tr} F(r; r; E) ; \quad (2.31)$$

where F is given by (2.29). To derive the gap equation we observe that

$$\begin{aligned} (r) &= \frac{g}{2} \int_0^Z (r) = \frac{g}{2} \int_0^Z \frac{dp_1}{(2)^3} \frac{dp_2}{(2)^3} e^{i(p_1 + p_2) \cdot r} \sim (p_1; p_2) \\ &= \frac{g}{2} \int_0^Z \frac{dE}{2} \frac{dp_1}{(2)^3} \frac{dp_2}{(2)^3} e^{i(p_1 + p_2) \cdot r} < y(p_1; E) > c(p_2; E) > \\ &= + i \frac{g}{2} \int_0^Z \frac{dE}{2} \frac{dp_1}{(2)^3} \frac{dp_2}{(2)^3} e^{i(p_1 - p_2) \cdot r} S^{21}(p_2; p_1) \\ &= + i \frac{g}{2} \int_0^Z \frac{dE}{2} S^{21}(r; r) ; \end{aligned} \quad (2.32)$$

which gives (2.31).

At finite temperature, introducing the Matsubara frequencies $\epsilon_n = (2n + 1) T$, the gap equation reads

$$(r) = \frac{g}{2} T \sum_{n=-1}^{\infty} \text{Tr} F(r; r; E)_{E = i\epsilon_n} : \quad (2.33)$$

B. Homogeneous superconductors

It is useful to specialize these relations to the case of homogeneous materials. In this case we have

$$(r) = \text{const} : \frac{2}{g} ; \quad (2.34)$$

$$\sim (p_1; p_2) = \frac{2}{g} \frac{1}{p_F^2} (2)^3 (p_1 + p_2) : \quad (2.35)$$

Therefore one gets

$$(p_1; p_2) = (p_1 - p_2) \quad (2.36)$$

and from (2.25) and (2.34)

$$(r) = (r) = : \quad (2.37)$$

Therefore $F(r; r; E)$ is independent of r and, from Eq. (2.29), one gets

$$\text{Tr} F(r; r; E) = \frac{1}{2} \int \frac{d^3 p}{(2\pi)^3} \frac{1}{(E - \frac{1}{2} \frac{p^2}{m})^2} \quad (2.38)$$

which gives the gap equation at $T = 0$:

$$= ig \int \frac{d^3 p}{(2\pi)^3} \frac{1}{(E - \frac{1}{2} \frac{p^2}{m})^2} ; \quad (2.39)$$

and at $T \neq 0$:

$$= g T \sum_{n=1}^{\infty} \int \frac{d^3 p}{(2\pi)^3} \frac{1}{(i\epsilon_n + \frac{1}{2} \frac{p^2}{m} - (p;))^2} ; \quad (2.40)$$

with

$$(p;) = \frac{g}{2 + \frac{p^2}{m}} ; \quad (2.41)$$

We now use the identity

$$\frac{1}{2} [n_u - n_d] = (p;) T \sum_{n=1}^{\infty} \frac{1}{(i\epsilon_n + \frac{1}{2} \frac{p^2}{m} - (p;))^2} ; \quad (2.42)$$

where

$$n_u(p) = \frac{1}{e^{(\frac{1}{2} \frac{p^2}{m}) - T} + 1} ; \quad n_d(p) = \frac{1}{e^{(\frac{1}{2} \frac{p^2}{m}) + T} + 1} ; \quad (2.43)$$

The gap equation can be therefore written as

$$= \frac{g}{2} \int \frac{d^3 p}{(2\pi)^3} \frac{1}{(p;)} (1 - n_u(p) - n_d(p)) ; \quad (2.44)$$

In the Landau theory of the Fermi liquid $n_u; n_d$ are interpreted as the equilibrium distributions for the quasiparticles of type $u; d$. It can be noted that the last two terms act as blocking factors, reducing the phase space, and producing eventually $\Delta \rightarrow 0$ when T reaches a critical value T_c (see below).

Before considering the solutions of the gap equations in the general case let us first consider the case $\Delta = 0$; the corresponding gap is denoted Δ_0 . At $T = 0$ there is no reduction of the phase space and the gap equation becomes

$$1 = \frac{g}{2} \int \frac{d^3 p}{(2\pi)^3} \frac{1}{(p;_0)} ; \quad (2.45)$$

whose solution is (we have assumed $d^3 p = p_F^2 dp/dp$)

$$\Delta_0 = \frac{2}{\sinh \frac{2}{g}} ; \quad (2.46)$$

Here

$$= \frac{p_F^2}{2v_F} \quad (2.47)$$

is the density of states and we have used $\rho_p = \rho(p - p_F)$, see Eqs. (2.16)–(2.19). In the weak coupling limit (2.46) gives

$$\Delta_0 = 2 \exp(-2/g) : \quad (2.48)$$

Let us now consider the case $\mu = 0$. By (2.44) the gap equation is written as

$$1 + \frac{g}{2} \int_0^{\Lambda} \frac{d^3 p}{(2\pi)^3} \frac{1}{\epsilon_p} = \frac{g}{2} \int_0^{\Lambda} \frac{d^3 p}{(2\pi)^3} \frac{n_u + n_d}{\epsilon_p} : \quad (2.49)$$

Using the gap equation for the BCS superconductor, the l.h.s. can be written, in the weak coupling limit, as

$$\text{l.h.s.} = \frac{g}{2} \ln \frac{\Lambda}{\Delta_0} ; \quad (2.50)$$

where we got rid of the cutoff by using Δ_0 , the gap at $\mu = 0$ and $T = 0$. Let us now evaluate the r.h.s. at $T = 0$. We get

$$\text{r.h.s.}_{T=0} = \frac{g}{2} \int_0^{\Lambda} \frac{d^3 p}{(2\pi)^3} [(1 - \frac{\mu}{\epsilon_p}) + (1 + \frac{\mu}{\epsilon_p})] : \quad (2.51)$$

The gap equation at $T = 0$ can therefore be written as follows:

$$\ln \frac{\Lambda}{\Delta_0} = \left(\frac{\mu}{\Delta_0} \right) \text{arcsinh} \frac{p_{\Lambda}}{\Delta_0} ; \quad (2.52)$$

ie.

$$\ln \frac{\Lambda}{\Delta_0 + \frac{p_{\Lambda}^2}{2}} = 0 : \quad (2.53)$$

One can immediately see that there are no solutions for $\mu > \Delta_0$. For $\mu = 0$ one has two solutions.

$$\text{a) } \Delta_0 = \mu ; \quad (2.54)$$

$$\text{b) } \Delta_0^2 = 2 \mu^2 : \quad (2.55)$$

The first arises since for $\mu = 0$ the l.h.s. of the Eq. (2.52) is zero. But since we may have solutions only for $\mu = 0$ the μ -function in Eq. (2.52) makes zero also the r.h.s.. The existence of this solution can also be seen from Eq. (2.39). In fact in this equation one can shift the integration variable as follows: $E \rightarrow E + \mu$, getting the result that, in the superconductive phase, the gap is independent of μ , ie. $\Delta_0 = \Delta_0$.

To compute the free energy we make use of the theorem saying that for small variations of an external parameter of the system all the thermodynamical quantities vary in the same way (Landau and Lifshitz, 1996). We apply this to the grand potential to get

$$\frac{\partial \Omega}{\partial g} = \frac{\partial \Omega_H}{\partial g} : \quad (2.56)$$

From the expression of the interaction hamiltonian (see Eq. (2.5)) we get immediately (cfr. (Abrikosov et al., 1963), cap. 7):

$$= \int \frac{dg}{g^2} \int d^3 x j(x) j(x) : \quad (2.57)$$

For homogeneous media this gives

$$\frac{\Omega}{V} = \int \frac{dg}{g^2} j j : \quad (2.58)$$

Using the result (2.48) one can trade the integration over the coupling constant g for an integration over Δ_0 , the BCS gap at $\mu = 0$, because $d\Delta_0 = -2dg = g^2$. Therefore the difference in free energy between the superconductor and the normal state is (we will use indifferently the symbol Ω for the grand potential and its density Ω/V)

$$\Omega = \frac{1}{2} \int_{\Delta_0}^{\Lambda} \frac{d\Delta_0}{\Delta_0} : \quad (2.59)$$

Here μ_f is the value of μ_0 corresponding to $\mu = 0$. $\mu_f = 0$ in the case a) of Eq. (2.54) and $\mu_f = 2$ in the case b) of Eq. (2.55); in the latter case one sees immediately that $\mu_0 > 0$ because from Eq. (2.55) it follows that $\mu_0 < 2$. The free energies for $\mu \neq 0$ corresponding to the cases a), b) above can be computed substituting (2.54) and (2.55) in (2.59). Before doing that let us derive the density of free energy at $T = 0$ and $\mu \neq 0$ in the normal non superconducting state. Let us start from the very definition of the grand potential for free spin 1/2 particles

$$\Omega_0(0; T) = - \frac{1}{2V} T \int_0^{\infty} \frac{d^3 p}{(2\pi)^3} \ln [1 + e^{-(\epsilon(p) - \mu)/T}] : \quad (2.60)$$

Integrating by parts this expression we get, for $T \rightarrow 0$,

$$\Omega_0(0) = - \frac{V}{12\pi^3} \int_0^{\infty} dp p^3 d\epsilon(p) : \quad (2.61)$$

From this expression we can easily evaluate the grand-potential for two fermions with different chemical potentials expanding at the first non-trivial order in μ . The result is

$$\Omega_0(\mu) = \Omega_0(0) - \frac{\mu^2}{2} : \quad (2.62)$$

Therefore from (2.54), (2.55) and (2.59) in the cases a), b) one has

$$a) \quad \Omega(\mu) = \Omega_0(\mu) - \frac{\mu^2}{4} (2\mu^2 + \mu_0^2) ; \quad (2.63)$$

$$b) \quad \Omega(\mu) = \Omega_0(\mu) - \frac{\mu^2}{4} (4\mu^2 + 4\mu_0^2) : \quad (2.64)$$

Comparing (2.63) and (2.64) we see that the solution a) has lower Ω . Therefore, for $\mu < \mu_0 = \frac{\sqrt{2}}{2}$ the BCS superconductive state is stable (Clogston, 1962). At $\mu = \mu_0 = \frac{\sqrt{2}}{2}$ it becomes metastable, as the normal state has a lower free energy. This transition would be first order since the gap does not depend on μ .

The grand potentials for the two cases a) and b) and for the gapless phase, Eq. (2.62), are depicted in Fig. 1, together with the corresponding gaps.

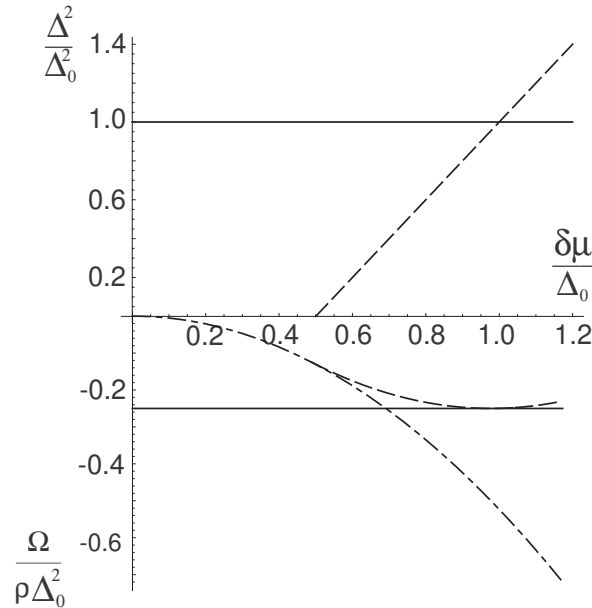


FIG. 1 Gap and grand potential as functions of μ for the two solutions a) and b) discussed in the text, see Eqs. (2.54), (2.55) and (2.63), (2.64). Upper solid (resp. dashed) line: Gap for solution a) (resp. solution b)). In the lower part we plot the grand potential for the solution a) (solid line) and solution b) (dashed line); we also plot the grand potential for the normal gapless state with $\mu \neq 0$ (dashed-dotted line). All the grand potentials are referred to the value $\Omega_0(0)$ (normal state with $\mu = 0$).

A different proof is obtained integrating the gap equation written in the form

$$\frac{\partial}{\partial} = 0 \quad (2.65)$$

The normalization can be obtained considering the homogeneous case with $\Delta = 0$, when, in the weak coupling limit, from Eqs. (2.57) and (2.48) one gets

$$= -\frac{1}{4} \frac{2}{0}; \quad (2.66)$$

see below Eq. (2.71). In this way one obtains again the results (2.63) and (2.64).

This analysis shows that at $\Delta = 1 = 0 = 2$ one would pass abruptly from the superconducting ($\Delta \neq 0$) to the normal ($\Delta = 0$) phase. However, as we shall discuss below, the real ground state for $\Delta > 1$ turns out to be an inhomogeneous one, where the assumption (2.37) of a uniform gap is not justified.

1. Phase diagram of homogeneous superconductors

We will now study the phase diagram of the homogeneous superconductor for small values of the gap parameter, which allows to perform a Ginzburg-Landau expansion of gap equation and grand potential. In order to perform a complete study we need to expand the grand-potential up to the 6th order in the gap. As a matter of fact in the plane (Δ ; T) there is a first order transition at $(\Delta_1; 0)$ and a second order one at $(0; T_c)$ (the usual BCS second order transition). Therefore we expect that a second order and a first order lines start from these points and meet at a tricritical point, which by definition is the meeting point of a second order and a first order transition line. A tricritical point is characterized by the simultaneous vanishing of the Δ^2 and Δ^4 coefficients in the grand-potential expansion, which is why one needs to introduce in the grand potential the 6th order term. For stability reasons the corresponding coefficient should be positive; if not, one should include also the Δ^8 term.

We consider the grand potential, as measured from the normal state, near a second order phase transition

$$= \frac{1}{2} \Delta^2 + \frac{1}{4} \Delta^4 + \frac{1}{6} \Delta^6; \quad (2.67)$$

Minimization gives the gap equation:

$$+ \Delta^3 + \Delta^5 = 0; \quad (2.68)$$

Expanding Eq. (2.40) up to the 5th order in Δ and comparing with the previous equation one determines the coefficients a , b and c up to a normalization constant. One gets

$$= 2g \text{ T Re } \sum_{n=0}^{\infty} \frac{\Delta^n}{(l_n^2 + \Delta^2)} = \frac{3}{(l_n^2 + \Delta^2)^2} + \frac{5}{(l_n^2 + \Delta^2)^3} + \dots; \quad (2.69)$$

with

$$l_n = l_n + i = (2n + 1) T + i; \quad (2.70)$$

The grand potential can be obtained, up to a normalization factor, integrating in Δ the gap equation. The normalization can be obtained by the simple BCS case, considering the grand potential as obtained, in the weak coupling limit, from Eqs. (2.57) and (2.48)

$$= -\frac{1}{4} \frac{2}{0}; \quad (2.71)$$

The same result can be obtained multiplying the gap equation (2.45) by Δ and integrating the result provided that we multiply it by the factor $2=g$, which fixes the normalization. Therefore

$$= \frac{2}{g} \left[1 - 2g \text{ T Re } \sum_{n=0}^{\infty} \frac{\Delta^n}{(l_n^2 + \Delta^2)} \right]; \quad (2.72)$$

$$= 4 \text{ T Re } \sum_{n=0}^{\infty} \frac{\Delta^n}{(l_n^2 + \Delta^2)^2}; \quad (2.73)$$

$$= 4 \text{ T Re } \sum_{n=0}^{\infty} \frac{\Delta^n}{(l_n^2 + \Delta^2)^3}; \quad (2.74)$$

In the coefficients and we have extended the integration in up to infinity since both the sum and the integral are convergent. To evaluate is less trivial. One can proceed in two different ways. One can sum over the Matsubara frequencies and then integrate over or one can perform the operations in the inverse order. Let us begin with the former method. We get

$$= \frac{2}{g} \left(1 - \frac{g}{4} \int_0^{\infty} \frac{dx}{x} \tanh \frac{x}{2T} + \tanh \frac{1}{2T} \right) : \quad (2.75)$$

Performing an integration by part we can extract the logarithmic divergence in . This can be eliminated using the result (2.46) valid for $T = 0$ in the weak coupling limit

$$1 = \frac{g}{2} \log \frac{2}{0} : \quad (2.76)$$

We find

$$= \left(\log \frac{2T}{0} + \frac{1}{4} \int_0^{\infty} dx \ln x \left[\frac{1}{\cosh^2 \frac{x+y}{2}} + \frac{1}{\cosh^2 \frac{x-y}{2}} \right] \right) ; \quad (2.77)$$

where

$$y = \frac{1}{T} : \quad (2.78)$$

Defining

$$\log \frac{0}{2T_c(y)} = \frac{1}{4} \int_0^{\infty} dx \ln x \left[\frac{1}{\cosh^2 \frac{x+y}{2}} + \frac{1}{\cosh^2 \frac{x-y}{2}} \right] ; \quad (2.79)$$

we get

$$(v; t) = \log \frac{t}{t_c(v=t)} ; \quad (2.80)$$

where

$$v = \frac{1}{0} ; \quad t = \frac{T}{0} ; \quad t_c = \frac{T_c}{0} : \quad (2.81)$$

Therefore the equation

$$t = t_c(v=t) \quad (2.82)$$

defines the line of the second order phase transition. Performing the calculation in the reverse order brings to a more manageable result for $t_c(y)$ (Buzdin and Kachkachi, 1997). In Eq. (2.72) we first integrate over obtaining a divergent series which can be regulated cutting the sum at a maximal value of n determined by

$$!_N =) N \frac{1}{2T} : \quad (2.83)$$

We obtain

$$= \frac{2}{g} \left(1 - \frac{g}{T} \operatorname{Re} \sum_{n=0}^N \frac{1}{!_n} \right) : \quad (2.84)$$

The sum can be performed in terms of the Euler's function $\zeta(z)$:

$$\operatorname{Re} \sum_{n=0}^N \frac{1}{!_n} = \frac{1}{2T} \operatorname{Re} \left(\frac{3}{2} + i \frac{y}{2} + N \left(\frac{1}{2} + i \frac{y}{2} \right) - \frac{1}{2T} \log \frac{1}{2T} \right) \operatorname{Re} \left(\frac{1}{2} + i \frac{y}{2} \right) : \quad (2.85)$$

Eliminating the cut-off as we did before we get

$$(v;t) = \log(4-t) + \operatorname{Re} \frac{1}{2} + i \frac{v}{2t} : \quad (2.86)$$

By comparing with Eq. (2.77) we get the following identity

$$\operatorname{Re} \frac{1}{2} + i \frac{y}{2} = \log(2) + \frac{1}{4} \int_0^1 dx \ln x \left[\frac{1}{\cosh^2 \frac{x+y}{2}} + \frac{1}{\cosh^2 \frac{x-y}{2}} \right] : \quad (2.87)$$

The equation (2.79) can be rewritten as

$$\log \frac{0}{4 - T_c(y)} = \operatorname{Re} \frac{1}{2} + i \frac{y}{2} : \quad (2.88)$$

In particular at $y = 0$, using (C the Euler-Mascheroni constant)

$$\frac{1}{2} = \log(4); \quad = \xi; \quad C = 0.5777777777777777 : : : ; \quad (2.89)$$

we find from Eq. (2.86)

$$(0; T=0) = \log \frac{T}{0}; \quad (2.90)$$

reproducing the critical temperature for the BCS case

$$T_c = -0.56693 : \quad (2.91)$$

The other terms in the expansion of the gap equation are easily evaluated integrating over Matsubara frequencies. We get

$$= T \operatorname{Re} \sum_{n=0}^{\infty} \frac{1}{i_n^3} = \frac{1}{16 T^2} \operatorname{Re}^{(2)} \frac{1}{2} + i \frac{1}{2 T}; \quad (2.92)$$

$$= \frac{3}{4} T \operatorname{Re} \sum_{n=0}^{\infty} \frac{1}{i_n^5} = \frac{3}{4 \cdot 768 T^4} \operatorname{Re}^{(4)} \frac{1}{2} + i \frac{1}{2 T}; \quad (2.93)$$

where

$$^{(n)}(z) = \frac{d^n}{dz^n} (z) : \quad (2.94)$$

Let us now briefly review some results on the grand potential in the GL expansion (2.67). We will assume $\epsilon > 0$ in order to ensure the stability of the potential. The minimization leads to the solutions

$$= 0; \quad (2.95)$$

$$^2 = ^2 = \frac{1}{2} \quad P \frac{1}{2^2 4} : \quad (2.96)$$

The discussion of the minima of depends on the signs of the parameters and . The results are the following:

$$1. \quad \begin{cases} > 0; > 0 \end{cases}$$

In this case there is a single minimum given by (2.95) and the phase is symmetric.

2. $\boxed{\begin{matrix} > 0; < 0 \end{matrix}}$

Here there are three minima, one is given by (2.95) and the other two are degenerate minima at

$$= + : \quad (2.97)$$

The line along which the three minima become equal is given by:

$$(0) = (+) ! = 4 \frac{r}{3} : \quad (2.98)$$

Along this line there is a first order transition with a discontinuity in the gap given by

$$\frac{2}{+} = \frac{4}{-} = \frac{3}{4} : \quad (2.99)$$

To the right of the first order line we have $(0) < (+)$. It follows that to the right of this line there is the symmetric phase, whereas the broken phase is in the left part (see Fig. 2).

3. $\boxed{\begin{matrix} < 0; > 0 \end{matrix}}$

In this case Eq. (2.95) gives a maximum, and there are two degenerate minima given by Eq. (2.97). Since for > 0 the two minima disappear, it follows that there is a second order phase transition along the line $= 0$. This can also be seen by noticing that going from the broken phase to the symmetric one we have

$$\lim_{! 0} \frac{2}{+} = 0 : \quad (2.100)$$

4. $\boxed{\begin{matrix} < 0; < 0 \end{matrix}}$

The minima and the maximum are as in the previous case.

Notice also that the solutions do not exist in the region $^2 < 4$. The situation is summarized in Fig. 2. Here we show the behavior of the grand potential in the different sectors of the plane $(= ; =)$, together with the transition lines. Notice that in the quadrant $(> 0; < 0)$ there are metastable phases corresponding to non absolute minima. In the sector included between the line $= \frac{2}{-}$ and the first order transition line the metastable phase is the broken one, whereas in the region between the first order and the $= 0$ lines the metastable phase is the symmetric one.

Using Eqs. (2.86), (2.92) and (2.93) which give the parameters $, ,$ and $$ in terms of the variables $v = = 0$ and $t = T = 0$, we can map the plane $$ and $$ into the plane $(= 0; T = 0)$. The result is shown in Fig. 3. From this mapping we can draw several conclusions. First of all the region where the previous discussion in terms of the parameters $, ,$ and $$ applies is the inner region of the triangular part delimited by the lines $= 0$. In fact, as already stressed, our expansion does not hold outside this region. This statement can be made quantitative by noticing that along the first order transition line the gap increases when going away from the tricritical point as

$$\frac{2}{+} = \frac{4}{-} = \frac{r}{3} : \quad (2.101)$$

Notice that the lines $(v;t) = 0$ and $(v;t) = 0$ are straight lines, since these zeroes are determined by the functions $^{(2)}$ and $^{(4)}$ which depend only on the ratio $v=t$. Calculating the first order line around the tricritical point one gets the result plotted as a solid line in Fig. 3. Since we know that $= 1 = 0 = \frac{2}{-}$ is a first order transition point, the first order line must end there. In Fig. 3 we have simply connected the line with the point with grey dashed line. To get this line a numerical evaluation at all orders in $$ would be required. This is feasible but we will skip it since the results will not be necessary in the following, see (Sama, 1963). The location of the tricritical point is determined by the intersection of the lines $= 0$ and $= 0$. One finds (Buzdin and Kachkachi, 1997; Combescot and Mora, 2002)

$$\frac{-}{0 \text{ tric}} = 0.60822; \quad \frac{T}{0 \text{ tric}} = 0.31833 : \quad (2.102)$$

We also note that the line $= 0$ should cross the temperature axis at the BCS point. In this way one reobtains the result in Eq. (2.91) for the BCS critical temperature, and also the value for the tricritical temperature

$$\frac{T_{\text{tric}}}{T_{\text{BCS}}} = 0.56149 : \quad (2.103)$$

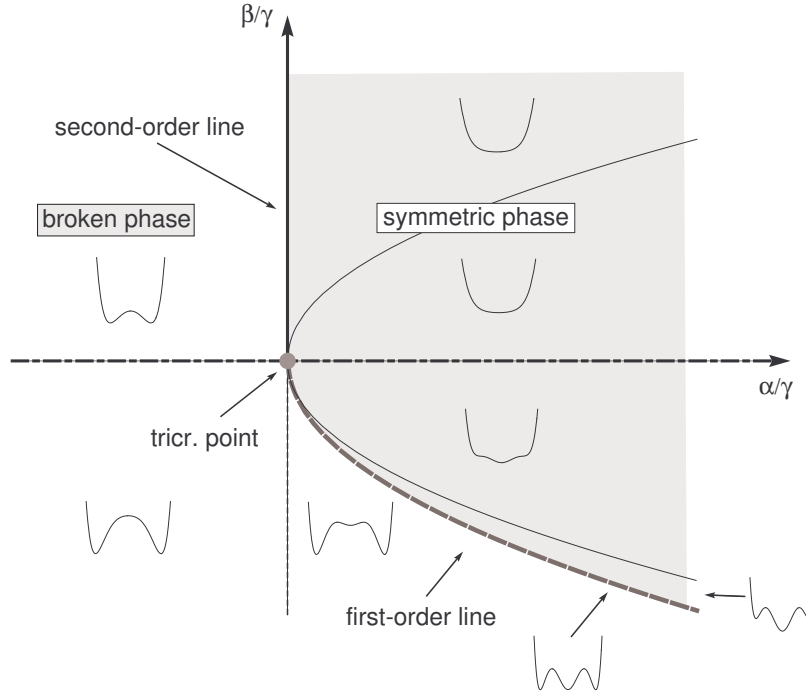


FIG. 2 The graph shows the first order and the second order transition lines for the potential of Eq. (2.67). We show the tricritical point and the regions corresponding to the symmetric and the broken phase. Also shown is the behavior of the grand potential in the various regions. The thin solid line is the locus of the points $\Delta^2 - 4\alpha = 0$. In the interior region we have $\Delta^2 - 4\alpha < 0$.

The results given in this Section are valid as long as other possible condensates are neglected. In fact, we will see that close to the first order transition of the homogeneous phase the LOFF phase with inhomogeneous gap can be formed.

C. Gap equation for anisotropic superconductor: One plane wave (FF state)

Let us now consider again the condensate wave function $\psi(r)$ of Eq. (2.9):

$$\psi(r) = \frac{1}{\sqrt{2}} \left(\psi_+(r) + \psi_-(r) \right) \quad (2.104)$$

Here ψ_{\pm} is the ground state. We develop it as follows

$$\psi_{\pm} = \sum_{N=0}^{\infty} c_N |N\rangle; \quad (2.105)$$

where N is even, the state $|N\rangle$ contains $N/2$ quark pairs of momenta

$$p_1 = +p + q; \quad p_2 = -p + q; \quad (2.106)$$

respectively for up and down species and the sum also implies an integration over the p variables and sum over spin. Clearly we have

$$\begin{aligned} \psi(r) &= \sum_N c_N \frac{1}{\sqrt{2}} \left(\psi_+(r) + \psi_-(r) \right) \\ &= \sum_N c_N \frac{1}{\sqrt{2}} \left(\psi_+(r) + \psi_-(r) \right) \\ &= \sum_N c_N \frac{1}{\sqrt{2}} e^{2iq_N} \psi_+(0) \psi_-(0) |N+2\rangle; \end{aligned} \quad (2.107)$$

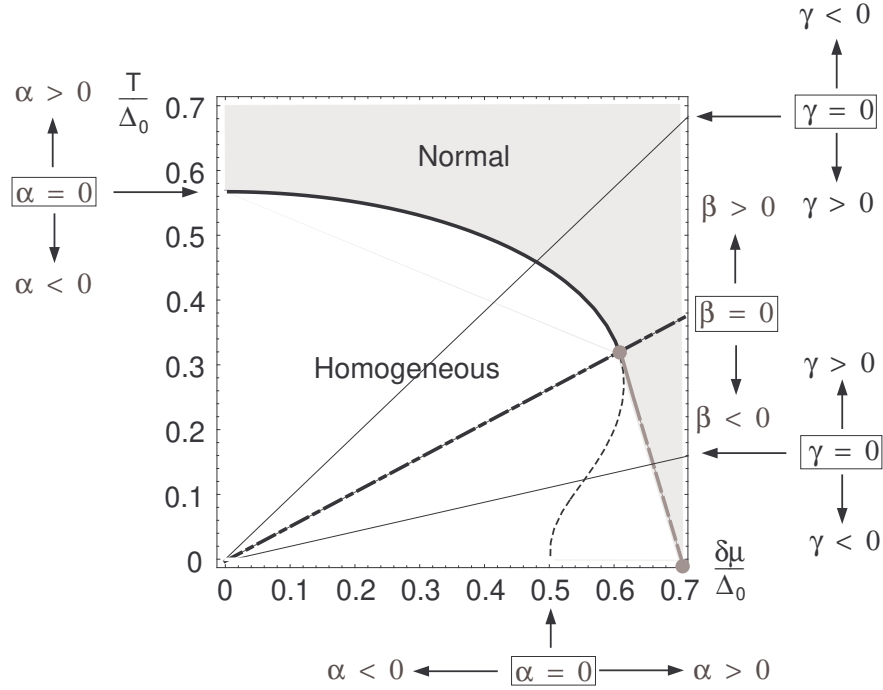


FIG. 3 The curve shows the points solutions of the equation $\epsilon = 0$ in the plane $(v; t) = (\delta\mu/\Delta_0; T/\Delta_0)$. The tricritical point at $(v; T) = (0.62; 0.28)\Delta_0$ is also shown. The upper part of the curve (solid line) separates the homogeneous phase from the normal one. Along the dashed line $\epsilon = 0$ but this is not the absolute minimum of the grand potential.

The homogeneous solution discussed in the previous subsection corresponds to the choice (Cooper pairs)

$$q_N = 0 \quad (\text{for all } N); \quad (2.108)$$

while $q_N \neq 0$ corresponds to the inhomogeneous state. Let us now assume that the interaction favors the formation of pairs with non zero total momentum and suppose that the values $q_1; q_2; \dots; q_P$ are possible. Clearly this hypothesis has to be tested by comparing the values of the free energies for the normal, homogeneous and non homogeneous state. In any event, under such hypothesis, since the gap is proportional to $\langle r \rangle$, one would get

$$\langle r \rangle = \sum_{m=1}^P X_m e^{2iq_m \cdot r}; \quad (2.109)$$

We will call the phase with $\langle r \rangle$ given by (2.109) inhomogeneous or LOFF superconducting. At the moment we shall assume the existence of a single q and therefore

$$\langle r \rangle = e^{2iq \cdot r}; \quad (2.110)$$

This is the simplest hypothesis, the one considered in (Fulde and Ferrell, 1964), see Fig. 4; it is therefore called FF state. The paper (Larkin and Ovcinnikov, 1964) examines the more general case (2.109); we will come to it below. The assumption (2.106) with $q \neq 0$ produces a shift in energy:

$$\epsilon_p = \epsilon(p - q_F) - \epsilon(p - q_F) = \epsilon_p - \epsilon_p; \quad (2.111)$$

with

$$\epsilon_p = \epsilon(p - q_F) = \epsilon(p) \cos \theta; \quad (2.112)$$

where the upper (resp. lower) sign refers to the d (resp. u) quasiparticle. Using the analogous result for the hole with $\epsilon^c(p)$, one can follow the same steps leading to (2.44) from (2.38); therefore the gap equation is still given by (2.44), but now the quasiparticle occupation numbers are

$$n_u(p) = \frac{1}{e^{(\epsilon_p - \epsilon_p)/T} + 1}; \quad n_d(p) = \frac{1}{e^{(\epsilon^c(p) - \epsilon^c(p))/T} + 1}; \quad (2.113)$$

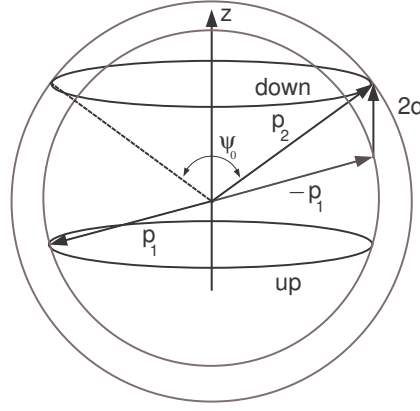


FIG. 4 Kinematics of the LOFF state in the case of one plane wave behavior of the condensate. The Cooper pair has a total momentum $2\mathbf{q} \neq 0$.

By (2.113), using the gap equation for the BCS superconductor with gap Δ_0 , the gap equation for the inhomogeneous superconductor is written as

$$\frac{g}{2} \ln \frac{\Delta_0}{2} = \frac{g}{2} \int \frac{d^3 p}{(2\pi)^3} [n_u(\mathbf{p}) + n_d(\mathbf{p})] : \quad (2.114)$$

Differently from the case with equal chemical potentials ($\mu = 0$), when there is phase space reduction at $T \neq 0$, now also at $T = 0$ the blocking factors reduce the phase space available for pairing. As a matter of fact the gap equation at $T = 0$ reads

$$\begin{aligned} \frac{g}{2} \ln \frac{\Delta_0}{2} &= \frac{g}{2} \int \frac{d^3 p}{(2\pi)^3} \frac{1}{\epsilon(\mathbf{p}; \pm)} (\epsilon(\mathbf{p}; -) + \epsilon(\mathbf{p}; +)) \\ &= \frac{g}{2} \int \frac{d^3 p}{(2\pi)^3} \frac{1}{4} \operatorname{arcsinh} \frac{C(\mathbf{p})}{q}; \end{aligned} \quad (2.115)$$

where

$$C(\mathbf{p}) = \frac{q}{q_F^2 v_F^2 (z_q - \cos \theta)^2} \quad (2.116)$$

and

$$z_q = \frac{\Delta_0}{q v_F} = \cos \frac{\theta_0}{2}; \quad (2.117)$$

where θ_0 is the angle depicted in Fig. 4. The angular integration is not over the whole Fermi surface, but only over region defined by $\theta(\mathbf{p}; \pm) < \theta_p$ or

$$q_F^2 v_F^2 (z_q - \cos \theta)^2 > \Delta_0^2 : \quad (2.118)$$

Notice that there are no solutions to this inequality for $q v_F + \Delta_0/2 > q_F$ (compare with Eq. (2.52)). Analyzing this inequality in terms of $\cos \theta$ we see that there are three regions, obtained comparing $q v_F + \Delta_0/2$ to q_F , characterized by different domains of angular integration. They are displayed Table I. As pointed out in (Fulde and Ferrell, 1964), the blocking regions correspond to regions in momentum space where fermions do not pair. In regions E and S fermions of one type (for instance spin up) do not pair, whereas in region D fermions of both types do not pair. The effect of the blocking regions is to reduce the phase space where pairing is possible. The complementary phase space is where the pairing is possible and therefore it will be called pairing region. It is formed by two rings that loosely speaking are around the two circles of Fig. 4. Since the pairing is possible not only on the Fermi surface, but also for modes just below and above it, each ring has a toroidal shape. $\theta_0 = 2 \arccos(z_q)$ is the aperture of the cone, with vertex at the origin of the spheres, intersecting the Fermi surfaces along the rings.

Once fixed the integration domain, the remaining integral in $\cos \theta$ is trivial and the result can be expressed, for the three cases, in the following uniform way

$$\ln \frac{\Delta_0}{2} = \frac{1}{2 q v_F} G \left(\frac{q v_F + \Delta_0/2}{q_F} \right) + G \left(\frac{q v_F - \Delta_0/2}{q_F} \right); \quad (2.119)$$

Region	Definition	Domain of integration in \cos
E	qv_F	$(-1; +1)$
S	$qv_F +$	$(-1; \cos \theta)$
D	$qv_F +$	$(\cos \theta; +1)$

TABLE I In the table the three blocking regions are shown. Here we have defined $\cos \theta = z_q (1 - \frac{1}{x})$

where the function $G(x)$ is defined as follows:

$$\begin{aligned} G(x) &= x \operatorname{arccosh}(x) - \frac{1}{x^2 - 1}; \quad |x| > 1; \\ G(x) &= 0; \quad |x| < 1; \\ G(x) &= -G(-x); \quad x < 0; \end{aligned} \quad (2.120)$$

1. Second Order phase transition point

The reduction of the available phase space implies a reduction of the gap, therefore one expects in general smaller gaps in comparison with the homogeneous case. In particular we see from Eq. (2.115) that increasing the effect of the blocking terms increases; eventually a phase transition to the normal phase occurs when μ approaches a maximum value μ_2 . Therefore the anisotropic superconducting phase can exist in a window

$$\mu_1 < \mu < \mu_2 : \quad (2.121)$$

One expects that μ_1 is near the Chandrasekhar-Clogston (Chandrasekhar, 1962; Clogston, 1962) limit $\mu_0 = \frac{p}{2}$ because Eq. (2.63) shows that near this point the difference in energy between the isotropic superconducting and the normal phases is small and one might expect that the LOFF state corresponds to the real ground state. We shall discuss the gap equation and prove this guess below. For the moment we determine μ_2 . For $\mu \rightarrow \mu_2$ the gap $\Delta \rightarrow 0$, and in the blocking regions E and D the domain of integration in $\cos \theta$ is $(-1; 1)$ (the region S disappears in the limit). Expanding the function $G(x)$ for $x \rightarrow 1$ we get from Eq. (2.119)

$$\ln \frac{\mu_0}{2} = -1 + \frac{1}{2} \frac{qv_F}{qv_F} \ln \frac{qv_F +}{qv_F} - \frac{1}{2} \ln \frac{1}{4(q^2 v_F^2 - 1)} \quad (2.122)$$

which can be rewritten as

$$(qv_F; \mu) = -1 + \frac{1}{2} \frac{qv_F}{qv_F} \ln \frac{qv_F +}{qv_F} - \frac{1}{2} \ln \frac{1}{4(q^2 v_F^2 - 1)} = 0 : \quad (2.123)$$

In terms of the dimensionless variables

$$y = \frac{\mu}{\mu_0}; \quad z = \frac{qv_F}{\mu_0} ; \quad (2.124)$$

the condition $\Delta = 0$ is equivalent to the equation

$$y + z = \frac{e}{2} \frac{z + y}{z - y} \frac{z - y}{2z} : \quad (2.125)$$

The critical line is plotted in Fig. 5.

Notice that the equation (2.122) can be written also in the form

$$\ln \frac{\mu_0}{2} = \frac{1}{2} f_0 \left(\frac{qv_F}{\mu_0} \right) = -1 + \frac{1}{2} \frac{qv_F}{qv_F} \ln \frac{qv_F +}{qv_F} - \frac{1}{2} \ln \frac{1}{(q^2 v_F^2 - 1)} ; \quad (2.126)$$

where

$$f_0(x) = \int_1^{x+1} du \ln(1 + xu) : \quad (2.127)$$

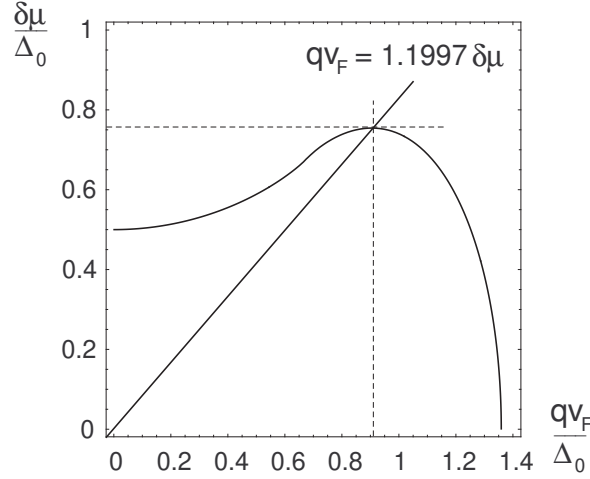


FIG. 5 The critical line for the LOFF phase at $T = 0$ in the plane $(q v_F = 0; \Delta = 0)$. Also the line determining $q v_F$ as a function of Δ is given.

We can fix x by minimizing the function Φ with respect to Δ . This is equivalent to minimize the grand potential close to the second order phase transition. This is obtained for x solution of the equation

$$x = \coth x; \quad (2.128)$$

i.e. at

$$x = \frac{q v_F}{2} = 1.1997 \quad x_c : \quad (2.129)$$

This can be also obtained from Fig. 5, intersecting the curve $\Phi = 0$ at its maximum value $\Delta = \Delta_0$ with a straight line passing from the origin.

The value of Δ at which the transition occurs is obtained by substituting this value in (2.126) and solving for Δ . One gets in this way

$$\Delta = 0.754 \Delta_0 : \quad (2.130)$$

Since $\Delta > \Delta_1 = 0.71 \Delta_0$, there exists a window of values of Δ where LOFF pairing is possible. We will prove below, using the Landau-Ginzburg approach, that the phase transition for the one-plane wave condensate at $T = 0$ and $\Delta = \Delta_2$ is second-order.

III. GINZBURG-LANDAU APPROXIMATION

The condensate wave function acts as an order parameter characterized by its non vanishing value in the superconducting phase. At the second order phase transition it vanishes and one can apply the general Ginzburg-Landau (GL) approach there (Ginzburg and Landau, 1950). We will begin by performing the GL expansion at $T = 0$ for a general inhomogeneous gap function (Bowers and Rajagopal, 2002; Larkin and Ovchinnikov, 1964). From this we will derive the grand potential measured with respect to the normal state and we will evaluate it explicitly for several cases. Next, in Section III D we will perform an analogous expansion at $T \neq 0$ around the tricritical point that we have shown to exist in Section II B (Alexander and M cR tague, 1978; Buzdin and Kachkachi, 1997; Combescot and Mora, 2002; Houzet and Buzdin, 2000b; Houzet et al., 2002, 1999). We will follow in this discussion the Ref. (Combescot and Mora, 2002). These authors have made a rather general analysis with the conclusion that in the generic case the favored state corresponds to a pair of antipodal wave vectors.

A. Gap equation in the Ginzburg-Landau approach

We will start this Section by considering the Ginzburg-Landau expansion of the Nambu-Gor'kov equations. Let us perform an expansion in Δ of the propagator F in Eq. (2.28). It is depicted in Fig. 6.

$$\text{thick line} = \text{black dot} + \text{black dot} - \text{empty circle} + \text{black dot} - \text{empty circle} - \text{black dot} - \text{empty circle} - \text{black dot} + \dots$$

FIG. 6 Ginzburg-Landau expansion of the propagator; the lines represent alternatively G_0 and G_0^+ , see Eq. (3.1). Full (resp. empty) circles represent (resp.) .

Formally it is written as follows

$$F = + G_0 G_0^+ + G_0 G_0^+ G_0 G_0^+ + G_0 G_0^+ G_0 G_0^+ G_0 G_0^+ : \quad (3.1)$$

The gap equation has an analogous expansion, schematically depicted in Fig. 7.

$$\text{line with dot} = \text{circle with dot} + \text{circle with 2 dots} + \text{circle with 4 dots} + \dots$$

FIG. 7 Ginzburg-Landau expansion of the gap equation; the lines represent alternatively G_0 and G_0^+ , see Eq. (3.2). Full (resp. empty) circles represent (resp.) .

It has the form

$$\begin{aligned} &= \frac{ig}{2} \text{Tr} \int \frac{dE}{2} \int dr_1 G_0(r; r_1) (r_1) G_0^+(r_1; r) \\ &+ \int dr_2 G_0(r; r_1) (r_1) G_0^+(r_1; r_2) (r_2) G_0(r_2; r_3) (r_3) G_0^+(r_3; r) \\ &+ \int dr_2 G_0(r; r_1) (r_1) G_0^+(r_1; r_2) (r_2) G_0(r_2; r_3) (r_3) G_0^+(r_3; r_4) \\ &+ \int dr_2 G_0(r; r_1) (r_1) G_0^+(r_1; r_2) (r_2) G_0(r_2; r_3) (r_3) G_0^+(r_3; r_4) \\ &+ \int dr_2 G_0(r; r_1) (r_1) G_0^+(r_1; r_2) (r_2) G_0(r_2; r_3) (r_3) G_0^+(r_3; r_4) \\ &+ \int dr_2 G_0(r; r_1) (r_1) G_0^+(r_1; r_2) (r_2) G_0(r_2; r_3) (r_3) G_0^+(r_3; r_4) : \end{aligned} \quad (3.2)$$

Substituting (2.109) we get

$$\begin{aligned} n &= \sum_k (q_k; q_n) \delta_{k, n} (q_k - q_n) \\ &+ \sum_k J(q_k; q_1; q_m; q_n) \delta_{k, m} (q_k - q_1 + q_m - q_n) \\ &+ \sum_{k, m, j, i} K(q_k; q_1; q_m; q_j; q_i; q_n) \delta_{k, m} \delta_{j, i} \\ &+ \sum_{k, m, j, i} (q_k - q_1 + q_m - q_j + q_i - q_n) : \end{aligned} \quad (3.3)$$

Here $(q_k - q_n)$ means the Kronecker delta: $\delta_{n, k}$ and

$$(q_1; q_2) = + \frac{ig}{2} \int \frac{d\omega}{4} \int \frac{dE}{2} f_1(E; \omega; q_1 q_2) ; \quad (3.4)$$

$$J(q_1; q_2; q_3; q_4) = + \frac{ig}{2} \int \frac{d\omega}{4} \int \frac{dE}{2} f_1(E; \omega; q_1 q_2 q_3 q_4) ; \quad (3.5)$$

$$K(q_1; q_2; q_3; q_4; q_5; q_6) = + \frac{ig}{2} \frac{d\hat{w}}{4} \frac{dE}{2} \frac{1}{\prod_{i=1}^6 (1 - \hat{w} q_i)} f_i(E; \hat{w}; f(qq)); \quad (3.6)$$

We have put $w = \hat{w}$ and

$$f_i(E; \hat{w}; f(qq)) = \frac{1}{E + i \operatorname{sign} E + \left(\frac{1}{2} \right) \prod_{k=1}^6 (1 - \hat{w} q_k)}; \quad (3.7)$$

Moreover the condition

$$\sum_{k=1}^M (1 - \hat{w} q_k) = 0 \quad (3.8)$$

holds, with $M = 2; 4; 6$ respectively for J , J and K .

For $(q) = (q; q)$ one gets

$$(q) = \frac{ig}{2} \frac{d\hat{w}}{4} \frac{dE}{2} \frac{1}{(E + i \operatorname{sign} E)^2}; \quad (3.9)$$

where $\hat{w} = \hat{w}(q)$ is defined in Eq. (2.112) and is identical to the function $C(\hat{w})$ of Eq. (2.116) with $\hat{w} = 0$. In performing the energy integration in (3.9) we use the fact that there are contributions only for $j > j_j$. Using the gap equation for the homogeneous pairing to get rid of the cutoff we obtain the result

$$(q) = 1 + \frac{g}{2} \left(1 + \frac{1}{2} \log \frac{2}{4j(qv_F)^2} \right) \frac{1}{2qv_F} \log \frac{qv_F +}{qv_F}; \quad (3.10)$$

(q) can be rewritten in terms of the function introduced in (2.123) as follows:

$$(q) = 2 \frac{1}{g} \frac{(q)}{g}; \quad (3.11)$$

Clearly the gap equation in the GL limit, $1 = (q)$, coincides with Eq. (2.123), which was obtained in the one plane wave hypothesis. The reason is that, since (q) depends only on j_j it assumes the same value for all the crystalline configurations; therefore (q) does not depend on the crystalline structure of the condensate and the transition point we have determined in Sec. II.C.1 is universal.

For the evaluation of J and K we have to specialize to the different LOFF condensate choices. This will be discussed below.

B. Grand potential

The grand potential is given in the GL approximation by

$$\begin{aligned} &= \frac{1}{g} \sum_{k,n=1}^P [(q_k; q_n) - 1] \frac{1}{k - n - q_k - q_n} \\ &+ \frac{1}{2} \sum_{k, m, n=1}^P J(q_k; q; q_m; q_n) \frac{1}{k - m - n - q_k - q + q_m - q_n} \\ &+ \frac{1}{3} \sum_{k, m, j, i, n=1}^P K(q_k; q; q_m; q_j; q_i; q_n) \frac{1}{k - m - j - i - n - q_k - q + q_m - q_j + q_i - q_n}; \end{aligned} \quad (3.12)$$

where P is the number of independent plane waves in the condensate. Let us assume that

$$q_k = -q_{-k} \quad (\text{for any } k); \quad (3.13)$$

so that we can rewrite (3.12) as follows:

$$= P \left(\frac{1}{2} + \frac{1}{4} + \frac{1}{6} \right); \quad (3.14)$$

where ϕ is related to q through (3.11) and

$$= \frac{2}{g} \sum_{k, m} X^P J(q_k; q; q_m; q_n) q_k q + q_m q_n; \quad (3.15)$$

$$= \frac{2}{g} \sum_{k, m} X^P K(q_k; q; q_m; q_j; q_i; q_n) q_k q + q_m q_j + q_i q_n; \quad (3.16)$$

It follows from the discussion in subsection II C 1 that, at $\phi = \phi_2$, ϕ vanishes; moreover $\phi < 0$ for $\phi < \phi_2$, see below, eq. (3.23). Exactly as in Section II B 1 we distinguish different cases:

1. $\phi > 0$, $\phi > 0$. In this case $\phi = 0$ is a maximum for ϕ , and the minima occur at the points given in Eq. (2.96), which now reads:

$$\phi_2 = \frac{\frac{P}{2} + \sqrt{\frac{P^2}{4} - 4P}}{2}; \quad (3.17)$$

Near the transition point one has

$$\phi_2 = \frac{P}{2}; \quad (3.18)$$

A phase transition occurs when $\phi = 0$, i.e. at $\phi = \phi_2$. The transition is second order since the gap goes continuously to zero at the transition point.

2. $\phi < 0$, $\phi > 0$. Both for $\phi < 0$ and for $\phi > 0$ ϕ_2 in (3.17) is a minimum for ϕ . In the former case it is the only minimum, as $\phi = 0$ is a maximum; in the latter case it competes with the solution $\phi = 0$. Therefore the LOFF phase can persist beyond ϕ_2 , the limit for the single plane wave LOFF condensate up to a maximal value ϕ_{max} . At $\phi = \phi_{\text{max}}$ the free energy vanishes and there are degenerate minima at

$$\phi = 0; \quad \phi_2 = \frac{3}{4}; \quad (3.19)$$

The critical point ϕ_{max} is obtained by Eq. (2.98) that in the present case can be written as

$$(q_V = 1.1997; \phi) = \frac{3}{16P}; \quad (3.20)$$

The phase transition from the crystalline to the normal phase at ϕ_{max} is first order.

3. $\phi < 0$, $\phi < 0$: In this case the GL expansion (3.14) is inadequate since ϕ is not bounded from below and another term $O(\phi^8)$ is needed.

In the case $\phi < 0$, $\phi > 0$ we can select the most favored structure by computing the free energy at a fixed value of ϕ . We choose $\phi = \phi_2$ where the FF state has a second order phase transition and $\phi = 0$. One has there

$$\phi_2 = -; \quad - = \frac{3}{12\phi^2}; \quad (3.21)$$

C. Crystalline structures

For any crystalline structure the function ϕ in the first term of the GL expansion is given by

$$\begin{aligned} &= 1 - \frac{1}{2} \log \frac{\phi_0^2}{4j(q_V)^2} + \frac{1}{2q_V} \log \frac{q_V + \phi}{q_V} \\ &= \log \frac{\phi_0}{2} + \frac{1}{2} f_0 \frac{q_V}{\phi}; \end{aligned} \quad (3.22)$$

where we have used Eqs. (2.126), (3.10) and (3.11); ϕ vanishes for $\phi = \phi_2$, which characterizes the second order transition point at $T = 0$, see (2.123) or (3.18); therefore we can write

$$\phi = \frac{\phi_0}{2}; \quad (3.23)$$

where

$$= x_2 \quad (3.24)$$

and we have expanded around x_2 and used the property of minimum of $f_0(x)$ at $x = x_2$. We observe that, for $x_2 < 0$, β is negative; therefore the transition at $T = 0$ is always second order if $\beta > 0$.

As to the other terms, we can use the results of Appendix A to get the first terms of the GL expansion for any crystal structure. The exception is the one-plane-wave case, where the free energy can be computed at any desired order.

1. One plane wave

Using the results of the Appendix A one gets for the Fulde-Ferrel one plane wave condensate:

$$J = J_0 - \frac{g}{8} \frac{1}{(qv_F)^2} x_2^2; \quad K = K_0 - \frac{g}{64} \frac{(qv_F)^2 + 3}{[(qv_F)^2]^{3/2}} x_2^2 \quad (3.25)$$

From (3.25) we get ($x_2 = qv_F = x_2 = 1.1997$):

$$\begin{aligned} &= \frac{1}{4 \frac{1}{2} (x_2^2 - 1)} = + \frac{0.569}{\frac{1}{2}}; \\ &= \frac{3 + x_2^2}{8 \frac{1}{2} (x_2^2 - 1)^{3/2}} = + \frac{1.637}{\frac{1}{2}}; \end{aligned} \quad (3.26)$$

Since $\beta > 0$ the β -term is ineffective near the transition point and Eq. (3.18) gives

$$x_2^2 = 4 - x_2^2 - 1 - x_2^2 = 1.757 - x_2^2 \quad (3.27)$$

We can get β from Eq. (3.14) with $P = 1$ and from Eqs. (3.23) and (3.26). The result is

$$\beta = \frac{x_2^2}{4} = 0.439 - (x_2^2)^2; \quad (3.28)$$

The same result could also be obtained using Eqs. (2.59) and (2.62).

2. Generic crystals

In the general case $P \neq 1$ and the evaluation of J and K is more complicated. First, one introduces Feynman parameterizations, then the integrals over energy, longitudinal momenta and angles are performed, along the lines sketched in Appendix A, mainly based on (Bowers and Rajagopal, 2002). Next, one has to perform the integration over the Feynman parameters. To do this it is useful to draw two pictures: a rhombus, with lines formed by the four vectors appearing in $J(q_k; q_l; q_m; q_n)$, implementing the condition $q_k - q_l + q_m - q_n = 0$, and an hexagon, with lines formed by the six vectors appearing in $K(q_k; q_l; q_m; q_j; q_i; q_n)$ that satisfy $q_k - q_l + q_m - q_j + q_i - q_n = 0$, see Fig. 8. Note that the rhombus and the hexagon need not be in a plane. The simplest example is provided by two plane waves.

3. Two plane waves

In this case $P = 2$; let the two vectors be $q_a; q_b$, forming an angle θ ; a simpler case is provided by an antipodal pair, $q_a = -q_b = q$ and $\theta = \pi$, with

$$r = 2 \cos \theta \quad (3.29)$$

To get from (A.5) one may notice that the integral J assumes two different values

$$J_0 = J(q_a; q_a; q_a; q_a); \quad J_\pi = J(q_a; q_a; q_b; q_b) \quad (3.30)$$

corresponding to Fig. 9.

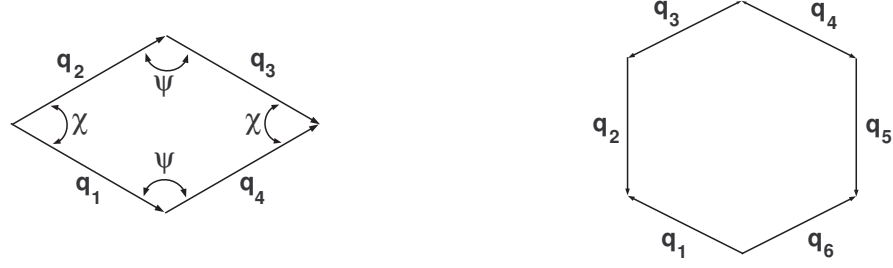


FIG. 8 Rhombic and hexagonal configurations for the vectors q_i . The vectors are assumed of the same length q and such that $q_1 + q_2 + q_3 + q_4 = 0$ for the rhombus and $q_1 + q_2 + q_3 + q_4 + q_5 + q_6 = 0$ for the hexagon. The vectors need not be all in the same plane.

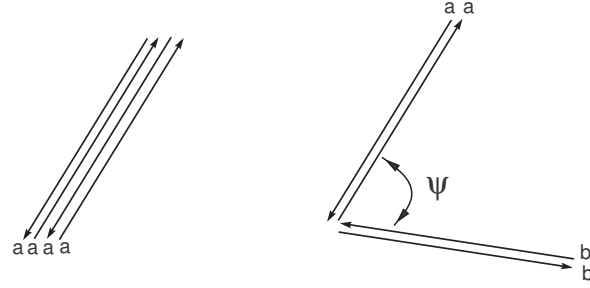


FIG. 9 The two rhombic structures corresponding to the integrals J_0 and J of Eqs. (3.30). The indices a and b refer to the vectors q_a and q_b respectively.

J_0 has been already computed, see Eq. (3.25); on the other hand

$$J = \frac{g}{2} \operatorname{Re} \frac{\arctan \frac{p}{2} \frac{x_2}{x_2^2 (1 + \cos \frac{\psi}{2})}}{2x_2 (\cos \frac{\psi}{2} - 1) (2 - \frac{x_2^2}{2} (1 + \cos \frac{\psi}{2}))}; \quad (3.31)$$

which for $\psi = 0$ gives

$$J = \frac{g}{8} \frac{x_2^2}{2}; \quad (3.32)$$

Using rotation and parity symmetry of the integrals one gets

$$(\psi) = \frac{2}{g} (2J_0 + 4J(\psi)); \quad (3.33)$$

The result for (ψ) as a function of ψ is reported in Fig. 10. In the case of the antipodal pair ($q; -q$), when $\psi = 180^\circ$, one gets

$$(\psi) = \frac{2}{g} (2J_0 + 4J(\psi)) = \frac{1}{2} \frac{1}{x_2^2 (1 - \cos \frac{\psi}{2})} - 1 = + \frac{0.138}{2}; \quad (3.34)$$

For K we have three possibilities (see Fig. 11):

$$K_0 = K(q_a; q_a; q_a; q_a; q_a; q_a); \quad K_1(\psi) = K(q_a; q_a; q_a; q_a; q_b; q_b); \quad K_2(\psi) = K(q_a; q_a; q_b; q_b; q_b; q_b); \quad (3.35)$$

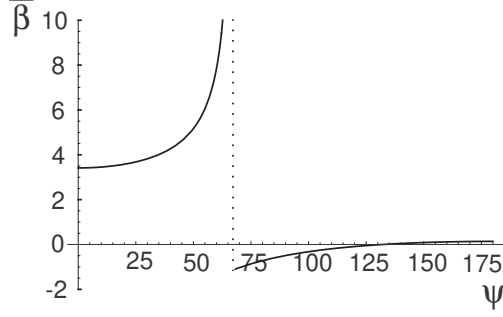


FIG. 10 $\bar{\beta} = \frac{\beta}{2}$ as a function of the opening angle ψ between the two plane wave vectors q_a and q_b ; $\psi_0 = 67.07^\circ$ is the angle defining the LOFF ring; $\beta_0 = 1.138$.

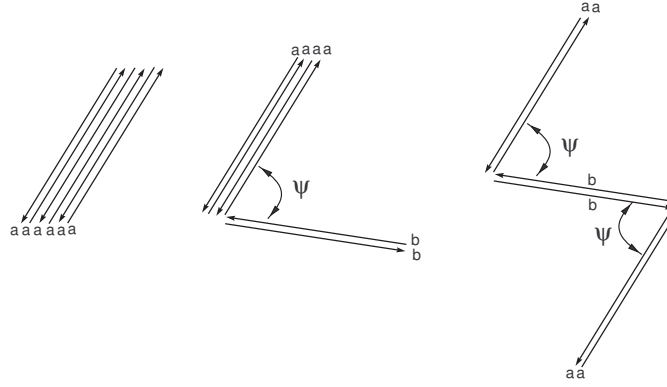


FIG. 11 The three hexagonal structures corresponding to the integrals K_0 , K_1 and K_2 of Eqs. (3.35). The indices a and b refer to the vectors q_a and q_b respectively.

Therefore we have

$$\beta(\psi) = \frac{2}{g} (2K_0 + 12K_1(\psi) + 6K_2(\psi)) : \quad (3.36)$$

K_0 has been already computed in (3.25), whereas K_1 and K_2 can be evaluated using the results given in Appendix A. $\beta(\psi)$ is plotted in Fig. 12. In the case of the antipodal pair, when $\psi = 180^\circ$, the result for β is in Table 2.

Figs. 10 and 12 show a divergence at

$$\psi_0 = 67.07^\circ = 2 \arccos \frac{2}{q v_F} : \quad (3.37)$$

ψ_0 is the opening angle depicted in Fig. 4. In this case, differently from the one plane wave situation, we have two different rings for each Fermi surface. For $\psi > \psi_0$ the two rings do not intersect, at $\psi = \psi_0$ they are contiguous, while for $\psi < \psi_0$ they overlap. The structure with $\psi < \psi_0$ is energetically disfavored because, being large and positive, the free energy would be smaller according to Eq. (3.18). According to the discussion in (Bowers and Rajagopal, 2002), this behavior seems universal, i.e. structures with overlapping rings are energetically disfavored in comparison with structures without overlaps. We will use this result in Section V D.

For $\psi_0 < \psi < 132^\circ$ β is negative. Therefore according to the discussion above we are in presence of a second order phase transition (β is always positive as it can be seen from Fig. 12). As it is clear from Eq. (3.21) the most favorable case from the energetic point of view occurs when β assumes its smallest value and j its largest, i.e. at $\psi = \psi_0$, when the rings are tangent. The values for this case are reported in Table II.

For comparison, at $\psi = 90^\circ$ we have $\frac{\beta}{2}(90^\circ) = 0.491$, $\frac{4}{2}(90^\circ) = 1.032$; the first order transition takes place at $\psi = 0.771 \psi_0$, only marginally larger than ψ_2 , and the dimensionless free energy $\beta = \beta(\frac{2}{q v_F})$ assumes at $\psi = \psi_2$ the value $\beta = 0.005$, which is larger than the value obtained for $\psi = \psi_0$, see Table II.

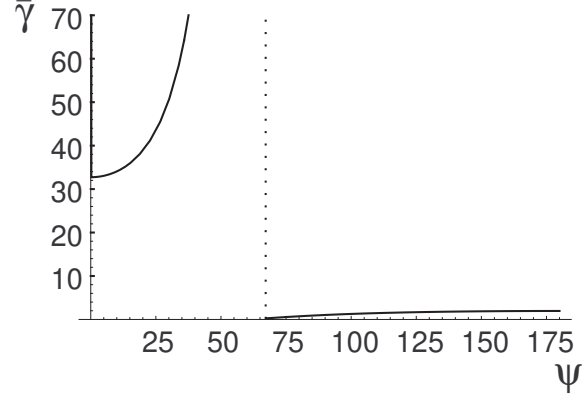


FIG. 12 $\bar{\gamma} = \frac{\gamma}{\gamma_0}$ as a function of the opening angle ψ between the two plane wave vectors q_a and q_b ; $\psi_0 = 67.07^\circ$ is the angle defining the LOFF ring; $\gamma_0 = 0.249$.

Structure	P	γ_1	γ_2	γ_3	γ_4
FF state	1	0.569	1.637	0	0.754
antipodal plane waves	2	0.138	1.952	0	0.754
Two plane waves ($\psi = \psi_0$)	2	-1.138	0.249	-1.126	1.229
Face centered cube	8	-110.757	-459.242	-	-

TABLE II Candidate crystal structures with P plane waves. $\psi = \frac{\pi}{2}$, $\psi = \frac{\pi}{2}$, $\psi = (\psi_0)$, with $\psi_F = (\psi_F)$, is the (dimensionless) minimum free energy computed at ψ_0 , obtained from (3.21). The phase transition (first order for $\psi < 0$ and $\psi > 0$, second order for $\psi > 0$ and $\psi > 0$) occurs at ψ_0 , given, for first order transitions, by Eq. (3.20).

4. Other structures

One could continue in the same way by considering other structures. An extensive analysis can be found in (Bowers and Rajagopal, 2002) where 23 different crystalline structures were considered. We refer the interested reader to Table I in this paper, as well as to its Appendix where the technical aspects of the integration over the Feynman parameters of the K integrals for the more complicated structures are worked out. From our previous discussion we know that the most energetically favored crystals are those which present a first order phase transition between the LOFF and the normal phase. Among the regular structures, with $\psi > 0$, examined in (Bowers and Rajagopal, 2002) the favored one seems to be the octahedron ($P = 6$), with $\psi_0 = 3.625^\circ$. Special attention, however, should be given to the face centered cube; we have reported the values of its parameters, as computed in (Bowers and Rajagopal, 2002), in our Table II. We note that $\psi < 0$ for this structure. The condensate in this case is given by

$$\langle \mathbf{r} \rangle = \sum_{k=1}^8 \langle \mathbf{r} \rangle_k = \sum_{k=1}^8 \exp(2i\mathbf{q}_k \cdot \mathbf{r}); \quad (3.38)$$

where \hat{n}_k are the eight unit vectors defining the vertices of the cube:

$$\begin{aligned} \hat{n}_1 &= \frac{1}{\sqrt{3}}(+1; +1; +1); & \hat{n}_2 &= \frac{1}{\sqrt{3}}(+1; -1; +1); \\ \hat{n}_3 &= \frac{1}{\sqrt{3}}(-1; -1; +1); & \hat{n}_4 &= \frac{1}{\sqrt{3}}(-1; +1; +1); \\ \hat{n}_5 &= \frac{1}{\sqrt{3}}(+1; +1; -1); & \hat{n}_6 &= \frac{1}{\sqrt{3}}(+1; -1; -1); \\ \hat{n}_7 &= \frac{1}{\sqrt{3}}(-1; -1; -1); & \hat{n}_8 &= \frac{1}{\sqrt{3}}(-1; +1; -1); \end{aligned} \quad (3.39)$$

Strictly speaking, since both γ_1 and γ_2 are negative, nothing could be said about the cube and one should compute the eighth order in the GL expansion, given by $\gamma_8 = 8$; the transition would be first order if $\psi > 0$. However (Bowers

and Rajagopal, 2002) argue that, given the large value of μ , this structure would necessarily dominate. Reasonable numerical examples discussed by the authors confirm this guess.

D. LOFF around the tricritical point

The LOFF phase can be studied analytically around the tricritical point (Buzdin and Kachkachi, 1997; Combescot and Mora, 2002) that we have considered in Section II B. Here we will follow the treatment of Ref. (Combescot and Mora, 2002). The tricritical point is the place where one expects the LOFF transition line to start. Close to it one expects that also the total pair momentum vanishes, therefore one can perform a simultaneous expansion in the gap parameter and in the total momentum. Starting from the expressions given in Section III (see Eqs. (3.4), (3.5) and (3.6)) and proceeding as in Section II B we find

$$\epsilon = \sum_{\mathbf{q}} \tilde{\epsilon}(\mathbf{q}) j_{\mathbf{q}}^2 + \frac{1}{2} \sum_{\mathbf{q}_1} \tilde{\epsilon}_1(\mathbf{q}_1) q_{1x} q_{2x} q_{3x} q_{4x} + \frac{1}{3} \sum_{\mathbf{q}_1} \tilde{\epsilon}_2(\mathbf{q}_1) q_{1x} q_{2x} q_{3x} q_{4x} q_{5x} q_{6x} : \quad (3.40)$$

Here we have used the momentum conservation in the fourth order and in the sixth order terms

$$q_1 + q_3 = q_2 + q_4; \quad q_1 + q_3 + q_5 = q_2 + q_4 + q_6; \quad (3.41)$$

with

$$\begin{aligned} \tilde{\epsilon}(\mathbf{q}) &= \epsilon_0 + \frac{2}{3} Q^2 + \frac{8}{15} Q^4; \\ \tilde{\epsilon}_1(\mathbf{q}_1) &= \epsilon_1 + \frac{4}{9} (Q_1^2 + Q_2^2 + Q_3^2 + Q_4^2 + Q_1 Q_2 + Q_2 Q_3 + Q_3 Q_4); \\ \tilde{\epsilon}_2(\mathbf{q}_1) &= \epsilon_2 + \frac{8}{9} (Q_1^2 + Q_2^2 + Q_3^2 + Q_4^2 + Q_1 Q_2 + Q_2 Q_3 + Q_3 Q_4); \end{aligned} \quad (3.42)$$

where ϵ_0 , ϵ_1 and ϵ_2 were defined in Eqs. (2.86), (2.92) and (2.93), and

$$Q = q v_F : \quad (3.43)$$

In Appendix B we show, as an example, how $\tilde{\epsilon}$ can be obtained from the expansion of $\epsilon(\mathbf{q})$ around $Q = 0$. In order to get a coherent expansion one has to consider the modulus of the pair total momentum of the same order of the gap. In fact, as we shall see, the optimal choice for Q turns out to be of order Δ . Correspondingly one has to expand the coefficient of the quadratic term in the gap up to the fourth order in the momentum and the fourth order term in the gap up to the second order in the momentum. In the form given in Eq. (3.40) one can easily apply the general analysis around the tricritical point used in Section II B. In particular for vanishing total momenta of the pairs we are back to the case of the homogeneous superconductor studied in Section II B.

It is interesting to write the expression for the grand potential in configuration space, because it shows that around the critical point the minimization problem boils down to solve a differential equation, whereas in a generic point the Ginzburg-Landau equations are integral ones. By Fourier transformation we get from Eq. (3.40)

$$\begin{aligned} \Omega &= \int \frac{d^3 r}{(2\pi)^3} j(\mathbf{r})^2 + \frac{2}{3} \int \tilde{\epsilon}(\mathbf{r}) j(\mathbf{r})^2 + \frac{8}{15} \int \tilde{\epsilon}^2(\mathbf{r}) j(\mathbf{r})^2 \\ &+ \int \frac{d^3 r}{(2\pi)^3} j(\mathbf{r})^4 + \frac{2}{9} \int (2 \tilde{\epsilon}(\mathbf{r}) j(\mathbf{r})^2)^2 + 3 (\tilde{\epsilon}^2(\mathbf{r})) (\tilde{\epsilon}^2(\mathbf{r})) + \frac{1}{8} \int \frac{d^3 r}{(2\pi)^3} j(\mathbf{r})^6 : \end{aligned} \quad (3.44)$$

Let us now recall from Section II B, see Eq. (2.98), that the first order phase transition is given by:

$$\mu_{\text{rst}} = \frac{r}{4} - \frac{1}{3}; \quad (3.45)$$

with a discontinuity in the gap given by

$$\Delta^2 = \Delta_{\text{rst}}^2 = \frac{3}{4}; \quad (3.46)$$

see Eq. (2.99). Let us now consider the possibility of a second order transition in the general LOFF case. Only the quadratic term in the gap is necessary for the discussion, and we have to look at its zero, given by $\tilde{\epsilon} = 0$. Since we

are considering only the quadratic term we can choose an optimal value for Q^2 by minimizing this term with respect to Q^2 . We find

$$Q^2 = \frac{5}{8} \frac{r}{\Delta_0}; \quad (3.47)$$

requiring $r < 0$. The corresponding value for T turns out to be

$$T = \frac{5}{24} \frac{r}{\Delta_0}; \quad (3.48)$$

or

$$T_{\text{second}} = \frac{r}{\frac{24}{5} \Delta_0}; \quad (3.49)$$

The LOFF second order transition line is higher than the first order transition line of the homogeneous case, since $T_{\text{second}} > T_{\text{first}}$ (see Fig. 13 showing the relevant lines in the plane $(\mu_0; T = \mu_0)$). Therefore the second order transition to the LOFF case overcomes the first order transition to the homogeneous symmetric phase as it can be checked by evaluating the grand potential for the LOFF state along the first order transition line.

The situation considered before corresponds to the physics of the problem only when the second order transition is a true minimum of the grand potential. This is not necessarily the case and we will explore in the following this possibility.

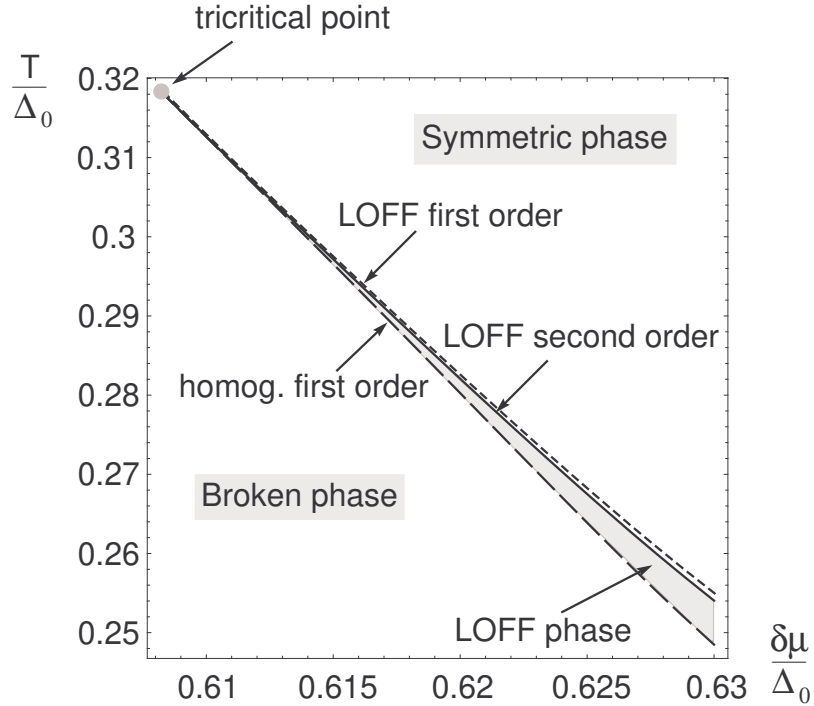


FIG. 13 The graph shows, in the plane $(\mu_0; T = \mu_0)$, the first order transition line (dashed line) from the homogeneous broken phase to the symmetric phase. The solid line corresponds to the second order transition from the LOFF phase to the symmetric one. The lines start from the tricritical point and ends when the Landau-Ginzburg expansion is not valid anymore.

1. The LO subspace

The second order term in the grand potential requires that the vectors Q have the same length along the second order transition line. It is natural to consider the subspace (LO) spanned by plane waves corresponding to momenta

with the same length Q_0 :

$$\langle r \rangle = \sum_{\mathbf{Q} \neq \mathbf{Q}_0}^{\mathbf{X}} e^{2i\mathbf{Q} \cdot \mathbf{r}}; \quad (3.50)$$

The authors of Ref. (Larkin and Ovchinnikov, 1964) have restricted their considerations to periodic solutions, but this is not strictly necessary, although the solution found in (Combescot and Mora, 2002) is indeed periodic. We will see that within this subspace the usual LOFF transition (the one corresponding to a single plane wave) is not a stable one. We will show that there is a first order transition that overcomes the second order line. In order that the LOFF line, characterized by Eqs. (3.47) and (3.48) is a true second order transition the coefficient of the fourth order term should be positive. However, in the actual case, the mixed terms in the scalar products of the vectors \mathbf{Q} could change this sign. In (Combescot and Mora, 2002) the mixed terms are studied by defining the following quantity

$$2bQ_0^2 \sum_{\mathbf{q}_i}^{\mathbf{X}} e^{i\mathbf{q}_1 \cdot \mathbf{r}} e^{i\mathbf{q}_2 \cdot \mathbf{r}} e^{i\mathbf{q}_3 \cdot \mathbf{r}} e^{i\mathbf{q}_4 \cdot \mathbf{r}} = \sum_{\mathbf{q}_i}^{\mathbf{X}} e^{i\mathbf{q}_1 \cdot \mathbf{r}} e^{i\mathbf{q}_2 \cdot \mathbf{r}} e^{i\mathbf{q}_3 \cdot \mathbf{r}} e^{i\mathbf{q}_4 \cdot \mathbf{r}} (Q_1 \cdot Q_2 + Q_2 \cdot Q_3 + Q_3 \cdot Q_4): \quad (3.51)$$

Clearly

$$b = 1 - \frac{1}{5}; \quad (3.52)$$

where $b = 1$ is reached in the case of a single plane wave. With this definition and for the optimal choice of Q_0 (see Eq. (3.47)), we get for the coefficients appearing in the expression of the grand potential (see Eqs. (3.40) and (3.42)):

$$\tilde{c} = \frac{5}{24} Q_0^2; \quad \tilde{b} = \frac{1}{9} (5b + 1); \quad \tilde{a} = \dots; \quad (3.53)$$

Therefore, for any order parameter such that

$$b < \frac{1}{5}; \quad (3.54)$$

it follows

$$\tilde{c} < 0 \quad (3.55)$$

and the LOFF line becomes unstable (we recall that close to the second order line $\tilde{c} < 0$). In fact, since $\tilde{c} = 0$ along this line and $\tilde{c} < 0$, a small order parameter is sufficient to make \tilde{c} negative. In other words one gains by increasing the order parameter as long as the sixth order term does not grow too much. But then we can make $\tilde{c} = 0$ (equal to its value in the symmetric phase) by increasing b . Therefore we have a new transition line in the plane $(b; \tilde{c})$ (or, which is the same in the plane $(\tilde{c} = 0; T = T_0)$) to the right of the LOFF line. (Combescot and Mora, 2002) also shows that necessarily

$$b \leq \frac{1}{3}; \quad (3.56)$$

The equality is reached for any real order parameter $\langle r \rangle$. In order to get a better feeling about the parameter b it is convenient to consider the following quantity

$$2cQ_0^2 \sum_{\mathbf{q}_i}^{\mathbf{X}} e^{i\mathbf{q}_1 \cdot \mathbf{r}} e^{i\mathbf{q}_2 \cdot \mathbf{r}} e^{i\mathbf{q}_3 \cdot \mathbf{r}} e^{i\mathbf{q}_4 \cdot \mathbf{r}} = \sum_{\mathbf{q}_i}^{\mathbf{X}} (Q_1 \cdot Q_2 + Q_2 \cdot Q_3 + Q_3 \cdot Q_4)^2 e^{i\mathbf{q}_1 \cdot \mathbf{r}} e^{i\mathbf{q}_2 \cdot \mathbf{r}} e^{i\mathbf{q}_3 \cdot \mathbf{r}} e^{i\mathbf{q}_4 \cdot \mathbf{r}}; \quad (3.57)$$

Expanding the right hand side of this equation and using $Q_1 \cdot Q_2 = Q_3 \cdot Q_4$ we find

$$c = 1 - b; \quad (3.58)$$

To minimize b is equivalent to maximize c . To this aim it is convenient to have opposite Q_1 and Q_2 because then $(Q_1 \cdot Q_2)^2$ reaches its maximum value equal to $4Q_0^2$. In this case we have

$$\mathbf{q}_1 = -\mathbf{q}_2; \quad (3.59)$$

This is equivalent to require that the order parameter is real in configuration space. Of course, it is not necessary that the amplitudes of the different pairs of plane waves are equal.

To proceed further one can introduce a measure of the size of the order parameter

$$\frac{1}{3} \int d^3r j(r) j^2 = \sum_{q_1}^X \sum_{q_2} N_2^2 \quad (3.60)$$

and

$$\frac{1}{3} \int d^3r j(r) j^4 = \sum_{q_1}^X \sum_{q_2} \sum_{q_3} \sum_{q_4} N_4^4; \quad (3.61)$$

$$\frac{1}{3} \int d^3r j(r) j^6 = \sum_{q_1}^X \sum_{q_2} \sum_{q_3} \sum_{q_4} \sum_{q_5} \sum_{q_6} N_6^6; \quad (3.62)$$

In the case of a single plane wave we get

$$N_2 = N_4 = N_6 = 1; \quad (3.63)$$

For a real gap the set of the vectors Q_i is made of $N=2$ pairs. If all the plane wave have the same amplitude one can show (Combes et al, 2002) that the quantities N_2 , N_4 and N_6 assume the following values

$$N_2 = 2N; \quad N_4 = 3N(N-1); \quad N_6 = 5N(3N^2 - 9N + 8); \quad (3.64)$$

With these notations the grand potential becomes

$$= N_2 + \frac{2}{3} Q_0^2 + \frac{8}{15} Q_0^4 + \frac{1}{2} N_4 + \frac{8}{3} a Q_0^2 + \frac{1}{3} N_6; \quad (3.65)$$

where

$$a = \frac{b+2}{3}; \quad \frac{1}{3} a \approx 1; \quad (3.66)$$

Minimizing this expression with respect to Q_0 we find

$$Q_0^2 = \frac{5}{8} - \frac{5}{4} a \frac{N_4}{N_2}; \quad (3.67)$$

Therefore a non zero solution for Q_0 is obtained if

$$\frac{1}{2a} - \frac{N_2}{N_4} = \frac{2}{\max}; \quad (3.68)$$

The corresponding expression for becomes

$$= N_2 - \frac{5}{24} \frac{2}{N_2} + \frac{1}{2} N_4 - \frac{5}{3} a \frac{4}{N_2} + \frac{1}{3} N_6 - \frac{5a^2}{2} \frac{N_4^2}{N_2 N_6}; \quad (3.69)$$

In order to have a transition from the symmetric phase we must allow $= 2$ to become negative. The zero of is reached for

$$= \frac{5}{24} \frac{2}{N_2} + \frac{3}{16} \frac{2}{N_4} - \frac{1}{\frac{N_2 N_6}{N_4^2} - \frac{5a^2}{2}}; \quad (3.70)$$

The value of corresponding to the zero of is given by

$$= \frac{3}{2} \frac{N_2}{N_4} - \frac{1}{\frac{N_2 N_6}{N_4^2} - \frac{5a^2}{2}}; \quad (3.71)$$

showing that this is a first order transition. We have shown that it is convenient to have b as small as possible and that the minimum is reached for $b = 1/3$ or $a = 5/9$. In correspondence with this value we have $\frac{1}{2} = 0$ and

$$> \frac{5}{24} : \quad (3.72)$$

We get

$$= \frac{5}{24} + \frac{1}{972} \frac{1}{\frac{N_2 N_6}{N_4^2} \frac{125}{162}} : \quad (3.73)$$

We see that it is convenient to take $N_2 N_6 = N_4^2$ as small as possible. However, notice that

$$\frac{N_2 N_6}{N_4} \geq 1 \quad (3.74)$$

as it follows from the Schwartz inequality

$$\frac{R_{d^3 r^2}(r) R_{d^3 r^6}(r)}{R_{d^3 r^4}(r)^2} \geq 1 : \quad (3.75)$$

Let us look for example at the case of pairs of plane waves with opposite q without any further constraint. In this case we get

$$\frac{N_2 N_6}{N_4^2} = \frac{5}{9} \frac{3N^2 + 9N + 8}{(N - 1)^2} : \quad (3.76)$$

This expression has a minimum at $N = 2$ (here N is even), where it holds $10/9$ and then it increases monotonically up to the value $15/9$. Notice that for crystalline structures the situation could be different. For instance, in the case of the cube the values of N_4 is not the one given by Eq. (3.64), i. e. 168, but rather 216. However, in Ref. (Combescot and Mora, 2002) it is shown that this expression gets indeed its minimum value for $N = 2$. This result is obtained assuming that the plane waves form a generic set of antipodal vectors, which means that the only way to satisfy the momentum conservation is through the cancellation of each momentum with the opposite one in the same pair. This excludes special configurations where other arrangements of vectors could give a zero result. The authors of Ref. (Combescot and Mora, 2002) argue that this result should hold in general, but a complete proof is lacking.

The value obtained for for the two plane wave case is

$$= \frac{1}{36} + \frac{5}{330} = \frac{1}{36} + \frac{5}{330} = 3 \cdot 10^{-3} : \quad (3.77)$$

In this case we have three lines, the first order line just found, the second order LOFF transition for $\beta = 5^2 = (24)$ and the first order transition to the homogeneous broken phase for $\beta = 3^2 = (16)$. The distance of these two last lines is given by

$$\frac{1}{16} - \frac{3}{24} = \frac{1}{48} = 2.1 \cdot 10^{-2} : \quad (3.78)$$

We know that these two lines stay close one to the other up to zero temperature. It turns out that the same is true for the new first order line as it has been shown in Ref. (Matsuo et al., 1998). These results are illustrated in Fig. 13. We notice that whereas in the expansion around the tricritical point the favored state seems to be the one corresponding to a pair of plane waves, with a first order transition between the LOFF and the normal state, at zero temperature one has a second order phase transition. Therefore the first order transition line must change into a second order line at low temperatures. In ref. (Matsuo et al., 1998) it has been shown that this happens at a temperature $T = T_{BCS} = 0.075$.

It is also interesting to see how things change varying the spatial dimensions. In fact it has been found in (Burkhardt and Rainer, 1994) that the first order transition found previously is second order in two spatial dimensions. This result is confirmed by (Buzdin and Kachkachi, 1997; Buzdin and Polonski, 1987; Buzdin and Tugushev, 1983; Machida and Nakanishi, 1989) which show that the transition is second order in one spatial dimension and furthermore it can be given an exact solution in terms of the Jacobi elliptic functions. This solution has the property that along the second

order transition line it reduces to the two plane wave case considered here. It is very simple to obtain the dependence on the number of dimensions. In fact the only place where the dimensions enter is in the angular integration as, for instance, in Eq. (B2). In general this is an average over the D -dimensional sphere and we need the following equations for the terms of order Q^2 and Q^4 respectively:

$$\int_{S_D} \frac{d\hat{w}}{S_D} \hat{w}_i \hat{w}_j = \frac{\delta_{ij}}{D}; \quad \int_{S_D} \frac{d\hat{w}}{S_D} \hat{w}_i \hat{w}_j \hat{w}_k \hat{w}_l = \frac{1}{D(D+2)} (\delta_{ij} \delta_{kl} + \delta_{ik} \delta_{jl} + \delta_{il} \delta_{jk}); \quad (3.79)$$

where S_D is the surface of the sphere with unitary radius in D -dimensions

$$S_D = \frac{2 \pi^{D/2}}{\Gamma(D/2)}; \quad (3.80)$$

Therefore the terms proportional to Q^2 are multiplied by $3=D$ and the ones proportional to Q^4 by $15=D(D+2)$. We get

$$\begin{aligned} \sim(q) &= + \frac{2}{D} Q^2 + \frac{8}{D(D+2)} Q^4; \\ \sim(q_i) &= + \frac{4}{3D} (Q_1^2 + Q_2^2 + Q_3^2 + Q_4^2 + Q_1 Q_2 + Q_1 Q_3 + Q_1 Q_4); \\ \sim(q_i) &= : \end{aligned} \quad (3.81)$$

Proceeding as before the grand potential evaluated at the optimal value of Q^2 is

$$= N_2 \left[1 - \frac{D+2}{8D} a^2 \right]^2 + \frac{1}{2} N_4 \left[1 - \frac{D+2}{D} a^4 \right] + \frac{1}{3} N_6 \left[1 - \frac{3(D+2)}{2D} a^2 \frac{N_4^2}{N_2 N_6} \right]^6; \quad (3.82)$$

We see from here that the critical dimension for the transition to change from first to second order is at the zero of the second term, that is

$$D = \frac{2a}{1-a} \quad (3.83)$$

and for $a = 5/9$, $D = 2.5$. This means that we have a first order transition for $D > 2.5$ and a second order one for $D < 2.5$ (remember that $a < 0$). The location of the transition is at $a = 5/9$

$$= \frac{D+2}{8D} a^2 + \frac{3}{20} \frac{a^2 (2D-5)^2}{D(7D-10)}; \quad (3.84)$$

The value of the gap along the transition line is given by

$$a^2 = \frac{6}{5} - \frac{2D}{7D} - \frac{5}{10}; \quad (3.85)$$

We see that $a^2 > 0$ for $D > 2.5$.

(Combescot and Mora, 2002) have considered also the possibility of solutions around the tricritical point not belonging to the LOFF subspace. In fact, the antipodal solution does not satisfy the Euler-Lagrange equation obtained from Eq. (3.44), due to the non-linear terms. If these are small it is reasonable to look for solutions close to $\cos(q \cdot r)$. This assumption simplifies the problem because the antipodal solution is essentially a one-dimensional solution characterized by the direction of q . Then (Combescot and Mora, 2002) have found that the corrections at $\cos(q \cdot r)$ expressed in terms of higher harmonics are indeed very small. Of course this is only a consistency argument, but it is an indication that the choice of the LOFF subspace is a good approximation to the full problem.

To conclude this Section let us say that in our opinion the status of the LOFF phase is not yet settled. Up to now we have considered the Ginzburg-Landau expansion both at $T = 0$ and at the tricritical point. The results in the three-dimensional case can be summarized as follows:

Zero temperature point: In (Larkin and Ovchinnikov, 1964) it is found that the favored phase has a gap with a phase modulation $\cos(q \cdot r)$ corresponding to a structure with two antipodal vectors. This phase and the normal alone are separated by a second order-transition line. However in (Bowers and Rajagopal, 2002), where a rather complete study of the possible crystalline structures has been done, it is argued that the most favorable structure would be the face-centered cube. The transition between the corresponding phase and the normal alone should be first-order.

Tricritical point: In (Buzdin and Kachkachi, 1997) the non-uniform phase has been studied in different dimensions with the result that the space modulation related to a single wave vector (i.e. $\exp(2iq \cdot r)$) is always unfavorable. These authors find also that the solution with two antipodal wave vectors is the preferred one. In 1 and 2 space dimensions the transition to the normal state is second-order, whereas it is first-order in 3 space dimensions. Analogous results have been found in (Houzet et al., 1999) (see also (Agterberg and Yang, 2001)), where the study has been extended to space modulations such as $\cos(qx) + \cos(qy)$ or $\cos(qx) + \cos(qy) + \cos(qz)$. These authors argue that there could be various transition lines at temperatures lower than the tricritical point. Finally, as thoroughly discussed in this Section, in (Combescot and Mora, 2002) the results of (Buzdin and Kachkachi, 1997) are confirmed.

There have been also numerical investigations about the full phase space. In particular (Burkhardt and Rainer, 1994) proved that in the two-dimensional case (layered superconductors) the phase transition from the normal phase to the one characterized by two antipodal vectors is second order. The second-order transition line from the phase with a single plane wave to the normal phase has been studied in (Saint-James et al., 1969; Samma, 1963). The two-dimensional case for type II superconductors has been studied in (Shimahara, 1998a). The author has considered states corresponding to single wave vectors and antipodal pairs together with configurations corresponding to triangular, square and hexagonal states. It is found that, according to the temperature, all these states may play a role. Finally (Matsuo et al., 1998), as already mentioned, make a numerical analysis based on the use of quasi-classical Green's functions. They find that in 3 dimensions the transition line between the normal phase and the antipodal vectors phase starts being first-order at the tricritical point and becomes second-order at $T = 0.0075 T_{CS}$. The two-dimensional case will be discussed again in Section VI D.

In conclusion the question of the preferred non-uniform state cannot be considered settled down yet. Let us discuss by way of example the 3 dimensional case. We have seen that there are strong indications that the favored state around the tricritical point is the one corresponding to two antipodal vectors. This being the case the natural question is: how the transition line extends down to zero temperature? If at $T = 0$ the preferred state were the antipodal pair a further tricritical point in the plane $(\vec{q}; T)$ would arise. In fact, recall that the transition is first order at the tricritical point and second-order at $T = 0$. However, if the conjecture in (Bowers and Rajagopal, 2002) is correct, the cubic phase would emerge in the path going to $T = 0$. A possibility is that one goes from one structure to another in analogy to what suggested by (Shimahara, 1998a) for the two-dimensional case. The other logical possibility is that the Combescot and Mora result at the tricritical point might be evaded by an exceptional arrangement of the wave vectors as, for instance, in the case of the face-centered cube. Therefore we think that more theoretical work is necessary in order to fill-in these gaps in our understanding of the non-uniform superconducting phase.

IV. SUPERCONDUCTIVITY IN QUANTUM CHROMODYNAMICS

Color superconductivity (CSC) is an old subject (Bailin and Love, 1984; Barrois, 1977; Collins and Perry, 1975; Frautschi, 1978) that has recently become one of the most fascinating research fields in Quantum Chromodynamics (QCD); these developments can be found in (Agasian et al., 1999; Alford et al., 1999a, 2000, 1998, 1999b; Carter and Diakonov, 1999; Hong et al., 2000; Pisarski and Rischke, 1999a, 2000b; Rapp et al., 1998; Schafer and Wilczek, 1999a,b,c,d; Shuster and Son, 2000); for reviews see (Rajagopal and Wilczek, 2001), (Hong, 2001), (Alford, 2001), (Hsu, 2000). It offers a clue to the behavior of strong interactions at high baryonic densities, an issue of paramount relevance both for the understanding of heavy ion collisions and the physics of compact stars. Color superconductivity arises because for sufficiently high baryon chemical potential and small temperature, the color interaction favors the formation of a quark-quark condensate in the color antisymmetric channel 3. In the asymptotic regime it is also possible to understand the structure of the condensates. In fact, consider the matrix element

$$\langle 0 | j_{ia} j_{jb} | 0 \rangle \quad (4.1)$$

where $i, j = 1, 2, 3$ are color indices, $a, b = 1, 2$ are spin indices and $i, j = 1, \dots, N$ are flavor indices. Its color, spin and flavor structure is completely fixed by the following considerations.

Antisymmetry in color indices (i, j) in order to have attraction.

Antisymmetry in spin indices (a, b) in order to get a spin zero condensate. The isotropic structure of the condensate is favored since a larger portion of the phase space around the Fermi surface is available.

Given the structure in color and spin, Pauli principles requires antisymmetry in flavor indices.

Since the quark and spin momenta in the pair are opposite, it follows that the left (right)-handed quarks can pair only with left (right)-handed quarks. In the case of 3 flavors the favored condensate is

$$\langle \bar{q}_{iL} q_{jL} \rangle = \langle \bar{q}_{iR} q_{jR} \rangle = \delta_{ij} \chi^3 \quad \text{C} = 1 \quad (4.2)$$

This gives rise to the so-called color{ flavor} locked (CFL) phase (Alford et al., 1999b; Schafer and Wilczek, 1999a). However at moderate densities other less attractive channels could play a role (Alford et al., 2003). The reason for the name is that simultaneous transformations in color and in flavor leave the condensate invariant. In fact, the symmetry breaking pattern turns out to be

$$SU(3)_C \times SU(3)_L \times SU(3)_R \times U(1)_B \rightarrow SU(3)_{C+L+R} \times Z_2;$$

where $SU(3)_{C+L+R}$ is the diagonal subgroup of the three $SU(3)$ groups. Both the chiral group and the color symmetry are broken but a diagonal $SU(3)$ subgroup remains unbroken. The Z_2 group arises from the invariance of the condensate when the quark fields are multiplied by -1 . We have 17 broken generators; since there is a broken gauge group, 8 of these generators correspond to 8 longitudinal degrees of the gluons, because the gauge bosons acquire a mass; there are 9 Nambu Goldstone bosons (NGB) organized in an octet associated to the breaking of the flavor group and in a singlet associated to the breaking of the baryonic number. The effective theory describing the NGB for the CFL model has been studied in (Casalbuoni and Gatto, 1999).

This is the typical situation when the chemical potential is much larger than the quark masses m_u, m_d and m_s (in these considerations one should discuss about density depending masses). However one can ask what happens when decreasing the chemical potential. At intermediate densities we have no more the support of asymptotic freedom, but all the model calculations show that one still has a sizeable color condensation. In particular if the chemical potential is much less than the strange quark mass one expects that the strange quark decouples, and the corresponding condensate should be

$$\langle \bar{q}_{iL} q_{jL} \rangle = \delta_{ij} \chi^3; \quad (4.3)$$

since due to the antisymmetry in color the condensate must necessarily choose a direction in color space. Notice that now the symmetry breaking pattern is completely different from the three-flavor case, in fact we have

$$SU(3)_C \times SU(2)_L \times SU(2)_R \times U(1)_B \rightarrow SU(2)_C \times SU(2)_L \times SU(2)_R \times U(1) \times Z_2;$$

The chiral group remains unbroken, while the original color symmetry group is broken to $SU(2)_C$, with generators T^A corresponding to the generators T^1, T^2, T^3 of $SU(3)_C$. As a consequence, three gluons remain massless whereas the remaining five acquire a mass. Even though the original $U(1)_B$ is broken there is an unbroken global symmetry that plays the role of $U(1)_B$. As for $U(1)_A$, this axial symmetry is broken by anomalies, so that in principle there is no Goldstone boson associated to its breaking by the condensate; however at high densities explicit axial symmetry breaking is weak and therefore there is a light would be Goldstone boson associated to the breaking of the axial $U(1)_A$. One can construct an effective theory to describe the emergence of the unbroken subgroup $SU(2)_L$ and the low energy excitations, much in the same way as one builds up chiral effective lagrangian with effective fields at zero density. For the two-flavor case this development can be found in (Casalbuoni et al., 2000; Rischke et al., 2001).

It is natural to ask what happens in the intermediate region of μ . It turns out that the interesting case is for $M_s^2 = \mu$. To understand this point let us consider the case of two fermions, one massive, $m_1 = M_s$ and the other one massless, at the same chemical potential μ . The Fermi momenta are of course different

$$p_{F1} = \sqrt{\mu^2 - M_s^2}; \quad p_{F2} = \mu; \quad (4.4)$$

The grand potential for the two unpaired fermions is

$$\Omega_{\text{unpair}} = 2 \int_0^{p_{F1}} \frac{d^3p}{(2\pi)^3} \mu - \frac{p^2}{2} - \frac{M_s^2}{2} + 2 \int_0^{p_{F2}} \frac{d^3p}{(2\pi)^3} (\mu - p^2); \quad (4.5)$$

For the two fermions to pair they have to reach some common momentum p_{com}^F , and the corresponding grand potential is

$$\Omega_{\text{pair}} = 2 \int_0^{p_{\text{com}}^F} \frac{d^3p}{(2\pi)^3} \mu - \frac{p^2}{2} - \frac{M_s^2}{2} + 2 \int_0^{p_{\text{com}}^F} \frac{d^3p}{(2\pi)^3} (\mu - p^2) - \frac{2}{4} \mu^2; \quad (4.6)$$

where the last term is the energy necessary for the condensation of a fermion pair, see Eq. (2.71). The common momentum $p_{\text{com m}}^{\text{F}}$ can be determined by minimizing ϵ_{pair} with respect to $p_{\text{com m}}^{\text{F}}$. The result is (expanding in M_s)

$$p_{\text{com m}}^{\text{F}} = \frac{M_s^2}{4} : \quad (4.7)$$

It is now easy to evaluate the difference $\epsilon_{\text{pair}} - \epsilon_{\text{unpair}}$ at the order M_s^4 , with the result

$$\epsilon_{\text{pair}} - \epsilon_{\text{unpair}} = \frac{1}{16} M_s^4 - \frac{1}{4} M_s^2 : \quad (4.8)$$

We see that in order to have condensation the condition

$$> \frac{M_s^2}{2} \quad (4.9)$$

must be realized. The problem of one massless and one massive flavor has been studied by (Kundu and Rajagopal, 2002). However, one can simulate this situation by letting the two quarks being both massless but with two different chemical potentials, which is equivalent to have two different Fermi spheres. The big advantage here is that one can use the LOFF analysis discussed in Section II C

Color superconductivity due to the non vanishing of the condensates (4.1) or (4.3) results from a mechanism analogous to the formation of an electron Cooper pair in a BCS superconductor and, similarly to the BCS superconductivity the only relevant fermion degrees of freedom are those near the Fermi surface. Therefore a two-dimensional effective field theory has been developed. We shall briefly review it below, but our main interest is to delineate another development of color superconductivity, i.e. the presence of a LOFF superconducting phase. Also in this case the condensation is generated by the attractive color interaction in the antitriplet channel. This phase of QCD has been mainly studied at small temperatures, see e.g. (Alford et al., 2001a,b; Bowers et al., 2001; Bowers and Rajagopal, 2002; Leibovich et al., 2001; Rajagopal, 2001). Similarly to the CFL and 2SC phases, the QCD LOFF phase can be studied by the effective theory, as shown in (Casalbuoni et al., 2002b, 2001a, 2002c,e; Nardulli, 2002b). This description is useful to derive the effective lagrangian for the Goldstone bosons associated to the breaking of the space symmetries, i.e. the phonons. It is based on an analogy with the Heavy Quark Effective Theory and is called High Density Effective Theory (HDET). To describe these developments we organize this Section as follows. In Subsection IV A we give an outline of the HDET. We specialize the formalism to the CFL phase in Subsection IV B and to the 2SC phase in Subsection IV C. The final Subsections are devoted to the LOFF phase in QCD. In Subsection IV D, after a general introduction to the subject, we consider a Nambu-Jona-Lasinio coupling for a QCD liquid formed by quarks with two flavors. Given the similarities with the BCS four-fermion interaction arising from the electron phonon interactions in metals, we can apply the same formalism discussed in previous Sections. In the present case, however the two species we consider are quarks of different flavors, up and down, with different chemical potentials μ_u, μ_d . We limit our analysis to the FF one plane wave state. However the results of Subsection III C are valid also for the QCD LOFF state; in particular the guess on the favored structure at $T = 0$ discussed in (Bowers and Rajagopal, 2002) and reviewed in Subsection III C.4 should point to the cubic structure as the most favorable LOFF crystal. In Subsection IV E we discuss the differences induced by considering the one-gluon interaction instead of the effective four fermion interaction. LOFF superconductivity in QCD can be induced not only by a difference in the quark chemical potential but also by mass differences among the quarks. This situation is discussed in Subsection IV F that shows the role the strange quark mass can play in favoring the LOFF phase.

A. High Density Effective Theory

At very high baryonic chemical potential and very small temperature ($T \rightarrow 0$) it is useful to adopt an effective description of QCD known as High Density Effective Theory (HDET), see (Beane et al., 2000; Casalbuoni et al., 2001b; Hong, 2000a,b), and, for reviews, (Casalbuoni, 2001; Nardulli, 2002a). Let us consider the fermion field

$$\psi(x) = \int \frac{d^4 p}{(2\pi)^4} e^{i p \cdot x} \psi(p) : \quad (4.10)$$

Since the relevant degrees of freedom are those near the Fermi surface, we decompose the fermion momentum as

$$p = v + \ell ; \quad (4.11)$$

where $v = (0; \mathbf{v})$, \mathbf{v} the Fermi velocity (for massless fermions $|\mathbf{v}| = 1$) and ℓ is a residual momentum. We also use $V = (1; \mathbf{v})$, $\bar{V} = (1; -\mathbf{v})$.

We now introduce the velocity-dependent positive-energy ψ_v and negative-energy $\bar{\psi}_v$ left-handed fields via the decomposition

$$\psi(x) = \int \frac{d^4 v}{4} e^{i v \cdot x} [\psi_v(x) + \bar{\psi}_v(x)] : \quad (4.12)$$

Here

$$\psi_v(x) = e^{i v \cdot \not{x}} \not{P}_+ \psi(x) = \int \frac{d^4 v}{(2\pi)^4} e^{i v \cdot \not{x}} \not{P}_+ \psi(v) \quad (4.13)$$

and

$$\bar{\psi}_v(x) = e^{i v \cdot \not{x}} \not{P} \bar{\psi}(x) = \int \frac{d^4 v}{(2\pi)^4} e^{i v \cdot \not{x}} \not{P} \bar{\psi}(v) : \quad (4.14)$$

\not{P} are projectors that for massless quarks are defined by

$$\not{P} = \not{P}(v) = \frac{1}{2} (1 + \not{v}) : \quad (4.15)$$

The extension to massive quarks is discussed in (Casalbuoni et al, 2002a, 2003). The cut-off satisfies while being much larger than the energy gap.

Using the identities

$$\begin{aligned} \psi_v \psi_v &= \not{V} \psi_v^0 \psi_v ; & \bar{\psi}_v \bar{\psi}_v &= \not{V} \bar{\psi}_v^0 \bar{\psi}_v ; \\ \psi_v \bar{\psi}_v &= \psi_v \not{?} \bar{\psi}_v ; & \bar{\psi}_v \psi_v &= \bar{\psi}_v \not{?} \psi_v ; \end{aligned} \quad (4.16)$$

and substituting into the Dirac part of the QCD lagrangian we obtain

$$L_D = \int \frac{d^4 v}{4} \bar{\psi}_v i \not{V} \not{D} \psi_v + \int \frac{d^4 v}{4} (2 + i \not{V} \not{D}) \psi_v + (\bar{\psi}_v i \not{D} \psi_v + h.c.) ; \quad (4.17)$$

$\not{D} = \not{D}_?$ and \not{D} is the covariant derivative: $\not{D} = \not{\partial} + i g \not{A}$. We note that here quark fields are evaluated at the same Fermi velocity; off-diagonal terms are subleading due to the Riemann-Lebesgue lemma, as they are cancelled by the rapid oscillations of the exponential factor in the $\Lambda \rightarrow \infty$ limit (Fermi velocity superselection rule). A similar behavior occurs in QCD in the $m_Q \rightarrow \infty$ limit, when one uses the Heavy Quark Effective Theory (Eichten and Hill, 1990; Georgi, 1990; Isgur and Wise, 1989, 1990), and for reviews, (Casalbuoni et al, 1997; Manohar and Wise, 2000; Neubert, 1994).

We can get rid of the negative energy solutions by integrating out the $\bar{\psi}_v$ fields in the generating functional; at tree level this corresponds to solve the equations of motion, which gives

$$i \not{V} \not{D} \psi_v = 0 \quad (4.18)$$

and

$$\psi_v = \frac{i}{2 + i \not{V} \not{D}} \not{D} \not{D}_? \psi_v ; \quad (4.19)$$

which shows the decoupling of $\bar{\psi}_v$ in the $\Lambda \rightarrow \infty$ limit. In the resulting effective theory for ψ_v only the energy and the momentum parallel to the Fermi velocity are relevant and the effective theory is two-dimensional.

It is useful to introduce two separate fields

$$\psi_v ; \quad (4.20)$$

therefore the average over the Fermi velocities is defined as follows:

$$\langle X \rangle = \int \frac{d^4 v}{8} : \quad (4.21)$$

The extra factor 1/2 occurs here because, after the introduction of the field with opposite velocity, one doubles the degrees of freedom, which implies that the integration is only over half solid angle.

In conclusion, if L_0 is the free quark lagrangian and L_1 represents the coupling of quarks to one gluon, the high density effective lagrangian can be written as

$$L_D = L_0 + L_1 + L_2 + (L + R); \quad (4.22)$$

where

$$L_0 = \sum_v \int d^3x \bar{\psi}_v \gamma_0 \psi_v + \int d^3x \bar{\psi}_v \gamma_0 \psi_v; \quad (4.23)$$

$$L_1 = ig \sum_v \int d^3x \bar{\psi}_v \gamma_\mu \psi_v A_\mu + \int d^3x \bar{\psi}_v \gamma_\mu \psi_v A_\mu; \quad (4.24)$$

and

$$L_2 = \sum_v \int d^3x \bar{\psi}_v \gamma_0 \psi_v \frac{1}{2 + iV} \bar{\psi}_v \gamma_0 \psi_v + \sum_v \int d^3x \bar{\psi}_v \gamma_0 \psi_v \frac{1}{2 + iV} \bar{\psi}_v \gamma_0 \psi_v; \quad (4.25)$$

L_2 is a non local lagrangian arising when one integrates over the ψ degrees of freedom in the functional integration. It contains couplings of two quarks to any number of gluons and gives contribution to the gluon Meissner mass. We have put

$$P = g \frac{1}{2} \int d^3x \bar{\psi} \gamma_\mu \psi + \int d^3x \bar{\psi} \gamma_\mu \psi; \quad (4.26)$$

This construction is valid for any theory describing massless fermions at high density provided one excludes degrees of freedom far from the Fermi surface.

B. CFL phase

Even though we shall consider the LOFF phase only for two flavors, for completeness we present HDET for the 3-flavor Color Flavor Locking phase as well. In the CFL phase the symmetry breaking is induced by the condensates

$$\bar{\psi}_i^L C^T \psi_j^L = \bar{\psi}_i^R C^T \psi_j^R = \frac{1}{2} \delta_{ij}; \quad (4.27)$$

where $\psi_i^{L,R}$ are Weyl fermions and $C = i\sigma_2$. Eq. (4.27) corresponds to the invariant coupling (χ_L):

$$\frac{1}{2} \sum_{i,j=1,3} \bar{\psi}_i^T C \psi_j = (L + R) + \text{h.c.}; \quad (4.28)$$

and $(\chi_L)_{ab} = \chi_{ab}$. Neglecting the negative energy components, for the Dirac fermions we introduce the compact notation

$$= \frac{1}{2} \bar{\psi} C \psi \quad (4.29)$$

in a way analogous to Equation (2.11). We also use a different basis for quark fields:

$$\psi_{v,i} = \sum_{A=1}^{X^0} \frac{(\psi_A)_i}{\sqrt{2}} \psi_A; \quad (4.30)$$

The CFL fermionic lagrangian has therefore the form :

$$L_D = L_0 + L_1 + L_2 = \sum_{v,A,B=1}^{X^0} \bar{\psi}_v \gamma_0 \psi_v + \int d^3x \bar{\psi}_v \gamma_\mu \psi_v A_\mu + \int d^3x \bar{\psi}_v \gamma_\mu \psi_v A_\mu + (L + R); \quad (4.31)$$

where

$$A_B = \text{Tr}[\psi_A^T \psi_B] \quad (4.32)$$

and

$$T_A = \frac{p_A}{2} : \quad (4.33)$$

Here $g_9 = g_0 = \frac{q}{3}$. We use the identity (any 3×3 matrix):

$$\text{Tr} g^T = g \quad \text{Tr} g ; \quad (4.34)$$

we obtain

$$A_B = A \quad A_B ; \quad (4.35)$$

where

$$1 = \frac{8}{8} \quad (4.36)$$

and

$$g_9 = \frac{2}{3} : \quad (4.37)$$

The CFL free fermionic lagrangian assumes therefore the form :

$$L_0 + L = \sum_{v, A=1}^X X^9 \quad A_Y \quad iV \quad @ \quad A \quad A + (L + R) : \quad (4.38)$$

Clearly the equations of motion following from this lagrangian are of the same type as the NG equations, see Eq. (2.15). For applications of HDET to the CFL phase we refer the reader to (Casalbuoni et al., 2001b).

C. 2SC phase

For the two flavor case, which encompasses both the 2SC model and the existing calculation in the LOFF phase, we follow a similar approach. The symmetry breaking is induced by the condensates

$$h_i^L C_j^L = h_i^R C_j^R = \frac{1}{2} \quad 3 \quad i,j ; \quad (4.39)$$

and the invariant coupling is (L):

$$L = \frac{1}{2} \quad C^T \quad (L + R) + \text{h.c.} ; \quad (4.40)$$

where

$$= i_2 : \quad (4.41)$$

We use a different basis for the fermion fields by writing the positive energy effective fields $v_{i,j}$ as follows:

$$v_{i,j} = \sum_{A=0}^X \frac{(\tilde{c}_A)_i}{\frac{p}{2}} \quad A : \quad (4.42)$$

The \tilde{c}_A matrices are defined in terms of the usual matrices as follows:

$$\tilde{c}_0 = \frac{1}{3} \quad 8 + \frac{r}{3} \quad 0 ; \quad \tilde{c}_A = A \quad (A = 1, 2, 3) ; \quad \tilde{c}_4 = \frac{4}{2} \quad i5 ; \quad \tilde{c}_5 = \frac{6}{2} \quad i7 : \quad (4.43)$$

We also define $\tilde{c} = i_2$. After the introduction, analogously to (4.29), of the fields \tilde{c}_A , the 2SC fermionic lagrangian assumes the form :

$$L_D = L_0 + L_1 + L$$

$$= \sum_{\nu} \sum_{A,B=0}^5 \text{Tr} [\bar{\psi}_A V_{AB} \psi_B] + (L \rightarrow R) : \quad (4.44)$$

Here

$$\begin{aligned} V_{AB} &= \frac{1}{2} \text{Tr} [\tilde{\psi}_A^T \tilde{\psi}_B] & (A,B = 0; \dots; 3); \\ V_{AB} &= 0 & (A,B = 4; 5) : \end{aligned} \quad (4.45)$$

and

$$T_A = \frac{\tilde{\psi}_A}{2} \quad (A = 0; \dots; 5) : \quad (4.46)$$

Analogously to (4.34) we use the identity:

$$\tilde{\psi}^T \tilde{\psi} = g \quad \text{Tr} g ; \quad (4.47)$$

we obtain

$$V_{AB} = V_A V_B ; \quad (4.48)$$

where V_A is defined as follows:

$$V_A = (+ ; ; ; ; 0; 0) : \quad (4.49)$$

Therefore the effective lagrangian for free quarks in the 2SC model can be written as follows

$$L_0 + L = \sum_{\nu} \sum_{A=0}^5 \text{Tr} [\bar{\psi}_A V_A \psi_A] + (L \rightarrow R) : \quad (4.50)$$

D. LOFF phase in QCD

We shall assume here that in the most interesting phenomenological applications, i.e. in compact stars (see Section VI G), there is a significant difference between the Fermi momenta of different flavors. Since this produces a difference in the densities, the BCS phase may be disrupted (Alford et al., 1999a; Schafer and Wilczek, 1999c) and a phase analogous to the LOFF phase might arise. The case of a LOFF phase in QCD was also discussed in Ref. (Son and Stephanov, 2001; Splittor et al., 2001) in the context of quark matter at large isospin density. Differences in the Fermi momenta in these examples arise both from the difference in the chemical potential, due to the weak equilibrium, and from the mass difference between the strange and the up and down quarks. A complete study requires to take into account both effects. This has been made in Ref. (Kundu and Rajagopal, 2002). We will discuss this paper below. Here we will consider a simpler case where all quarks are massless but have different chemical potentials (Alford et al., 2001b). To simplify further the problem we will restrict ourselves to the case of two massless quarks with chemical potentials μ_u and μ_d given by

$$\mu_u = \mu + \mu_3 ; \quad \mu_d = \mu : \quad (4.51)$$

These equations are the same as (2.2) but now up and down refer to flavor.

Everything goes according to the discussion made in Sections II B and II C except that now the density of gapped states at the Fermi surface is multiplied by a factor 4, coming from the two colors and the two flavors. In fact, the condensate has the form

$$h_{ij} = \frac{1}{2} \delta_{ij} ; \quad (4.52)$$

where $i, j = 1; 2; 3$ and $i, j = 1; 2$ are respectively color and flavor indices. Other differences are in the value of the Fermi velocity, which is $v_F = 1$, since we deal with massless fermions, and in the Fermi momentum which is given by $p_F = \mu$. As a consequence the density of states is now

$$= 4 \frac{\mu^2}{2} : \quad (4.53)$$

It follows that the first order transition from the homogeneous phase to the normal one, in the weak coupling limit, is given, using (2.63), by

$$(\chi) = 0 \quad (\chi) = -\frac{1}{4} (2^{-2} - \frac{2}{0}) = -\frac{1}{2} (2^{-2} - \frac{2}{0}) = 0 : \quad (4.54)$$

Applying the results obtained in the Section II.C to color superconductivity requires some care. For instance, although only two colors are gapped, in order to describe the mixed phase it is necessary the use of a proper treatment of the two ungapped quarks (Bedaque, 2002). Another situation that can be present in QCD but not in condensed matter is the case of equal chemical potentials with different Fermi momenta due to unequal masses. This is discussed in Ref. (Alford et al., 1999a; Schafer and Wilczek, 1999c). However in the realistic case different chemical potentials must be considered.

We will describe also the LOFF phase using the formalism of fields close to the Fermi surface, although in the present case the corrections to the leading order are expected to be larger since we are not considering asymptotic values of the chemical potential. This formalism is very close to the NG formalism developed in Section II. We consider a four-fermion interaction modelled on one-gluon exchange, that is

$$L_I = -\frac{3}{8} G \quad a \quad a ; \quad (4.55)$$

where a are Gell-Mann matrices. We then introduce the fields ψ_{i+} through the procedure outlined in Section IV.C. We perform the same transformation $\exp(i \psi^\dagger x)$ for both flavors. For simplicity, in the rest of this Section we will denote the fields ψ_{i+} by ψ_i . Separating the left-handed and the right-handed modes the previous interaction can be written as

$$L_I = -\frac{G}{2} (3 \quad)_{a \underline{c} \underline{b} d} \psi_a^{y_i} \psi_c^{y_j} \psi_{\underline{b}} \psi_d \quad V \quad y_i y_j \quad i \quad j ; \quad (4.56)$$

where in the last expression the sum over the spin indices, $a; c; b; d$ is understood and

$$V = -\frac{G}{2} (3 \quad) : \quad (4.57)$$

In obtaining this result we have used the identities

$$\sum_{a=1}^8 X^a \quad (a) \quad (a) = \frac{2}{3} (3 \quad) \quad (4.58)$$

and

$$(\quad)_{ab} (\sim)_{dc} = 2 \quad a \underline{c} \underline{b} d : \quad (4.59)$$

Here

$$= (1; \quad); \quad \sim = (1; \quad); \quad (4.60)$$

with the Pauli matrices. As in Section II we divide L_I in two pieces

$$L_{\text{cond}} = V \quad (y_i y_j h_{i \quad j} i + \quad i \quad j h \quad y_i y_j i) + (L + R) \quad (4.61)$$

and

$$L_{\text{int}} = V \quad (y_i y_j \quad h \quad y_i y_j i) (\quad i \quad j \quad h_{i \quad j} i) + (L + R) : \quad (4.62)$$

The first piece can be written as

$$L_{\text{cond}} = \frac{1}{2} \quad 3 \quad ij (\quad i \quad j \quad e^{2iq \cdot r + c \cdot x}) + (L + R); \quad (4.63)$$

where we have defined

$$s \quad e^{2iq \cdot r} = \frac{1}{2} \quad 3 \quad ij h \quad i \quad j i \quad (4.64)$$

and

$$= G_s : \quad (4.65)$$

The quadratic part of the lagrangian L_{cond} in terms of the NG fields can be written as

$$L_{\text{cond}}^{(2)} = \frac{1}{2} \sum_{ij} \sum_{\alpha} (S^{-1})_{ij}^{\alpha} \phi_j^{\alpha} ; \quad (4.66)$$

where, in momentum space

$$(S^{-1})_{ij}^{\alpha} = \frac{(i j | V_{\alpha} + \frac{1}{2} \delta_{ij} (\psi^{\alpha} - \bar{\psi}^{\alpha}))}{3 \delta_{ij} (\psi^{\alpha} - \bar{\psi}^{\alpha} - 2q)} - \frac{3 \delta_{ij} (\psi^{\alpha} + 2q)}{(i j | V_{\alpha} + \frac{1}{2} \delta_{ij} (\psi^{\alpha} - \bar{\psi}^{\alpha}))} ; \quad (4.67)$$

and $q = (0; q)$. Using this expression and performing the same derivation as in Section II we find the gap equation

$$= 2ig \int \frac{d^4 p}{4} \frac{d^4 k}{2} \text{Tr} \frac{1}{(V_{\alpha} (\psi + q) + \frac{1}{2} \delta_{ij} (\psi^{\alpha} - \bar{\psi}^{\alpha})) + \frac{1}{2} \delta_{ij} (\psi^{\alpha} - \bar{\psi}^{\alpha})} ; \quad (4.68)$$

Comparing this result with Eq. (2.39), one notices a factor 2 coming from the trace on the color; the remaining trace is on the flavor indices where the matrix δ_{ij} acts. Performing the trace and making explicit the prescriptions for the energy integration we find

$$= i \frac{g}{2} \int \frac{d^4 p}{4} \frac{d^4 k}{2} \frac{1}{(E_k + i \text{sign} E_k)^2 + \frac{1}{2} \delta_{ij} (\psi^{\alpha} - \bar{\psi}^{\alpha})} ; \quad (4.69)$$

where $\rho = 4 \pi^2 \rho$ is the relevant density at the Fermi surface and we have defined $E = \epsilon_k$ and $\psi = \psi_k$ to emphasize the similarity with the original LOFF equation (see Section II.C). Moreover

$$= \frac{1}{2} \frac{1}{\psi - \bar{\psi}} : \quad (4.70)$$

Performing the integration over the energy we get

$$1 = \frac{g}{2} \int \frac{d^4 p}{4} \frac{d^4 k}{2} \frac{1}{\psi - \bar{\psi}} \left(\frac{1}{2} \delta_{ij} (\psi^{\alpha} - \bar{\psi}^{\alpha}) \right) : \quad (4.71)$$

Since

$$\left(\frac{1}{2} \delta_{ij} (\psi^{\alpha} - \bar{\psi}^{\alpha}) \right) = 1 \left(\frac{1}{2} \delta_{ij} (\psi^{\alpha} - \bar{\psi}^{\alpha}) \right) + \frac{1}{2} \delta_{ij} (\psi^{\alpha} - \bar{\psi}^{\alpha}) ; \quad (4.72)$$

we get exactly the LOFF gap equation (compare with Eq. (2.115)), except for the different definition of the density of states.

We have already shown that in the present case there is a first order transition in ρ , between the homogeneous state (that from now on will be referred to as the BCS state) and the normal state. Furthermore, from Section II.C we know that there is a second order transition between the LOFF state and the normal one. These results are valid also in the present case with the only change in the density of gapped states at the Fermi surface, which, as already stressed, is now a factor of four larger than the one for electrons. We recall from that analysis that around the second order critical point $\rho_c = 0.754 \rho_0$ (with ρ_0 the BCS gap) we have (see Eq. (3.27))

$$\rho_{\text{LOFF}} = \frac{\rho}{1.757 \rho_0} = 1.15 \rho_0 : \quad (4.73)$$

As for the grand potential, we have from Eq. (2.63)

$$\Omega_{\text{BCS}} - \Omega_{\text{normal}} = \frac{1}{4} (2 \rho^2 - \rho_0^2) \quad (4.74)$$

and from Eq. (3.28)

$$\Omega_{\text{LOFF}} - \Omega_{\text{normal}} = 0.439 \left(\frac{\rho}{\rho_0} \right)^2 : \quad (4.75)$$

These results are summarized in Fig. 14, where we plot the grand potentials for the different phases.

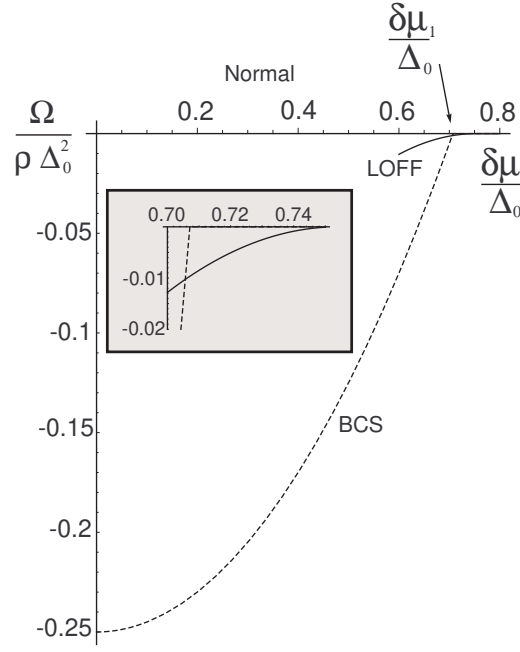


FIG. 14 The figure shows the differences between the grand potential for the BCS and the normal state and that between the LOFF and the normal state plotted vs. Ω . The grand potentials are normalized to Δ_0^2 . The inset shows the intersection of the two curves close to $\Omega = 0.7$. The solid lines correspond to the LOFF case, whereas the dotted ones to the BCS case.

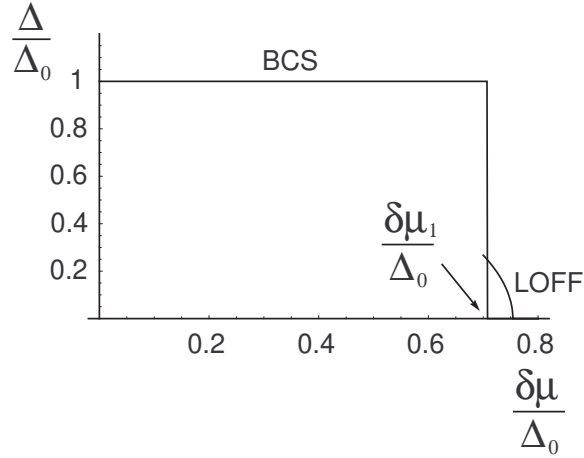


FIG. 15 The figure shows the condensates of the BCS and LOFF phases vs. Ω .

Since the interval $(\Omega_1; \Omega_2)$ is rather narrow there is practically no difference between the values of Ω corresponding to the BCS-normal transition ($\Omega_1 = \Omega_0 = \frac{1}{2}$) and the value corresponding to the BCS-LOFF transition. This can be visualized easily from Figs. 14 and 15. The figures have been obtained by using the previous equations in the Ginzburg-Landau expansion around Ω_2 , but they are a very good approximation of the curves obtained numerically (Alford et al., 2000; Takada and Izuyama, 1969)

All the discussion here has been done in the weak coupling limit. For a more correct treatment see (Alford et al., 2000) where the results from the numerical integration of the gap equation are given. In particular we want to stress

the results on the size of the window obtained by these authors. If μ_1 and μ_2 are evaluated for a general coupling and at the same time one takes into account corrections from the chemical potential in the measure of integration, the windows get smaller and smaller for increasing BCS gap Δ_0 . The corrections in the chemical potential arise from the momentum integration, which is made on a shell of height 2 but with an integration measure given by $p^2 dp$, rather than $p_F^2 dp$ as usually done in the treatment of the BCS gap in the weak coupling limit. The results are illustrated in Fig. 16, where the behavior of the critical points vs. the BCS gap are shown. The curves are plotted for a range of values of the cutoff ranging from 0.8 to 1.6 GeV. The cutoff dependence is not very strong, in particular for μ_2 , moreover the window closes for Δ_0 between 80 to 100 MeV, according to the chosen value of Λ .

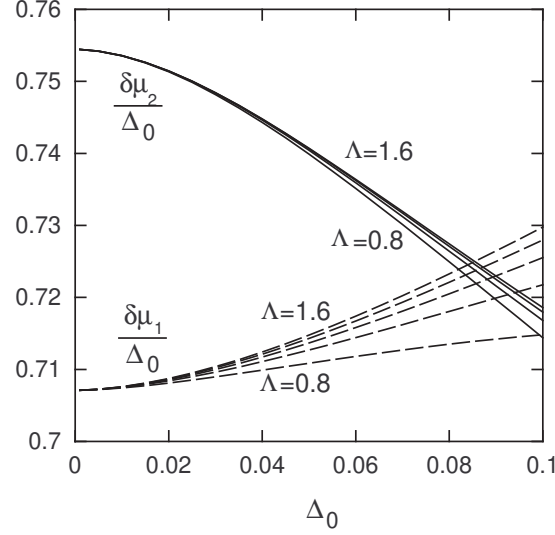


FIG. 16 The figure shows the critical points μ_1 (solid lines) and μ_2 (dashed lines) in Δ_0 units vs. Δ_0 , for cutoff values $\Lambda = 0.8$ to 1.6 GeV and for $\mu = 0.4$ GeV. This figure is taken from (Alford et al., 2001b).

In (Alford et al., 2000) the presence of a vector condensate in the QCD LOFF phase is also discussed. The reason why this condensate can be formed in QCD but not in condensed matter is the following. Both in the BCS and in the LOFF phases the coupling is between fermions of the same helicity. In the BCS phase the fermions have also opposite momentum giving rise to a $J = 0$ pair. On the other hand in the LOFF phase momenta are not exactly aligned, therefore a small component of $J = 1$ condensate may arise. A spin 1 state is symmetric in the spin indices and therefore Fermi statistics forbids it for electron pairing. On the other hand in QCD with two flavors one can form a state antisymmetric in color and symmetric in flavor, and the Pauli principle is satisfied. Therefore the structure of the vector condensate is (Alford et al., 2000)

$$h(1)_{ij} = \frac{1}{3} \epsilon_{ijk} \epsilon_{lmn} \sigma_{ij} \sigma_{kl} = \frac{2}{3} \frac{q_i^j}{q_j} v e^{2iq \cdot r} \quad (4.76)$$

The ratio $v = s$ is practically constant within the LOFF window varying between 0.121 at μ_1 and 0.133 at μ_2 . However this condensate does not contribute to the grand potential in the present case (Alford et al., 2000); therefore it does not change the original LOFF results. The situation is different if, instead of using the NJL interaction (4.55), use is made of the following interaction

$$L_I = \frac{3}{8} G_E (\bar{\psi} \gamma_0 \psi) (\bar{\psi} \gamma_0 \psi) + G_M (\bar{\psi} \gamma_i \psi) (\bar{\psi} \gamma_i \psi) \quad (4.77)$$

This expression is not Lorentz invariant, but since we are trying to model QCD at finite density, there is no reason to use a Lorentz invariant effective action. For instance, at high density the electric gluons are expected to be screened, whereas the magnetic ones are Landau damped. In particular, it has been shown by (Son, 1999) that at high density the magnetic gluon exchange is dominating in the pairing mechanism, which can be simulated assuming $G_E \ll G_M$.

For the following discussion it is convenient to introduce the quantities

$$G_A = \frac{1}{4} (G_E + 3G_M); \quad G_B = \frac{1}{4} (G_E - G_M) \quad (4.78)$$

For $G_E = G_M = G$, as discussed above one has

$$G_A = G; \quad G_B = 0: \quad (4.79)$$

At zero density we expect $G_B = 0$, whereas at high density we expect $G_E = 0$ or $G_B = G_A = 1/3$. Therefore the relevant physical region for $G_B = G_A$ should be given by

$$\frac{1}{3} \leq \frac{G_B}{G_A} \leq 0: \quad (4.80)$$

The gap parameters are now defined by

$$\Delta = G_A \Delta_S; \quad \Delta_V = G_B \Delta_V: \quad (4.81)$$

Since the grand potential and the quasi-particle energy are determined by the gap, for the Lorentz invariant case, $G_B = 0$, there is no contribution from the vector condensate. For $G_B \neq 0$, one has to solve two coupled gap equations (Alford et al., 2000). The most interesting result found by these authors is about the LOFF window which is modified by the presence of the $J = 1$ gap. The result is shown in Fig. 17.

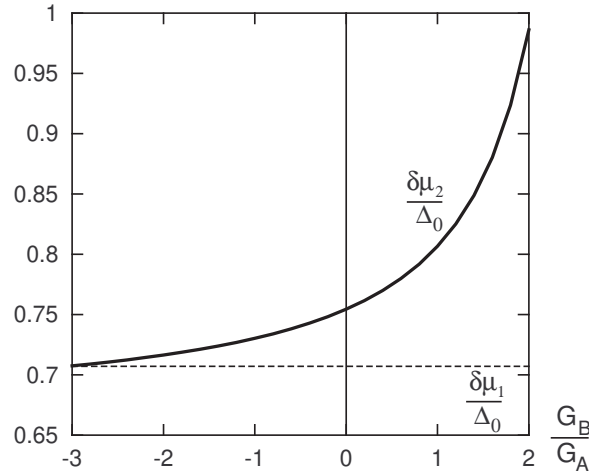


FIG. 17 The figure shows the variation of the criticalpoints $\mu_1 = 0$ (dotted line) and $\mu_2 = 0$ (solid line) with $G_B = G_A$. This figure is taken from (Alford et al., 2001b).

The LOFF window closes at $G_B = G_A = 1/3$ and increases with increasing $G_B = G_A$. For $G_B = G_A$ inside the physical region (see Eq. (4.80)) the maximal opening is for $G_B = 0$. However, inside the physical region the variation of the window is rather small. Since μ_1 is essentially defined by the BCS-normal state transition, it is given by $\mu_1 = \mu_2$ independently of the vector condensate. However, the second order criticalpoint μ_2 is rather sensitive to $G_B = G_A$, the reason being that, for $G_A = 0$, the $J = 1$ channel is attractive for $G_B > 0$ and repulsive for $G_B < 0$. Therefore the stability of the LOFF state is reinforced by the vector condensate in the region $G_B > 0$.

Let us close this Section considering a different pairing discussed in (Deryagin et al., 1992; Park et al., 2000; Rapp et al., 2001; Shuster and Son, 2000). It is a quark-hole pairing with non-zero momentum at large baryon density. This produces a hqqi condensate varying in space with a wave number $2\vec{q}$, to be contrasted with $2\vec{q} \rightarrow 2\vec{q} \rightarrow 2\vec{q}$. This state is energetically favorable only for very large values of the number of colors (Deryagin et al., 1992). (Park et al., 2000; Shuster and Son, 2000) found that N_c should be larger than about 1000.

E. One-gluon exchange approximation

The previous results have been obtained in the case of a NJL interaction. In (Leibovich et al., 2001) the case of the one-gluon exchange interaction has been studied. Of course this would be a realistic case only at very high densities (Rajagopal and Shuster, 2000) where, presumably, the CFL phase dominates over the LOFF phase. However the

study of different interactions allows to understand the model dependence of the LOFF window. In (Leibovich et al., 2001) the standard QCD vertex is used in conjunction with the following propagator for the gluon

$$D = \frac{P^T}{p^2 - G(p)} + \frac{P^L}{p^2 - F(p)}; \quad (4.82)$$

where

$$P_{ij}^T = \delta_{ij} \frac{p_i p_j}{p^2}; \quad P_{00}^T = P_{01}^T = 0; \\ P^L = \frac{p^0 p^0}{p^2} - P^T; \quad (4.83)$$

Here

$$G(p) = -m^2 \frac{p^0}{p^2} \quad (4.84)$$

describes the Landau damping and

$$F(p) = m^2; \quad (4.85)$$

where m^2 is the Meissner mass evaluated for 2 flavors

$$m^2 = g^2 \frac{2}{2}: \quad (4.86)$$

The expressions for $F(p)$ and $G(p)$ are obtained in the hard-loop approximation (Le Bellac, 1996) and evaluated here for $p_0 = p_j$ (we recall that μ is the average chemical potential). Solving the gap equation it is found that the LOFF window is enlarged of about a factor 10 at average chemical potential $\mu = 400$ MeV. In fact, whereas μ_1 , as already noticed, is essentially fixed by the BCS-normal state transition at the value $\mu_1 = \mu_0 = \frac{p^0}{2}$, μ_2 increases in a dramatic way. At $\mu = 400$ MeV the authors of Ref. (Leibovich et al., 2001) find

$$\mu_2 = 1.24 \mu_0) \quad \mu_2 - \mu_1 = 0.55 \mu_0; \quad (4.87)$$

to be compared with the NJL case, where

$$\mu_2 = 0.754 \mu_0) \quad \mu_2 - \mu_1 = 0.05 \mu_0: \quad (4.88)$$

At $\mu = 10^3$ MeV the window is about 60 times larger than the window for the point-like case. In general, by increasing μ , μ_2 increases as well. The interpretation of these results, according to (Leibovich et al., 2001), goes as follows. For weak coupling the $q-q$ scattering via one-gluon exchange is mostly in the forward direction. This implies that, after the scattering has taken place, quarks remain close at the angular position possessed before the scattering, meaning that the theory is essentially 1+1 dimensional. In fact, in this case the only possible value for $2j_j$ is $d_{\text{eff}} = 2$. This is not exactly the case in 3+1 dimensions. In fact, as it can be seen from Fig. 4, $2j_j$ is generally bigger than 2. Furthermore, it is known from the 1+1 dimensional case (Buzdin and Polonski, 1987; Buzdin and Tugushev, 1983) that in the weak coupling limit $\mu_2 = \mu_0 + 1$. Both these features have been found in (Leibovich et al., 2001).

A similar analysis has been done in Ref. (Giannakis et al., 2002). The results found here are somewhat different from the ones discussed before. In particular it is found that at weak coupling:

$$\mu_2 = 0.968 \mu_0) \quad \mu_2 - \mu_1 = 0.26 \mu_0; \quad (4.89)$$

with an enhancement of the window of a modest factor 5 with respect to the point-like interaction. However, the evaluation made in this paper consists in an expansion around the tricritical point (called by these authors μ_{on}) implying, in particular, an expansion in j_j . In order to compare the results of these two groups one should extrapolate the results of Ref. (Giannakis et al., 2002) to zero temperature. It is not evident, at least to us, that this can be safely made. Of course, also the physical interpretation is different. According to (Giannakis et al., 2002) in 3+1 dimensions, increasing μ implies a reduction of the phase space and therefore a smaller gap and a smaller μ_2 . This reduction effect, according to these authors, overcomes the enhancement due to the 1+1 dimensional effect discussed before.

In our opinion the case of the one-gluon exchange in the LOFF phase deserves further studies. In fact a sizeable increase of the LOFF window would make the LOFF state very interesting as far as the applications to compact stellar objects are concerned.

F. Mass effects

In Ref. (Kundu and Rajagopal, 2002) the combined effect of having two quarks with different chemical potentials and one of the two quarks being massive has been studied. In the free case the Fermi momenta are given by (assuming that the pair contains an up and a strange quark)

$$p_F^u = \frac{1}{2} \sqrt{(\mu_1 + \mu_2)^2 - M_s^2}; \quad p_F^s = \frac{1}{2} \sqrt{(\mu_1 - \mu_2)^2 - M_s^2} \quad (4.90)$$

Assuming both $\mu_1 = \mu_2 = \mu$ and $m_s = 0$ to be much smaller than one, one finds

$$p_F^u = p_F^s = \frac{1}{2} \sqrt{(\mu_1 + \mu_2)^2 - M_s^2} \quad (4.91)$$

The effect of $M_s \neq 0$ amounts to something more than the simple shift $\mu \rightarrow \mu - \frac{M_s^2}{4}$. In fact, let us recall that at $M_s = 0$ the BCS condensate is not changed by μ as long as $\mu < \mu_1$. However Δ_0 decreases with M_s , see the results in (Kundu and Rajagopal, 2002) and (Casalbuoni et al, 2002a). Furthermore, for $M_s^2 = 2\mu$ the decreasing is practically linear. This produces corrections in the grand potential of order $\frac{1}{2} \Delta_0(0) M_s^2$. For small values of $M_s^2 = 2\mu$ we have BCS pairing, whereas for large values there is no pairing and the system is in the normal phase. Therefore the BCS-normal transition is M_s dependent and occurs for μ approximately given by

$$\frac{M_s^2}{4} = \frac{\mu_0(M_s)}{2} \quad (4.92)$$

It can be noted that differently from the case $M_s = 0$ this condition is not symmetric for μ_1 and the LOFF phase can exist in two different windows in μ , above ($\mu > \mu_1$) and below ($\mu < \mu_1$) the BCS region; in any case, for $M_s = 0$ one gets back the Clogston-Chandrasekhar limit. In order to discuss the size of the window the correct variable is

$$\frac{\mu_2(M_s) - \mu_1(M_s)}{\mu_0(M_s)} \quad (4.93)$$

At weak coupling (small $\mu_0(0)$) it is found that the window is essentially the same as for the case $M_s = 0$. Otherwise the window generally increases with M_s as shown in Fig. 18 for various values of M_s . We have plotted both the cases $\mu > 0$ (left panel) and $\mu < 0$. This shows that the LOFF phase is rather robust for $M_s \neq 0$.

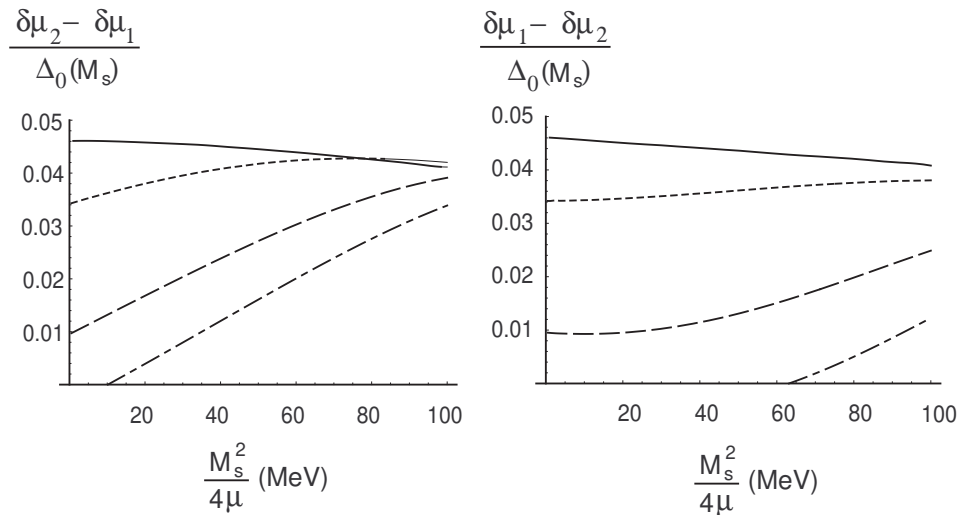


FIG. 18 In the left (right) panel the width of the LOFF window above (below) the BCS region is reported. The four curves correspond to the following values of $\mu_0(0)$ (MeV): 10 (solid line), 40 (dotted line), 80 (dashed line), 100 (dash-dotted line). This figure is taken from (Kundu and Rajagopal, 2002).

V. PHONON AND GLUON EFFECTIVE LAGRANGIANS

Translational and rotational invariance are spontaneously broken within a LOFF phase. The energy gap is not uniform and actually is expected to vary according to some crystalline structure, as result of the analysis developed in the previous Sections. The crystal defined by the space modulation of the gap can fluctuate and its local deformations define phonon fields⁽ⁱ⁾ that are the Nambu-Goldstone bosons associated to the breaking of the translational symmetry. The number of the phonon fields is equal to the number of the broken generators of the translation group. The existence of long wavelength oscillations with phonon dispersion law was already noted in (Fulde and Ferrell, 1964). More recently an effective lagrangian for phonons in a QCD medium has been developed in (Casalbuoni et al., 2002b, 2001a, 2002c,e) and we wish to review it in this Section, dominantly dedicated to the QCD LOFF phase. For color superconductivity only the $T \rightarrow 0$ case is physically interesting and we shall consider only this limit. However the theory developed in this Section could be extended to $T \neq 0$ as well as to other physical cases (solid state, nuclear physics).

Being long wavelength oscillations of the crystalline LOFF structure, the phonons exist only if the quarks of the Cooper pair are in the pairing region. This is a portion of the phase space around the Fermi surface and is formed by a few annular rings, that are likely to be contiguous, according to the discussion in (Bowers and Rajagopal, 2002), see also the discussion in Section III C. The effective theory for the phonon fields⁽ⁱ⁾ has to display this behavior and therefore the phonon-quark coupling must vanish outside the pairing region. The mathematical formalization of this behavior is rather involved and some approximation is needed. (Casalbuoni et al., 2002b,c) write the phonon-quark interaction using the HDET discussed in Section IV A. They introduce effective velocity dependent fermion fields and the lagrangian as a sum of terms, each characterized by its own Fermi velocity v . Also the quark-phonon coupling constant becomes velocity-dependent and is proportional to

$$\mathcal{L}_{eff} / \sum_{\mathbf{k}} \sum_{\mathbf{v}} \frac{1}{R} \hat{n}_{\mathbf{v}} [\mathbf{v} \cdot \hat{\mathbf{n}}_{\mathbf{k}}] : \quad (5.1)$$

Here $\hat{\mathbf{n}}_{\mathbf{k}}$ are the vectors defining the LOFF crystal, R is a parameter and $\hat{n}_{\mathbf{v}} [\mathbf{v} \cdot \hat{\mathbf{n}}_{\mathbf{k}}]$ is a function that vanishes outside the pairing region. More precisely, it reaches its maximum when the pairing quarks are on the Fermi surface and decreases when they leave it. By this approximation an evaluation of the phonon effective lagrangian is possible. In Subsection V A we consider the HDET for the inhomogeneous LOFF state and write the quark-phonon lagrangian. Below, we discuss two crystalline structures. First we consider the Fulde-Ferrell one plane wave, which is the benchmark case for the whole LOFF theory; next we shall examine the cubic structure, already studied in Subsection III C.4, because this seems the most favored crystalline structure according to (Bowers and Rajagopal, 2002). On the basis of symmetry arguments one can write down the effective phonon lagrangians for the two cases. This is done in Subsections V B and V D, whereas in Subsections V C and V E we show how the parameters of the effective lagrangian can be computed by the HDET. Let us mention here that the parameter R appearing in (5.1) should be fixed by a comparison of the gap equation computed in the HDET and the approach discussed in Subsection II C for the FF state and in Section III for generic structures. This comparison has not yet been done and therefore, in the discussion below, we leave R as a parameter, even though, in the case of a cubic structure, the requirement that the annular rings are contiguous can be used to fix its value. We conclude this Section with a discussion in V F on the modifications induced by the LOFF pairing of quarks on the gluon lagrangian.

A. Effective lagrangian for the LOFF phase

Let us begin by writing the gap term in the lagrangian in presence an inhomogeneous condensate. As in Section II C we write the following formula for the LOFF condensate

$$\langle \bar{\psi} \psi \rangle = \sum_{m=1}^P e^{2iq_m \cdot \mathbf{r}} \quad (5.2)$$

We will consider only two cases below :

- a) One plane wave: $P = 1$
- b) Cubic structure: $P = 8$.

In the former case we shall take into account the possibility of having both a $J = 0$ and a $J = 1$ condensate as discussed above. In the case of the cubic structure we will consider only spin zero condensate; we will take $\mathbf{m} = 0$,

real, $q_m = \hat{n}_m q$ with \hat{n}_m the eight unit vectors defined in Eq. (3.39). To describe the quark condensate in the case of the single plane wave, we consider the lagrangian term :

$$L = L^{(s)} + L^{(v)} = \frac{e^{2iq \cdot r}}{2} \sum_{i,j} \bar{\psi}_i(x) C^{(s)}_{ij} \psi_j + \hat{n}^{(v)}_{ij} \frac{1}{2} \bar{\psi}_i(x) (L + R) \psi_j + h.c.; \quad (5.3)$$

which includes both the scalar and the vector condensate.

We introduce velocity-dependent fields as in Eq. (4.13), with factors $\exp(i \mathbf{v}_i \cdot \mathbf{x})$, and we take into account only the positive energy part that we write as $\psi_{i,j}$ for a quark with flavor i and color j ; we keep track of the velocities of the two quarks that are not opposite in the LOFF phase. We have:

$$L = \frac{1}{2} \sum_{\mathbf{v}_i, \mathbf{v}_j} \exp(i \mathbf{r} \cdot (\mathbf{v}_i + \mathbf{v}_j)) f(\mathbf{v}_i, \mathbf{v}_j; q) \sum_{i,j} \bar{\psi}_{i,j}(\mathbf{x}) C^{(s)}_{ij} \psi_j + \hat{n}^{(v)}_{ij} \frac{1}{2} \bar{\psi}_{i,j}(\mathbf{x}) (L + R) \psi_j + h.c.; \quad (5.4)$$

where

$$f(\mathbf{v}_i, \mathbf{v}_j; q) = 2q \cdot (\mathbf{v}_i + \mathbf{v}_j); \quad (5.5)$$

We also define

$$= \frac{1 + 2}{2}; \quad = \frac{1 - 2}{2}; \quad (5.6)$$

Since $q = 0$ ($\neq 0$), the condition

$$\mathbf{p}_1 + \mathbf{p}_2 = 2\mathbf{q} \quad (5.7)$$

gives in the $\rightarrow 1$ limit

$$\mathbf{v}_1 + \mathbf{v}_2 = 0 \quad (5.8)$$

Taking into account that $P_+(-\mathbf{v}) C^k P_+(\mathbf{v}) = v^k P_+(-\mathbf{v}) C P_+(\mathbf{v})$ we can rewrite (5.4) as follows

$$L = \frac{1}{2} \sum_{\mathbf{v}_i, \mathbf{v}_j} \exp(i \mathbf{r} \cdot (\mathbf{v}_i + \mathbf{v}_j)) f(\mathbf{v}_i, \mathbf{v}_j; q) \sum_{i,j} \bar{\psi}_{i,j}(\mathbf{x}) C^{(s)}_{ij} \psi_j + \hat{n}^{(v)}_{ij} \frac{1}{2} \bar{\psi}_{i,j}(\mathbf{x}) (L + R) \psi_j + h.c.; \quad (5.9)$$

These equations can be easily generalized to the case of the face centered cube. We shall discuss this generalization below.

B. One plane wave structure

Let us rewrite (5.9) as follows:

$$L = \frac{1}{2} e^{2i\mathbf{r} \cdot \mathbf{q}} \sum_{\mathbf{v}_i, \mathbf{v}_j} e^{i(\mathbf{v}_i + \mathbf{v}_j) \cdot \mathbf{r}} \sum_{i,j} \bar{\psi}_{i,j}(\mathbf{x}) C^{(s)}_{ij} \psi_j + \hat{n}^{(v)}_{ij} \frac{1}{2} \bar{\psi}_{i,j}(\mathbf{x}) (L + R) \psi_j + h.c.; \quad (5.10)$$

There are two sources of space-time symmetry breaking in (5.10), one arising from the exponential term $\exp(2i\mathbf{r} \cdot \mathbf{q})$, which breaks both translation and rotation invariance, and another one in the vector condensate breaking rotation invariance. On the other hand the factor $\exp(i \mathbf{v}_i \cdot \mathbf{x} - i \mathbf{v}_j \cdot \mathbf{x})$ breaks no space symmetry, since it arises from a field redefinition in a lagrangian which was originally invariant. For definiteness' sake let us take the z-axis pointing along the direction of \mathbf{q} . As a consequence of the breaking of translational invariance along the z-axis, Goldstone's theorem predicts the existence of one scalar massless particle, the Nambu-Goldstone Boson (NGB) associated to the spontaneous symmetry breaking (SSB). The symmetry breaking associated to the vector condensate is not independent of the SSB arising from the exponential term $\exp(2i\mathbf{r} \cdot \mathbf{q})$, because the direction of \mathbf{q} coincides with the direction \hat{n} of the vector condensate. For this reason, while there are in general three phonons associated to the breaking of space symmetries here one NGB is sufficient. The argument is sketched in Fig. 19 and follows from the fact that rotations and translations are not independent transformations, because the result of a translation plus a rotation is locally equivalent to a pure translation.

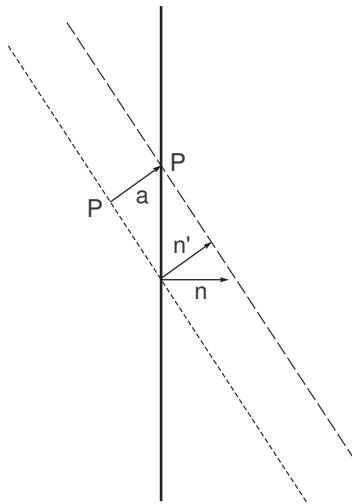


FIG. 19 In the point P the effect of the rotation $n \rightarrow n'$ and the effect of the translation $r \rightarrow r + a$ tend to compensate each other.

The lagrangian (5.10) induces a lattice structure given by parallel planes perpendicular to \hat{n} :

$$\hat{n} \cdot r = \frac{k}{q} \quad (k = 0; 1; 2; \dots) : \quad (5.11)$$

We can give the following physical picture of the lattice structure of the LOFF phase: Due to the interaction with the medium, the Majorana masses of the red and green quarks oscillate in the direction \hat{n} , reaching on subsequent planes maxima and minima. The NGB is a long wavelength small amplitude variation of the condensate $\langle \bar{\psi} \psi \rangle$; formally it is described by the substitution

$$\langle \bar{\psi} \psi \rangle = e^{2iq\hat{n} \cdot r} \rightarrow e^{i\phi} ; \quad (5.12)$$

with

$$\frac{\delta \mathcal{L}}{\delta \phi} = 2q(\hat{n} + \mathbf{n}) \cdot (\mathbf{r} + \mathbf{r}') \frac{\delta \mathcal{L}}{\delta \mathbf{r}} + 2q\hat{n} \cdot \mathbf{r} \quad (5.13)$$

and $\hbar = 0$. We assume

$$\hat{n} + \mathbf{n} = 0 ; \quad (5.14)$$

$$\hbar \cdot \mathbf{n} = 0 : \quad (5.15)$$

Let us introduce the auxiliary functions R and T ,

$$R = \hat{n} + \mathbf{n} ; \quad T = 2qR \cdot \mathbf{r} : \quad (5.16)$$

The lattice fluctuation describes, in second quantization, the phonon field. Since it must be small, T and R are not independent fields and T must depend functionally on R , i.e. $T = T[R]$, which means

$$\frac{\delta \mathcal{L}}{\delta \mathbf{r}} = 2qR \cdot \mathbf{r} + T[R] - G[R; \mathbf{r}] : \quad (5.17)$$

The solution of this functional relation has the form

$$R = h[\mathbf{r}] ; \quad (5.18)$$

where \mathbf{h} is a vector built out of the scalar function ϕ . By this function one can only³ form the vector \mathbf{r} ; therefore we get

$$\mathbf{R} = \frac{\mathbf{r}}{r} \phi; \quad (5.19)$$

which satisfies (5.14). In terms of the phonon field the vector field \mathbf{R} is given (up to the second order terms in ϕ) by the expression

$$\mathbf{R} = \hat{\mathbf{n}} + \frac{1}{2fq} [\mathbf{r} - \hat{\mathbf{n}}(\hat{\mathbf{n}} \cdot \mathbf{r})] + \frac{\hat{\mathbf{n}}}{8f^2q^2} 3(\hat{\mathbf{n}} \cdot \mathbf{r}^2) \mathbf{r} - \frac{\mathbf{r}}{4f^2q^2} (\hat{\mathbf{n}} \cdot \mathbf{r}): \quad (5.20)$$

We stress that the only dynamical field is ϕ , \mathbf{h} is an auxiliary field with a non vanishing vacuum expectation value $\mathbf{h}|_0 = 2q \mathbf{r}$; as to $\hat{\mathbf{n}}, \mathbf{R}$ and \mathbf{r} , they can all be expressed in terms of ϕ . In conclusion, the interaction term with the NGB field is contained in

$$L_{\text{int}} = \frac{1}{2} e^{i\phi} \sum_{\mathbf{v}_i, \mathbf{v}_j} e^{i(\mathbf{v}_i + \mathbf{v}_j) \cdot \mathbf{r}} \sum_{i,j} \mathbf{v}_j^T C_{\mathbf{v}_j, i}^{(s)}(\mathbf{x}) C_{\mathbf{v}_j, j}^{(v)}(\mathbf{x}) \mathbf{R}^{(v)} \frac{1}{i_j} \mathbf{v}_j; j(\mathbf{x}) (\mathbf{L} \cdot \mathbf{R}) + \text{h.c.}; \quad (5.21)$$

where the fields \mathbf{r} and \mathbf{R} have been introduced in such a way to reproduce Eq. (5.10) in the ground state. At the first order in the fields one gets the following three-linear coupling:

$$L = \frac{i}{2f} \sum_{\mathbf{v}_i, \mathbf{v}_j} e^{i\mathbf{r} \cdot \mathbf{f}(\mathbf{v}_i, \mathbf{v}_j; q)} \sum_{i,j} \mathbf{v}_j^T C_{\mathbf{v}_j, i}^{(s)}(\mathbf{x}) \mathbf{R}^{(v)} \frac{1}{i_j} \mathbf{v}_j; j(\mathbf{x}) C_{\mathbf{v}_j, j}^{(v)}(\mathbf{x}) (\mathbf{L} \cdot \mathbf{R}) + \text{h.c.}; \quad (5.22)$$

We also write down the quadrilinear coupling:

$$L = \frac{2}{4f^2} \sum_{\mathbf{v}_i, \mathbf{v}_j} e^{i\mathbf{r} \cdot \mathbf{f}(\mathbf{v}_i, \mathbf{v}_j; q)} \sum_{i,j} \mathbf{v}_j^T C_{\mathbf{v}_j, i}^{(s)}(\mathbf{x}) \mathbf{R}^{(v)} \frac{1}{i_j} \mathbf{v}_j; j(\mathbf{x}) C_{\mathbf{v}_j, j}^{(v)}(\mathbf{x}) (\mathbf{L} \cdot \mathbf{R}) + \text{h.c.}; \quad (5.23)$$

Through a bosonization procedure one can derive an effective lagrangian for the NGB field. This will be done below. For the moment we derive the general properties of the phonon effective lagrangian. It must contain only derivative terms. Polynomial terms are indeed forbidden by translation invariance, since ϕ is not an invariant field. In order to write the kinetic terms it is better to use the auxiliary field \mathbf{h} which behaves as a scalar under both rotations and translation. To avoid the presence of polynomial terms in the phonon lagrangian one has to exclude polynomial terms in the auxiliary field \mathbf{h} as well; therefore the lagrangian should be constructed only by derivative terms. The most general invariant lagrangian will contain a tower of space-derivative terms (Casalbuoni et al., 2001a). In fact, since $\mathbf{h}|_0 = 2q \mathbf{r}$ is not a small quantity, we cannot limit the expansion in the spatial derivatives of ϕ to any finite order. Therefore we write

$$L(\phi; \partial) = \frac{f^2}{2} \sum_{n=1}^{\infty} \sum_{\mathbf{X}} c_n (\mathbf{X} \cdot \partial)^n \phi^{\mathbf{X}}; \quad (5.24)$$

In this lagrangian ϕ must be thought as a function of the phonon field ϕ .

³ In principle there is a second vector, \mathbf{r} , on which \mathbf{R} could depend linearly, but this possibility is excluded because \mathbf{R} is a vector field transforming under translations as $\mathbf{R}(\mathbf{r}) \rightarrow \mathbf{R}^0(\mathbf{r}^0) = \mathbf{R}(\mathbf{r})$

Since

$$\dot{x}_k \dot{x}_k = 4q^2 + \frac{4q}{f} \dot{\eta} \quad r + \frac{1}{f^2} \dot{x}_k \dot{x}_k; \quad (5.25)$$

with similar expression for higher powers. At the lowest order in the derivatives of the phonon field we get, neglecting a constant term:

$$L(\dot{x}; \partial) = \frac{1}{2} \hbar \omega_k^2 \dot{x}_k \dot{x}_k + \frac{1}{2} \omega_k^2 4q f r_k + \dot{x}_k \dot{x}_k^i; \quad (5.26)$$

where $r_k = \dot{\eta} \cdot r$, and $\omega_k^2 v^2$ are constants.

C. Parameters of the phonon effective lagrangian: one plane wave

In order to derive the parameters of the phonon lagrangian (5.26) it is useful to make an approximation. We assume that $\lim_{\hbar \rightarrow 0} \omega_k = 0$. Clearly we cannot take simply the $\hbar \rightarrow 0$ limit in the exponential term $\exp(i \int \dot{x}_k v_j; q_k) g$ in Eq. (5.9); therefore we consider a smeared amplitude as follows:

$$\lim_{\hbar \rightarrow 0} \exp(i \int \dot{x}_k v_j; q_k) g = \lim_{\hbar \rightarrow 0} \int_{-1}^1 dr^0 \exp(i \int \dot{x}_k v_j; q_k) g(r; r^0); \quad (5.27)$$

We assume the following smearing function:

$$g(r; r^0) = g(r - r^0) = \frac{Y^3 \sin \frac{q(r_k - r_k^0)}{R}}{(r_k - r_k^0)^3} \quad (5.28)$$

and we evaluate (5.27) in the $\hbar \rightarrow 0$ limit by taking q along the z axis, and using the following identity:

$$\int_{-1}^1 dr^0 \exp(i \int \dot{x}_k v_j; q_k) g(r - r^0) = \exp(i \int \dot{x}_k v_j; q_k) \frac{f}{2q}; \quad (5.29)$$

where

$$f_R(x) = \begin{cases} \frac{R}{2} & \text{for } |x| < \frac{R}{2} \\ 0 & \text{elsewhere.} \end{cases} \quad (5.30)$$

For the components x and y of f we get

$$j(v_1 + v_2)_{x,y} j < \frac{q}{R}; \quad (5.31)$$

i.e. approximately (for $\hbar \rightarrow 0$)

$$j(v_1 + v_2)_{x,y} j < \frac{q}{R}; \quad (5.32)$$

From this, in the high density limit, it follows

$$v_1 = v_2 + O(\hbar): \quad (5.33)$$

We used already this result in Eq. (4.17), in connection with the Riemann-Lebesgue lemma and in Eq. (5.8). A more accurate result is as follows. If θ_1 and θ_2 are the angles of v_1 and v_2 with respect to the z -axis one gets

$$\theta_1 = \theta_2 + \frac{2}{\hbar} \tan \theta_2; \quad (5.34)$$

For the z component we get

$$f_z = 2qh(\cos \theta_2); \quad (5.35)$$

where

$$h(x) = 1 + \frac{x^2}{2q} \left(1 + \frac{4}{x^2} \right)^{\frac{s}{2}}; \quad (5.36)$$

and, neglecting corrections of order $\frac{1}{q}$,

$$h(x) = 1 - \frac{\cos q}{x}; \quad \cos q = \frac{1}{q}; \quad (5.37)$$

Notice that $q = \theta = 2$ where θ is the angle depicted in Fig. 4, see also Eq. (2.117). The two factors $\frac{1}{q}$ arising from the x and y components are absorbed into a wave function renormalization of the quark fields, both in the kinetic and in the gap terms. As for the z component one remains with the factor

$$\frac{1}{R} e^{i2qhz} \frac{1}{R} [h(v \cdot \hat{n})] = \frac{1}{R} [h(v \cdot \hat{n})] \quad (5.38)$$

in the gap term, whereas for the kinetic term we get a factor of 1. We have assumed $\exp[i2qhz] = 1$ in Eq. (5.38) owing to the presence of the $\frac{1}{R}$ function, that, in the $R \rightarrow \infty$ limit, enhances the domain of integration where $h = 0$. We will discuss this approximation below.

Eq. (5.30) defines a region where $R \neq 0$, i.e. a domain where pairing between the two quarks can occur; it corresponds to the pairing region in the analysis of (Fukushima and Ferrell, 1964) and (Bowers et al., 2001), in contrast with the blocking region, where $R = 0$. The pairing region intersects the Fermi surface with a 'ring' whose size depends on the value of R . As we noticed above, $R = 1$ implies the vanishing of the pairing region and therefore one expects $R \rightarrow \infty$ at the second order phase transition (Casalbuoni et al., 2002b). The precise value of R should be fixed by the gap equation; since this calculation is still missing, for the purpose of this paper we leave R as a parameter.

In conclusion we can approximate Eq. (5.9) as follows

$$L = \frac{1}{2} \sum_v \frac{1}{R} [h(v \cdot \hat{n})] \sum_{i,j} T_{v,i}^{(s)}(x) C_{ij}^{(s)} v \cdot \hat{n} \frac{1}{ij} v_{ij}(x) (L \rightarrow R) + h.c.: \quad (5.39)$$

Using the same notations as in Section IV C we can write the effective lagrangian as follows:

$$L_0 + L_1 + L = \sum_{v,A,B=0}^X \sum_{A,B=0}^5 A_Y [i \text{Tr} [\Gamma_A^Y V_{AB} D_B]] + \sum_{A,B=0}^Y A_B [i \text{Tr} [\Gamma_A^Y V_{AB} D_B]] + (L \rightarrow R): \quad (5.40)$$

Here

$$A = \frac{1}{2} \left(C + \frac{A}{A} \right) \quad (5.41)$$

and

$$T_A = \frac{\tilde{A}}{2} \quad (A = 0; \dots; 5): \quad (5.42)$$

The matrix A_{AB} vanishes for A or $B = 4$ or 5 , while, for $A, B = 0; \dots; 3$, is given by

$$A_{AB} = \frac{(s)}{\text{eff}} A_{AB} v \cdot \hat{n} \frac{(v)}{\text{eff}} A_{AB}; \quad (5.43)$$

with

$$A_{AB} = \begin{pmatrix} 0 & 1 & 0 & 0 & 0 \\ 1 & 0 & 0 & 0 & 0 \\ 0 & 0 & 1 & 0 & 0 \\ 0 & 0 & 0 & 1 & 0 \\ 0 & 0 & 0 & 0 & 1 \end{pmatrix}; \quad A_{AB} = \begin{pmatrix} 0 & 0 & 0 & 1 \\ 0 & 0 & i & 0 \\ 0 & +i & 0 & 0 \\ +1 & 0 & 0 & 0 \end{pmatrix}; \quad (5.44)$$

and

$$\frac{(s)}{\text{eff}} = \frac{(s)}{R} [h(v \cdot \hat{n})]; \quad \frac{(v)}{\text{eff}} = \frac{(v)}{R} [h(v \cdot \hat{n})]: \quad (5.45)$$

In the present approximation the quark propagator is given by

$$D_{AB}(\gamma; \omega) = (2)^{4-4} (\gamma \omega) \times \begin{matrix} 0 & 1 \\ \begin{matrix} \text{B} \\ \text{C} \end{matrix} & \begin{matrix} \text{A} \\ \text{A} \end{matrix} \end{matrix} \begin{matrix} \frac{\gamma}{D_{CB}(\gamma)} & \frac{\gamma_{AC}}{D_{CB}(\gamma)} \\ \frac{\gamma_{AC}}{D_{CB}(\gamma)} & \frac{\gamma}{D_{CB}(\gamma)} \end{matrix} \begin{matrix} \text{C} \\ \text{A} \end{matrix}; \quad (5.46)$$

where

$$D_{CB}(\gamma) = \gamma \gamma \gamma \gamma \gamma_{CB}; \quad D_{CB}(\gamma) = \gamma \gamma \gamma \gamma \gamma_{CB}; \quad (5.47)$$

On the other hand the propagator for the elds ^{4,5} does not contain gap mass terms and is given by

$$D(\gamma; \omega) = (2)^{4-4} (\gamma \omega) \begin{matrix} 0 & 1 \\ \text{C} & \text{A} \end{matrix} \begin{matrix} \frac{\gamma}{D_{CB}(\gamma)} & \frac{\gamma_{AC}}{D_{CB}(\gamma)} \\ \frac{\gamma_{AC}}{D_{CB}(\gamma)} & \frac{\gamma}{D_{CB}(\gamma)} \end{matrix} \begin{matrix} \text{C} \\ \text{A} \end{matrix}; \quad (5.48)$$

For the other elds ^A, $A = 0; 3$, it is useful to go to a representation where γ and γ are diagonal. It is accomplished by performing a unitary transformation which transforms the basis ^A into the new basis \tilde{A} defined by

$$\tilde{A} = R_{AB} B; \quad (5.49)$$

with

$$R_{AB} = \frac{1}{2} \begin{matrix} 0 & 1 \\ \text{B} & \text{C} \end{matrix} \begin{matrix} 1 & 0 & 0 & 1 \\ 0 & 1 & i & 0 \\ 0 & +i & 1 & 0 \\ 1 & 0 & 0 & 1 \end{matrix} \begin{matrix} \text{C} \\ \text{C} \\ \text{A} \\ \text{A} \end{matrix}; \quad (5.50)$$

In the new basis we have

$$\begin{matrix} \gamma \\ \gamma \end{matrix} \begin{matrix} A \\ A \end{matrix} B = \begin{matrix} A \\ \tilde{A} \end{matrix} \begin{matrix} A \\ A \end{matrix} B; \quad (5.51)$$

where

$$0 = 2 = \sim 2 = \sim 3 = \left(\frac{(s)}{\text{eff}} \gamma \hat{n} \frac{(v)}{\text{eff}} \right)^2; \quad 1 = 3 = \sim 0 = \sim 1 = \left(\frac{(s)}{\text{eff}} + \gamma \hat{n} \frac{(v)}{\text{eff}} \right)^2; \quad (5.52)$$

For further reference we also define

$$c = \left(\frac{(s)}{\text{eff}} \gamma \hat{n} \frac{(v)}{\text{eff}}; \frac{(s)}{\text{eff}} + \gamma \hat{n} \frac{(v)}{\text{eff}}; \frac{(s)}{\text{eff}} \gamma \hat{n} \frac{(v)}{\text{eff}}; \frac{(s)}{\text{eff}} + \gamma \hat{n} \frac{(v)}{\text{eff}} \right); \quad (5.53)$$

In the basis \sim the 3-point and 4-point couplings (5.22) and (5.23) are written as follows:

$$L_3 + L_4 = \sum_{v=A=0} X^3 \begin{matrix} \sim^A \gamma \\ \gamma \end{matrix} \begin{matrix} 0 & \gamma \\ \gamma & \gamma \end{matrix} \begin{matrix} \gamma \\ \gamma \end{matrix} \begin{matrix} \sim^B \\ \sim^B \end{matrix}; \quad (5.54)$$

Here

$$g_3 = \frac{i}{f} \frac{(s)}{\text{eff}} \begin{matrix} \text{A} \\ \text{A} \end{matrix} B + \hat{O}[\] \begin{matrix} \text{A} \\ \text{A} \end{matrix} B; \quad (5.55)$$

$$g_4 = \frac{2}{2f^2} \frac{(s)}{\text{eff}} \begin{matrix} \text{A} \\ \text{A} \end{matrix} B + \frac{i}{f} \hat{O}[\] + \hat{Q}[\] \begin{matrix} \text{A} \\ \text{A} \end{matrix} B; \quad (5.56)$$

with

$$\hat{O}[\] = \frac{1}{2fq} \gamma \left[\gamma \hat{n} (\hat{n} - r) \right] \frac{(v)}{\text{eff}}; \quad (5.57)$$



FIG. 20 Self-energy (a) and tadpole (b) diagrams.

$$\hat{Q}[\eta] = \frac{v_{eff}^{(v)}}{4f^2 q^2} \frac{v_{eff}}{2} 3(\eta^2 - r^2) \eta^2 (v_{eff} - r \eta(r)); \quad (5.57)$$

Terms in g_3 and g_4 that are proportional to η_{AB} arise from the expansion of $\exp i = f$ alone, whereas terms proportional to η_{AB} get also contribution from the expansion of R in the vector condensate. The effective action for the NGB is obtained at the lowest order by the diagrams in Fig. 20.

The result of the calculation of the two diagrams at the second order in the momentum expansion is as follows:

$$\begin{aligned} (p)_{se} &= \frac{i^2}{16^3 f^2} \frac{X^3 Z}{v_{c=0}} d^2 \frac{h}{D_C^2(\gamma)} \frac{4^2 c V}{D_C^2(\gamma)} \frac{V}{D_C^2(\gamma)} \frac{1}{q^2} \frac{v_{eff}^{(v)}}{q^2} \frac{1}{D_C^2(\gamma)} + \frac{1}{D_C^2(\gamma)} \frac{i}{q^2}; \\ (p)_{tad} &= \frac{i^2}{16^3 f^2} \frac{X^3 Z}{v_{c=0}} \frac{d^2}{D_C^2(\gamma)} \frac{h}{4^2 c} \frac{v_{eff}^{(v)}}{q^2} \frac{1}{q^2} \frac{1}{D_C^2(\gamma)} + \frac{1}{D_C^2(\gamma)} \frac{i}{q^2}; \end{aligned} \quad (5.58)$$

where

$$D_C(\gamma) = \gamma_0^2 - \gamma_k^2 - c + i; \quad (5.59)$$

c defined in (5.53) and

$$\eta(p) = p - v_{eff}(\eta)(v_{eff} - r\eta); \quad (5.60)$$

To perform the calculation we will take the limit $R \rightarrow 1$, when the R function becomes the Dirac delta. We handle the R functions according to the Fermi trick in the Golden Rule; in the numerator, in presence of a product of two R , we substitute one R function with the Dirac delta and for the other one we take

$$\frac{R[h(x)]}{R} \rightarrow \frac{R(0)}{R} \rightarrow 1; \quad (5.61)$$

A similar substitution is performed in the denominator. Moreover we use

$$\frac{d^2}{D_C^2(\gamma)} = \frac{i}{2^2 c}; \quad (5.62)$$

Therefore one has

$$\frac{R[h(v_{eff})]}{R} \frac{R[h(v_{eff})]}{R} \rightarrow \frac{R[h(v_{eff})]}{R} = \frac{1}{q v_{eff}} = k_R - v_{eff} \frac{1}{q}; \quad (5.63)$$

with

$$k_R = \frac{j}{qR}; \quad (5.64)$$

At the second order in the momentum expansion one gets

$$(\mathbf{p}) = \frac{2k_R}{2f^2} X \mathbf{v} \cdot \hat{\mathbf{n}} - \frac{h}{q} \mathbf{V} \cdot \nabla \mathbf{p} \cdot \mathbf{p} + {}^{(v)}(\mathbf{p})^i : \quad (5.65)$$

Here

$$\begin{aligned} {}^{(v)}(\mathbf{p}) = & \frac{{}^{(v)}\mathbf{p}^2}{q} {}^{(s)}(\mathbf{p})^2 - \frac{1}{2} \frac{X^3}{c=0} \operatorname{arcsinh} \frac{X}{j_c j} + \\ & + \frac{{}^{(v)}(\mathbf{p})^3}{2q^2} \frac{X^3}{c=0} \operatorname{arcsinh} \frac{X}{j_c j} \\ & - 2 \frac{{}^{(v)}\mathbf{p}^2}{q} \frac{1}{2} \log \frac{2}{(s)} {}^{(s)}(\mathbf{p})^2 + \mathbf{v} \cdot \hat{\mathbf{n}} {}^{(p)}(\mathbf{p}) ; \end{aligned} \quad (5.66)$$

where we have used the result (Alford et al., 2001b) ${}^{(v)}(\mathbf{p})^2$ and

$$(\mathbf{p}) = 3p_z^2 - p^2 \mathbf{v} \cdot \hat{\mathbf{n}} - 2p_z p_x \quad (5.67)$$

From

$$L_{\text{eff}}(\mathbf{p}) = \frac{2k_R}{2f^2} X \mathbf{v} \cdot \hat{\mathbf{n}} - \frac{h}{q} \mathbf{V} \cdot \nabla \mathbf{p} \cdot \mathbf{p} ; \quad (5.68)$$

after averaging over the Fermi velocities we obtain

$$L_{\text{eff}} = \frac{1}{2} h (\mathbf{k})^2 - v_z^2 (\partial_x \mathbf{k})^2 - v_y^2 (\partial_y \mathbf{k})^2 - v_k^2 (\partial_z \mathbf{k})^2 : \quad (5.69)$$

One obtains canonical normalization for the kinetic term provided

$$f^2 = \frac{2k_R}{4} : \quad (5.70)$$

On the other hand

$$v_z^2 = \frac{1}{2} \sin^2 \theta_q + 1 - 3 \cos^2 \theta_q - 1 - \log \frac{2}{0} - \frac{{}^{(v)}\mathbf{p}^2}{q} ; \quad v_k^2 = \cos^2 \theta_q : \quad (5.71)$$

In conclusion we get the anisotropic phonon dispersion law

$$E(\mathbf{p}) = \frac{q}{v_z^2 (p_x^2 + p_y^2) + v_k^2 p_z^2} : \quad (5.72)$$

Besides the anisotropy related to $v_z \neq v_k$, there is another source of anisotropy, due to the fact that p_z , the component of the momentum perpendicular to the planes (5.11), differently from p_x and p_y is a quasimomentum and not a real momentum. The difference can be better appreciated in coordinate space, where the effective lagrangian reads

$$L = \frac{1}{2} (\mathbf{k})^2 - v_z^2 (\partial_x \mathbf{k})^2 - v_y^2 (\partial_y \mathbf{k})^2 - v_k^2 \frac{q}{2} (\mathbf{k} - \mathbf{k}_1)^2 : \quad (5.73)$$

The effective action for the field ϕ , $S[\phi]$, is obtained by the lagrangian as follows

$$S = \int dtdx dy \frac{1}{q} \int_{k=-1}^{k=1} L(\mathbf{k}; \mathbf{x}; \mathbf{y}; \mathbf{k} = \mathbf{q}) : \quad (5.74)$$

In the action bilinear terms of the type $\phi_{\mathbf{k}} \phi_{\mathbf{k}^0}$ with $\mathbf{k} \in k^0$ may arise. In the continuum limit these terms correspond to derivatives with respect to the z direction. However, in the long distance limit $\mathbf{k} = \mathbf{q}$, the set of fields $\phi_{\mathbf{k}}(\mathbf{x}; \mathbf{y})$ becomes a function $\phi(\mathbf{x}; \mathbf{y}; z)$ and the last term in (5.73) can be approximated by $v_k^2 (\partial_z)^2$.

D . Cubic structure

The space dependence of the condensate corresponding to this lattice is as follows

$$\langle \bar{\psi} \psi \rangle(\mathbf{r}) = \frac{X^8}{R} \exp \left(2i \mathbf{q} \cdot \mathbf{r} \right) \quad (5.75)$$

where the eight unit vectors \hat{n}_k are given in (3.39) and

$$\mathbf{q} = \frac{\pi}{a} \mathbf{a} : \quad (5.76)$$

In Fig. 21 some of the symmetry axes of this cube are shown: they are denoted as C_4 (the three 4-fold axes), C_3 (the four 3-fold axes) and C_2 (the six 2-fold axes).

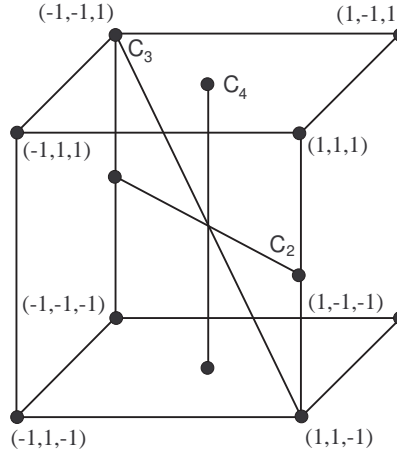


FIG .21 Symmetry axes C_2 , C_3 and C_4 of the cube.

To describe the quark condensate we add a term L completely analogous to (5.10). By the same procedure used for the plane wave condensate one has

$$L = \frac{X^8}{2} \sum_{k=1}^8 \frac{1}{R} \text{Tr} [\bar{\psi} \psi \hat{n}_k]_{ij} \sum_{v,i}^T (\mathbf{x}) C_{v,j} (\mathbf{x}) (L + R) + \text{h.c.} : \quad (5.77)$$

$L_0 + L_1 + L$ is still given by Eq. (5.40) but now

$$\langle \bar{\psi} \psi \rangle_{\text{eff}} = \frac{X^8}{R} \sum_{k=1}^8 \text{Tr} [\bar{\psi} \psi \hat{n}_k] ; \quad (5.78)$$

the quark propagator is given by (5.46) with $\langle \bar{\psi} \psi \rangle_{\text{eff}}$ given by (5.78).

An interesting point should be noted. This equation shows that the pairing region for the cubic LOFF condensate is formed by eight distinct rings; each ring is associated to one vertex of the cube and has as its symmetry axis one of the threefold axes C_3 . According to the analysis of (Bowers and Rajagopal, 2002), the LOFF vacuum state corresponds to a situation where these domains have at most one common point. Given the symmetry of the cubic structure we can limit the analysis to one pair of rings, for example those associated to the vertices $n_1; n_5$. The common point between these two rings lies on the axis C_2 and has $\mathbf{v} = \frac{1}{\sqrt{2}}(1; 1; 0)$: Since it must also belong to the boundary of the two pairing regions we have the condition:

$$\text{Tr} [\bar{\psi} \psi \hat{n}_1] = \frac{1}{2R} ; \quad (5.79)$$

which implies

$$R = \frac{p}{2h} : \quad (5.80)$$

Using Eq. (5.36) one gets

$$R = 18 : \quad (5.81)$$

The condensate (5.75) breaks both translations and rotations. It is however invariant under the discrete group O_h , the symmetry group of the cube. This can be seen by noticing that the condensate is invariant under the following coordinate transformations

$$\begin{aligned} R_1 : & x_1 \rightarrow x_1; x_2 \rightarrow x_3; x_3 \rightarrow x_2; \\ R_2 : & x_1 \rightarrow x_3; x_2 \rightarrow x_2; x_3 \rightarrow x_1; \\ R_3 : & x_1 \rightarrow x_2; x_2 \rightarrow x_1; x_3 \rightarrow x_3; \\ I : & x_1 \rightarrow x_1; x_2 \rightarrow x_2; x_3 \rightarrow x_3; \end{aligned} \quad (5.82)$$

that is rotations of $\pi/2$ around the coordinate axes, and the inversion with respect to the origin. Since the group O_h is generated by the previous 4 elements the invariance follows at once.

The crystal defined by the condensate (5.75) can fluctuate and its local deformations define three phonon fields⁽ⁱ⁾ that are the Nambu-Goldstone bosons associated to the breaking of the translational symmetry. They can be formally introduced following the same procedure discussed for the single plane wave case. One effects the substitution in (5.75)

$$2qx^i \rightarrow \frac{(i)}{f}(\mathbf{x}) = \frac{2}{a}x^i + \frac{(i)}{f}(\mathbf{x}); \quad (5.83)$$

where the three auxiliary scalar fields⁽ⁱ⁾ satisfy

$$\frac{D}{f} \frac{(i)}{0} E = \frac{2}{a} x_i; \quad (5.84)$$

whereas for the phonon fields one has

$$h^{(i)}(\mathbf{x})_{i_0} = 0; \quad (5.85)$$

We have therefore three fluctuating fields⁽ⁱ⁾_{k₁ k₂ k₃} for any elementary cube defined by discrete coordinates

$$x_{k_1} = \frac{k_1}{q}; y_{k_2} = \frac{k_2}{q}; z_{k_3} = \frac{k_3}{q}; \quad (5.86)$$

i.e.

$$\frac{(i)}{k_1 k_2 k_3} (t; x_{k_1}; y_{k_2}; z_{k_3}) : \quad (5.87)$$

The interaction term with the NGB fields is therefore given by an equation similar to (5.74):

$$S_{int} = \int dt \frac{1}{q} \sum_{k_1, k_2, k_3=1}^3 \sum_{v=1}^3 \sum_{m=1}^8 \exp[i \sum_{i=1}^3 \mathbf{r}_i \cdot \mathbf{q}_i] \mathbf{f}_{ij}^{(m)} \mathbf{C}_{v;j}^T (\mathbf{L} \cdot \mathbf{R}) + h.c.; \quad (5.88)$$

where

$$\mathbf{f}_{k_1 k_2 k_3}^{(m)} = \sum_{i=1}^3 \mathbf{X}_i^3 \frac{(m)}{i} \frac{(i)}{k_1 k_2 k_3} \quad (5.89)$$

and the eight vectors^(m) are given by

$$\frac{(m)}{i} = \frac{p}{3} \hat{n}_m : \quad (5.90)$$

The complete effective action for the NGB elds $\phi^{(i)}$ will be of the form

$$S = \int dt \frac{1}{q} \sum_{k_1, k_2, k_3 = 1}^3 \mathbf{x}^1 L(\phi^{(i)}(t; k_1 = q; k_2 = q; k_3 = q)) ; \quad (5.91)$$

In the low energy limit, i.e. for wavelengths much longer than the lattice spacing $l=q$, the elds $\phi_{k_1, k_2, k_3}^{(i)}$ vary almost continuously and can be imagined as continuous functions of three space variables x, y and z .

The coupling of the quark elds to the NGB elds generated by the condensate will be written as

$$T C \sum_{i=1}^N \exp i(\phi_1^{(1)} + \phi_2^{(2)} + \phi_3^{(3)}) ; \quad (5.92)$$

making the theory invariant under translations and rotations. These symmetries are broken spontaneously in the vacuum defined by Eq. (5.84). In order to write down the effective lagrangian for the phonon elds $\phi^{(i)}$ it is useful to start with the effective lagrangian for the auxiliary elds $\phi^{(i)}$ that has to enjoy the following symmetries: rotational and translational invariance; O_h symmetry on the elds $\phi^{(i)}$. The latter requirement follows from the invariance of the coupling (5.92) under the group O_h acting upon $\phi^{(i)}$. The phonon elds $\phi(x)$ and the coordinates x^i must transform under the diagonal discrete group obtained from the direct product of the rotation group acting over the coordinates and the O_h group acting over $\phi^{(i)}(x)$. This is indeed the symmetry left after the breaking of translational and rotational invariance. The most general low-energy effective lagrangian displaying these symmetries is

$$L = \frac{f^2}{2} \sum_{i=1,2,3} \mathbf{x} (-\partial_\mu \phi^{(i)})^2 + L_s(I_2(\mathbf{x}^{(i)}); I_4(\mathbf{x}^{(i)}); I_6(\mathbf{x}^{(i)})) ; \quad (5.93)$$

where

$$I_2(\mathbf{x}_i) = x_1^2 + x_2^2 + x_3^2; \quad I_4(\mathbf{x}_i) = x_1^2 x_2^2 + x_2^2 x_3^2 + x_3^2 x_1^2; \quad I_6(\mathbf{x}_i) = x_1^2 x_2^2 x_3^2; \quad (5.94)$$

are the three basic symmetric functions of three variables. At the lowest order in the elds $\phi^{(i)}$ and at the second order in the derivatives one gets (Casalbuoni et al., 2002e)

$$L = \frac{1}{2} \sum_{i=1,2,3} \mathbf{x} (-\partial_\mu \phi^{(i)})^2 - \frac{a}{2} \sum_{i=1,2,3} \mathbf{x} \partial_\mu \phi^{(i)} \partial^\mu \phi^{(i)} - \frac{b}{2} \sum_{i=1,2,3} \mathbf{x} (\partial_\mu \phi^{(i)})^2 - c \sum_{i < j=1,2,3} \mathbf{x} \partial_\mu \phi^{(i)} \partial^\mu \phi^{(j)} ; \quad (5.95)$$

which depends on three arbitrary parameters.

E. Parameters of the phonon effective lagrangian: cubic crystal

The parameters $a; b; c$ appearing in (5.95) are computed by a method similar to the one used in Section V.C. One puts

$$\phi^{(m)}(t; \mathbf{x}) = \sum_{i=1}^3 \mathbf{x}^i \phi_i^{(m)}(t; \mathbf{x}) ; \quad (5.96)$$

which allows to write the 3-point and the 4-point couplings as follows:

$$L_3 + L_4 = \sum_{\mathbf{v}, A=0}^3 \mathbf{x}^A \mathbf{x}^3 \sim^A \mathbf{y} \quad 0 \quad \mathbf{y}^3 \quad \mathbf{y}^4 \quad \sim^B ; \quad (5.97)$$

Here

$$g_3 = \sum_{m=1}^8 \frac{\mathbf{x}^8}{R} \mathbf{R} [\mathbf{h}(\mathbf{v}, \hat{\mathbf{n}}_m)] \frac{i^{(m)}}{f} \mathbf{A} \mathbf{B} ;$$

$$g_4 = \sum_{m=1}^8 \frac{\mathbf{x}^8}{R} \mathbf{R} [\mathbf{h}(\mathbf{v}, \hat{\mathbf{n}}_m)] \frac{(\mathbf{v}^{(m)})^2}{2f^2} \mathbf{A} \mathbf{B} ; \quad (5.98)$$

to be compared with Eqs. (5.55) and (5.56) valid for the one-plane wave form of the condensate (we have here neglected the vector condensate). To perform the calculation one employs the propagator given in Eq. (5.46) with ϵ_{eff} given in (5.78) and the interaction vertices in (5.97). The result of the calculation of the two diagrams in Fig. 20 at the second order in the momentum expansion is

$$L_{eff}(p)_{s\pi} = i \frac{4}{16} \frac{4^2 X^8}{3f^2} \sum_{v, m, k=1}^Z \frac{1}{2} \frac{1}{R} \sum_{R} [h(v, \hat{n}_m)](i^{(m)})_R [h(v, \hat{n}_k)](i^{(k)})^Z \frac{d^2 v}{D(v)D(v+p)} \quad (5.99)$$

$$L_{eff}(p)_{tad} = i \frac{4}{16} \frac{4^2 X^8}{3f^2} \sum_{v, m=1}^Z \frac{d^2 v}{D(v)} \frac{1}{R} \sum_{R} [h(v, \hat{n}_m)](i^{(m)})^2; \quad (5.100)$$

where

$$D(v) = v_0^2 - v_k^2 - \epsilon_{eff}^2 + i; \quad (5.101)$$

and, analogously to (5.45),

$$\epsilon_{eff} = \frac{X^8}{R} \sum_{k=1}^Z [h(v, \hat{n}_k)]: \quad (5.102)$$

From (5.99) and (5.101) one can easily control that the Goldstone theorem is satisfied and the phonons are massless. As a matter of fact one has

$$L_{mass} = L_{eff}(0)_{s\pi} + L_{eff}(0)_{tad} = i \frac{4}{16} \frac{4^2 X^8}{3f^2} \sum_{v, m, k=1}^Z \frac{d^2 v}{D(v)} \frac{1}{R} \sum_{R} [h(v, \hat{n}_m)](i^{(m)})_R [h(v, \hat{n}_k)](i^{(k)}) + \epsilon_{eff} \sum_{m=1}^Z [h(v, \hat{n}_m)](i^{(m)})^2; \quad (5.103)$$

In the double sum in the r.h.s. of Eq. (5.103) only the terms with $m = k$ survive and one immediately verifies the validity of the Goldstone's theorem, i.e. the vanishing of (5.103). Notice that in this approximation the masses of the Goldstone bosons vanish because the pairing regions are not overlapping, signaling that when they do overlap one is not at the minimum of the free-energy, see (Bowers and Rajagopal, 2002).

At the second order in the momentum expansion one has

$$L_{eff}(p) = i \frac{4}{16} \frac{4^2 X^8}{3f^2} \sum_{v, m, k=1}^Z \frac{1}{2} \frac{1}{R} \sum_{R} [h(v, \hat{n}_m)](i^{(m)})_R [h(v, \hat{n}_k)](i^{(k)})^Z \frac{d^2 v}{D(v)^3} \frac{2 \epsilon_{eff}^2 v \cdot p}{p^2}; \quad (5.104)$$

Using the result

$$\sum_{R} \frac{d^2 v}{D(v)^3} = \frac{i}{2 \epsilon_{eff}^4}; \quad (5.105)$$

and the absence of off-diagonal terms in the double sum, we get the effective Lagrangian in the form

$$L_{eff}(p) = \frac{2}{2^2 f^2} \sum_{v, k=1}^Z \frac{X^8}{R} \frac{(\sum_{R} [h(v, \hat{n}_k)])^2}{2 \epsilon_{eff}^2} (v \cdot p)^{2k} \frac{1}{v \cdot p^{(k)}}; \quad (5.106)$$

To perform the calculation one can exploit the large value found per R , and use the same approximations of Section V.C. The sum over k in (5.106) gives

$$\sum_{k=1}^Z \sum_{R} [h(v, \hat{n}_k)]^{(k)} \sum_{R} [h(v, \hat{n}_k)]^{(k)} = \frac{R}{2} \sum_{k=1}^Z [h(v, \hat{n}_k)]^{(k)}^2 =$$

$$= \frac{R}{k=1} \sum_{k=1}^8 \frac{1}{q^k} \left(\sum_{i,j=1}^3 \frac{1}{q} \right)^2 = \frac{R^2}{2} k_R \sum_{k=1}^8 \frac{1}{q^k} \left(\sum_{i,j=1}^3 \frac{1}{q} \right)^2; \quad (5.107)$$

with

$$k_R = \frac{j}{qR} j; \quad (5.108)$$

Therefore one gets

$$L_{\text{eff}}(p) = \frac{2k_R}{2 \cdot 2f^2} \sum_{i,j=1}^3 \sum_{k=1}^8 \frac{1}{q^k} \sum_{\nu} \frac{1}{q} \sum_{\nu} \left(\sum_{i,j=1}^3 \frac{1}{q} \right)^2 p^{(i)} p^{(j)}; \quad (5.109)$$

The integration over the Fermi velocities requires special attention. We use the result

$$\sum_{k=1}^8 \left(\sum_{i,j=1}^3 \frac{1}{q} \right)^2 = 8 \delta_{ij}; \quad (5.110)$$

this fixes the constant multiplying the time derivative term in the effective lagrangian at the value (taking into account (4.21))

$$\frac{8 \cdot 2k_R}{2 \cdot 4 \cdot 2f^2}; \quad (5.111)$$

Therefore one obtains canonical normalization for the kinetic term provided

$$f^2 = \frac{8 \cdot 2k_R}{4 \cdot 2}; \quad (5.112)$$

The parameters a ; b ; c of the effective lagrangian (5.95) can be now evaluated and one finds (Casalbuoni et al., 2002b):

$$\begin{aligned} L_{\text{eff}}(p) &= \frac{1}{2} p^{02} \delta_{(i)^2} - \frac{1}{8} \sum_{lm} p^l p^m \delta_{(i)^2} \delta_{(j)^2} = \\ &= \frac{1}{2} p^{02} \delta_{(i)^2} - \frac{p^2}{12} \delta_{(i)^2} - \frac{3 \cos^2 \varphi}{6} \frac{1}{X} \sum_{i < j=1,2,3} p^i p^j \delta_{(j)^2}; \end{aligned} \quad (5.113)$$

i.e., comparing with Eq. (5.95),

$$a = \frac{1}{12}; \quad b = 0; \quad c = \frac{3 \cos^2 \varphi}{12} \frac{1}{X}; \quad (5.114)$$

F. Gluon dynamics in the LOFF phase

1. One plane wave structure

In this Section and in the subsequent one we wish to derive the effective lagrangian for the gluons of the unbroken $SU(2)_c$ subgroup of the two-flavor LOFF phase. To begin with we assume the crystal structure given by a plane wave and we neglect the vector condensate, so that we write

$$L_{\text{eff}} = \frac{1}{R} \text{Tr} [h(v \cdot \hat{n})]; \quad (5.115)$$

The effective action allows the evaluation of the one loop diagram with two external gluon lines and internal quark lines similar to those in Fig. 20. If one writes

$$\Pi_{ab}(p) = \Pi_{ab}(0) + \Pi_{ab}(p); \quad (5.116)$$

then the Meissner mass vanishes

$$\Pi_{ab}^{ij}(0) = 0 \quad (5.117)$$

and the Debye screening mass is non-vanishing

$$m_D = \frac{g}{1 + \frac{\cos_a \cos_b}{2}}; \quad (5.118)$$

where \cos_a and \cos_b ($1 - \cos_a - \cos_b = 1$) are the solutions of the equation

$$h(\cos) = \frac{1}{2R}; \quad (5.119)$$

Next consider $\chi_{ab}(\mathbf{p})$. The only non vanishing contribution to $\chi_{ab}(\mathbf{p})$ comes from the pairing region, i.e. where $\epsilon_{eff} \neq 0$. In the approximation of small momenta ($|\mathbf{p}| \ll 1$) one finds (Casalbuoni et al., 2002c)

$$\chi_{ab}(\mathbf{p}) = \frac{g^2}{12} \sum_{\mathbf{v}; \text{pairing}} \frac{v_i v_j (\mathbf{v} \cdot \mathbf{p})}{\epsilon_{eff}^2} + v_i v_j: \quad (5.120)$$

That is

$$\chi_{ab}^{00}(\mathbf{p}) = \frac{g^2}{3} \sum_{\mathbf{v}; \text{pairing}} \frac{v_i v_j}{2} p_i p_j = \frac{g^2}{3} \frac{R^2}{2^4} \sum_{\text{pairing}} \frac{d \cos \theta}{8} \frac{v_i v_j}{(R h(\cos \theta))^2} p_i p_j; \quad (5.121)$$

where $\mathbf{v} = (\sin \theta \cos \phi; \sin \theta \sin \phi; \cos \theta)$. The integration domain is defined by $\cos_a < \cos \theta < \cos_b$. Therefore we get

$$\chi_{ab}^{00}(\mathbf{p}) = k_{ab} f(R) p_i^2 + g(R) p_k^2; \quad (5.122)$$

where k is given by (ϕ_0 the homogeneous condensate):

$$k = \frac{g^2}{18} \frac{1}{2^2} \quad (5.123)$$

and

$$f(R) = \frac{3}{4} \sum_{\text{pairing}} d \cos \theta (1 - \cos^2 \theta); \quad (5.124)$$

$$g(R) = \frac{3}{2} \sum_{\text{pairing}} d \cos \theta \cos^2 \theta \quad (5.125)$$

are functions of the parameter R and are reported in Fig. 22.

It is interesting to note the anisotropy of the polarization tensor exhibited by these results. One has always $g > f$; for large R , and neglecting ϕ_0 corrections, one finds approximately

$$\frac{g(R)}{f(R)} \approx \frac{2}{\frac{1}{1}}; \quad (5.126)$$

Let us finally write down the remaining components of the polarization tensor. From (5.120) we get

$$\chi_{ab}^{ij}(\mathbf{p}) = \frac{g^2}{3} \sum_{\mathbf{v}; \text{pairing}} \frac{v_i v_j}{2} p_0^2 = k p_0^2 f(R) (\delta_{i1} \delta_{j1} + \delta_{i2} \delta_{j2}) + g(R) \delta_{i3} \delta_{j3} \quad (5.127)$$

and

$$\chi_{ab}^{0i}(\mathbf{p}) = k p_0 p^j f(R) (\delta_{i1} \delta_{j1} + \delta_{i2} \delta_{j2}) + g(R) \delta_{i3} \delta_{j3}; \quad (5.128)$$

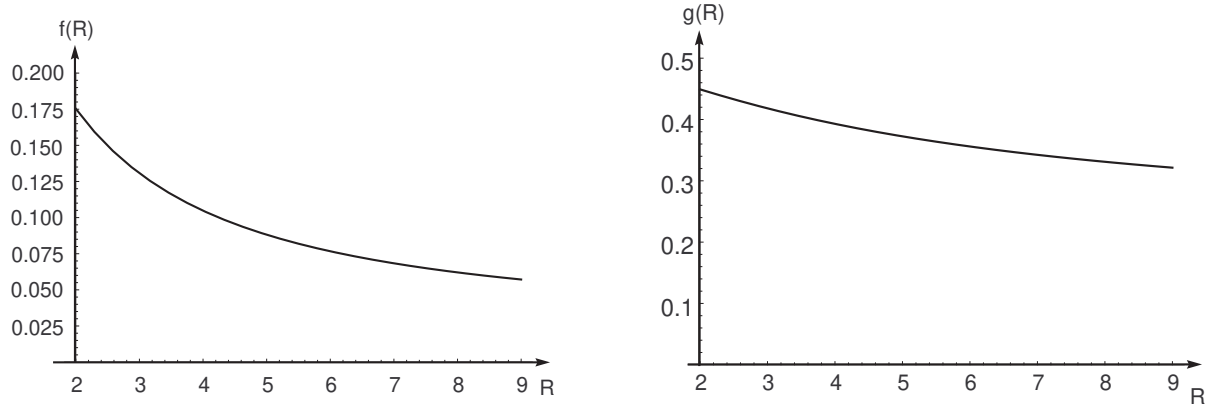


FIG. 22 Plots of the functions $f(R)$ and $g(R)$.

These results complete the analysis of the LOFF model in the one plane wave approximation. From ϵ_{ab} we get the dispersion law for the gluons at small momentum. The lagrangian at one loop is⁴

$$L = \frac{1}{4} F_a^\mu F_\mu^a - \frac{1}{2} \epsilon_{ab} A^\mu_a A_\mu^b : \quad (5.129)$$

(sum over the repeated color indices $a, b = 1, 2, 3$). Introducing the fields $E_i^a = F_{0i}^a$ and $B_i^a = \frac{1}{2} \epsilon_{ijk} F_{jk}^a$, and using (5.122), (5.127) and (5.128) we can rewrite the lagrangian (5.129) as follows

$$L = \frac{1}{2} \epsilon_{ij} E_i^a E_j^a - B_i^a B_i^a + \frac{1}{2} m_D^2 A_a^0 A_a^0 ; \quad (5.130)$$

where

$$\epsilon_{ij} = \begin{pmatrix} 1 + kf(R) & 0 & 0 \\ 0 & 1 + kf(R) & 0 \\ 0 & 0 & 1 + kg(R) \end{pmatrix} : \quad (5.131)$$

This means that the medium has a non-isotropic dielectric tensor and a magnetic permeability $\mu = 1$. These results have been obtained taking the total momentum of the Cooper pairs along the z direction. Therefore we distinguish the dielectric constant along the z axis, which is

$$\epsilon_k = 1 + kg(R) ; \quad (5.132)$$

and the dielectric constant in the plane perpendicular to the z axis

$$\epsilon_\perp = 1 + kf(R) : \quad (5.133)$$

This means that the gluon speed in the medium depends on the direction of propagation of the gluon; along the z axis the gluon velocity is

$$v_k = \frac{1}{kg(R)} ; \quad (5.134)$$

while for gluons which propagate in the $x-y$ plane we have

$$v_\perp = \frac{1}{kf(R)} \quad (5.135)$$

⁴ We do not include here the 3 and 4-gluon vertices that however can be handled as in (Casalbuoni et al., 2002d), with the result that the local gauge invariance of the one-loop lagrangian is satisfied.

and in the limit of large R , and neglecting $\propto R^{-2}$ corrections,

$$v_k = \frac{1}{2} \tan^{-1} v_0 : \quad (5.136)$$

with $\cos \theta_q$ defined in Eq. (5.37).

2. Cubic structure

The condensate in this case is given by Eq. (5.75), so that we will use the results of Section V A with ϵ_{eff} given by (5.78). The calculations are similar to the previous case and, similarly, the $SU(2)_c$ gluons have vanishing Meissner mass and exhibit partial Debye screening. However the dispersion law of the gluons is different.

As a matter of fact we write the one loop Lagrangian for the $SU(2)_c$ gluons as

$$L = \frac{1}{2} (\mathbf{E}_i^a \mathbf{E}_i^a - \mathbf{B}_i^a \mathbf{B}_i^a) + L ; \quad (5.137)$$

with

$$L = \frac{1}{2} \sum_{ab} A^a A^b : \quad (5.138)$$

In the approximation $p_j \ll 1$, ϵ_{ab} is again given by Eq. (5.120), but now ϵ_{eff} is given by (5.78). One gets

$$L = \mathbf{E}_i^a \mathbf{E}_j^b \sum_{ab} \frac{g^2}{6} \frac{Z}{2} \underbrace{\frac{d \cos \theta}{8}}_{\text{pairing}} \frac{v_i v_j}{2 \epsilon_{eff}} + A_0^a A_0^b \sum_{ab} \frac{g^2}{4} \frac{Z}{2} \underbrace{d \cos \theta}_{\text{blocking}} : \quad (5.139)$$

Evaluating the integrals one finds

$$L = \frac{1}{2} (\tilde{\gamma}_{ij} \mathbf{E}_i^a \mathbf{E}_j^a - \mathbf{B}_i^a \mathbf{B}_i^a) + \frac{1}{2} M_D^2 A_0^a A_0^a ; \quad (5.140)$$

with the tensor $\tilde{\gamma}^{ij}$ given by

$$\tilde{\gamma}_{ij} = \gamma_{ij} [1 + k t(R)] : \quad (5.141)$$

and

$$M_D = \frac{g}{1 + 8 \frac{\cos \theta_a + \cos \theta_b}{2}} : \quad (5.142)$$

where $\cos \theta_{ab}$ are solutions of Eq. (5.119). The tensor $\tilde{\gamma}^{ij}$ is isotropic. This result can be easily explained noticing that the Lagrangian should be a quadratic function of the field strengths and should also satisfy the cubic symmetry. Therefore it must be constructed by the invariants $I_2(\mathbf{E}_i)$ and $I_2(\mathbf{B}_i)$ that are isotropic. As shown in (Casalbuoni et al., 2002c) $t(R)$ is given by

$$t(R) = \frac{8}{3} [2f(R) + g(R)] : \quad (5.143)$$

It should also be noted that the values of the parameter R for the cube and the plane wave can be different. A plot of the function $t(R)$ is in Fig. 23. Even if the crystalline structure is not isotropic, the dielectric properties of the medium will be isotropic and the velocity of propagation of the gluons will be the same in all the directions.

VI. INHOMOGENEOUS SUPERCONDUCTIVITY IN CONDENSED MATTER, NUCLEAR PHYSICS AND ASTROPHYSICS

As observed in the introduction, the main focus of this review is on the theoretical methods rather than phenomenological consequences. However, for completeness, in this Section we give a review of the different approaches developed so far to detect the inhomogeneous phase in superconductors. The LOFF is expected to be ubiquitous, therefore one might expect to find it in completely different physical systems. For obvious reasons research in solid state physics is

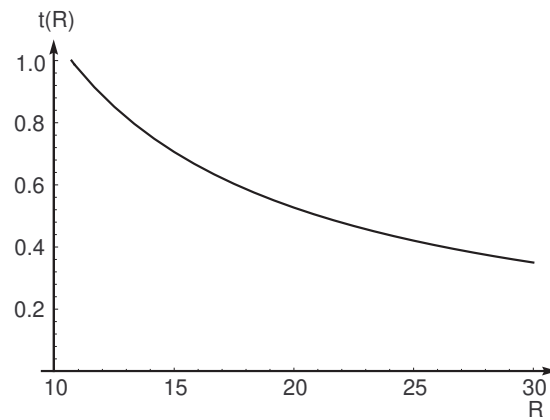


FIG. 23 Plot of the function $t(R)$.

much more advanced and indeed signals of formation of the LOFF phase have been reported in the literature. In the first part of this Section we review them. In order to produce the effective exchange interaction of Eq. (2.1) a sufficiently high magnetic field is needed to produce an appreciable difference between the chemical potentials. This could be done in type I superconductors, but the required fields are likely to destroy superconductivity altogether. This issue is discussed in Subsection VIA. To overcome this difficulty, type II superconductors must be used; moreover they should be free of impurities and have large electron mean free path; the needed requirements and the associated phenomenology are discussed in Subsection VIB and VIC. Another way to overcome the effects of high magnetic fields that are detrimental to electron superconductivity is to use layered superconductors and magnetic fields parallel to the layers. Superconductors of this type are rather different from the ones considered in the original LOFF papers; in particular organic superconductors are compounds with these features and are therefore good candidates. They will be discussed in Subsection VID, while in Subsection VIE we briefly discuss future possible developments in the area of atomic physics. The final part of this Section is devoted to phenomenological implications of the LOFF phase in nuclear physics (Subsection VIF) and QCD (Subsections VIG and VIH). In particular, in this last Subsection we discuss a possible role of the QCD LOFF phase in the explanation of a peculiar phenomenon of pulsars, i.e. the periodic glitches in their angular velocity.

A. Type I superconductors

In the original LOFF papers (Larkin and Ovchinnikov, 1964), (Fulde and Ferrell, 1964) the difference in chemical potentials between spin up and spin down electrons arises from an interaction of a magnetic field with the electron magnetic dipole moments. The magnetic field can hardly be the external field H_{ext} , which exerts a stronger influence on the orbital motion than on the electron spin. Therefore the inhomogeneous phase was thought to arise in nonmagnetic metals in presence of paramagnetic impurities. Under an external field the host impurities display ferromagnetic alignment; decreasing the temperature the material becomes a superconductor while the ferromagnetic alignment persists, leading to a constant self-consistent exchange field, proportional to the average spin of the impurities. This field is at the origin of the modulated order parameter. The value $H_0 = 2$ above which LOFF phase can exist corresponds to a critical value of the magnetic field that can be derived as follows (Clogston, 1962), (Chandrasekhar, 1962). The susceptibility of an electron gas in the normal phase at $T = 0$ is

$$\chi_n = \frac{2}{B} ; \quad (6.1)$$

where $\rho_F = g_F^2 = (2 \cdot 2 v_F)$ is the density of states at the Fermi surface, B is the Bohr magneton and $g = 2$ is the electron degeneracy factor. On the other hand the susceptibility in the superconducting phase at $T = 0$ vanishes: $\chi_s = 0$, because to polarize the superconductor one has to break the Cooper pair, which costs energy. The free energy per unit volume f_s of the superconductor, in absence of paramagnetic effects, is:

$$f_s = f_n - \frac{H_c^2(T)}{8} ; \quad (6.2)$$

where f_n is the free energy of the normal phase and $H_c(T)$ is the critical field. Including the Pauli paramagnetism implies adding the Hamiltonian a term

$$H_B = \mu_B \sum_i \sigma_i H; \quad (6.3)$$

while (6.2) becomes

$$f_s = f_n + \frac{(\chi_n - \chi_s)H^2}{2} - \frac{H_c^2(T)}{8}; \quad (6.4)$$

Therefore the BCS superconductivity will survive at $T = 0$ for magnetic fields satisfying

$$H \leq \frac{H_c^2(0)}{4(\chi_n - \chi_s)} = H_P(0); \quad (6.5)$$

Now $H_c^2(0) = 8 \times 10^4$ and therefore the Pauli limiting field at $T = 0$ is

$$H_P(0) = \frac{1}{2} \frac{H_c^2(0)}{(\chi_n - \chi_s)}; \quad (6.6)$$

The identification $\chi_1 = \chi_B H_P(0)$ arises by the comparison between (6.3), (6.6) and (2.1).

For a type I superconductor it is difficult to reach the Pauli limit (6.6) because, while $H_P(0)$ is typically of the order of 300 K Oe, $H_c(0)$ is of the order 1 K Oe. Therefore superconductivity will be broken by the magnetic field well before the Clogston-Chandrasekhar limit is achieved. This implies the LOFF phase is unlikely to be produced by these materials and one has to turn to type II superconductors (Saint-James et al., 1969) because for some of these superconductors the upper critical field H_{c2} can be very high.

B. "Clean" and strongly type II superconductors

To evaluate the possibility of the LOFF state one has to take into account not only Pauli paramagnetism of the electrons but also the orbitale effects (Ginzburg, 1957). Before doing that, let us first distinguish between "clean" and "dirty" superconductors (Anderson, 1959). One calls "clean" the superconductors in which the electron mean free path l is much larger than the superconducting coherence length ξ_0 :

$$l \gg \xi_0; \quad (6.7)$$

while "dirty" superconductors are characterized by the opposite condition $l \ll \xi_0$. In "clean" superconductors electrons at the Fermi surface move with velocity v_F , while in "dirty" superconductors the electron motion is described by a diffusion equation. "Dirty" superconductors are characterized by the presence of impurities, which can narrow and even destroy the LOFF state (Aslamazov, 1969; Takada, 1970). Therefore materials with small l , e.g. PbMoS₈, should not display the LOFF phase, see e.g. Decroux and Fischer, 1982). On the other hand the so called heavy-fermion superconductors are favored: these materials are indeed characterized by the small Fermi velocity of their quasiparticles (Rauchschwalbe, 1982); since

$$\xi_0 = \frac{\hbar v_F}{k_B T_c}; \quad (6.8)$$

for small enough v_F the condition (6.7) is satisfied. For example in the heavy fermion compound UPdAl₃ the superconducting coherence length is $\xi_0 \approx 85 \text{ \AA}$, much smaller than the electronic free mean path $l \approx 700 \text{ \AA}$; therefore it can be considered as a "clean" superconductor.

To evaluate the possibility of the LOFF state in type II superconductors one has to take into account not only Pauli paramagnetism of the electrons, but also the orbitale effects. This analysis was first performed by (Guenberg and Gunther, 1966). These authors followed the variational method of (Werthamer et al., 1966), by making an ansatz for the condensate. In general there is a competition between the orbital and the paramagnetic effect, the former trying to organize a structure of Abrikosov vortices and the latter a periodic LOFF structure; therefore the orbitale effect reduces the possibility of the LOFF state that can exist only for sufficiently high H_{c2} . The quantitative criterion at $T = 0$ for clean superconductors with isotropic dispersion law is as follows. The LOFF state can persist in a type II superconductor provided

$$\frac{H_{c2}(0)}{H_P(0)} > 1.8; \quad (6.9)$$

Here κ is the parameter first introduced in (Maki, 1964), $H_{c2}(0)$ is the Gorkov upper critical field at $T = 0$ in absence of paramagnetic effects (Gorkov, 1960) and $H_p(0)$ is the Pauli limiting field defined in (6.6).

In conclusion good experimental conditions to observe the LOFF state should be provided by a clean superconductor with a large κ value. These features are not easily found in the most common superconductors and therefore experimental investigations consider unconventional superconductors, e.g. heavy-fermion, organic or high T_c superconductors. As a matter of fact many of these materials are strongly type II superconductors, which means that the condition (6.9) can be satisfied. Moreover they have often a layered structure, which implies that, applying the magnetic field parallel to the layers, the orbital effect is minimum and the Zeeman effect, on which the LOFF phase is based, is dominant.

The condition of being very clean and simultaneously strong type II superconductors should be more easily realized in d-wave superconductors like high T_c cuprate superconductors and organic superconductors like $-(\text{ET})_2$ or $-(\text{ET})_2$ salts. They will be discussed in more detail below; suffice it here to say that in d-wave superconductors the region of the LOFF phase is much more extended than in s-wave superconductors. The analysis of (Maki and Won, 1996), where this conclusion was drawn, has been extended in (Won and Maki, 2002) to the calculation of the LOFF free energy, specific heat and magnetic susceptibility; in particular for these layered d-wave superconductors the energetically favored structure at $T = 0$ is found to be

$$(\kappa; \gamma) / \cos \alpha_x + \cos \alpha_y : \quad (6.10)$$

Other materials where the possible existence of LOFF phase has been investigated are ferromagnetic metals or alloys (Pickett et al., 1999), (Dyugaev et al., 2001). The study of the possible coexistence of ferromagnetism and superconductivity was initiated by (Ginzburg, 1957) who noted that, though the two orderings can in principle coexist, their simultaneous presence is practically impossible under ordinary conditions. As a matter of fact the presence in ferromagnets of a spontaneous magnetization M_0 produces at $T = 0$ an internal magnetic induction $B_0 = 4\pi M_0$ even in absence of external magnetic field. For superconductivity to exist, B_0 should be smaller than the lower critical field at $T = 0$, in absence of ferromagnetism:

$$B_0 < H_{c1}^0(0) : \quad (6.11)$$

However, the induction B_0 at $T = 0$ is of the order of 10 K Oe (e.g. 22, 18.5, 6.4, 24.8 K Oe respectively for Fe, Co, Ni, Gd), while the critical field is in general much smaller, of the order of a few K Oe or less. Superconductivity of ferromagnets is therefore difficult unless special conditions render the condition (6.11) possible. They might be, for example, a reduced size of the sample, with dimensions of the order of the penetration depth. The formation of the vortex phase in type II superconductors, however, screens locally the internal magnetic induction, and allows to avoid Ginzburg's negative conclusion (Krey, 1973). As a matter of fact superconductivity was recently reported in the ferromagnetic alloy $\text{RuSr}_2\text{GdCu}_2\text{O}_8$ (Bernhard, 1999; Hadjiev, 1999; Pringle, 1999; Tallon, 1999). This layered material becomes first ferromagnetic at $T = 132$ K; superconductivity appears at $T = 35 - 40$ K and finally, at $T = 2.6$ K Gd ions acquire an antiferromagnetic order. The theoretical study of (Pickett et al., 1999) confirms these reports, but suggests that the superconducting phase is of the LOFF type, because the coupling between ferromagnetism and superconducting layers appears to be sufficiently weak to permit superconductivity, but strong enough to require the inhomogeneous phase. In a similar context (Dyugaev et al., 2001) consider the possibility of creating the LOFF phase using ferromagnetic materials instead of nonmagnetic bulks with paramagnetic impurities as in the original LOFF papers. Since the impurities create not only an exchange interaction, but also an electromagnetic interaction, using nuclear ferromagnetism, as they propose, would reduce the latter, since the effective field would be proportional to the nuclear magneton and not to the Bohr magneton. They show that in some metals, e.g. Rh, W, the BCS condensate imbedded in a matrix of ferromagnetically ordered nuclear spins should manifest the LOFF phase.

All the proposals we have discussed so far are rather different from the one discussed in the original LOFF papers. An extension of the LOFF analysis to these materials and unconventional superconductors is beyond the scope of the present review. We will therefore limit our presentation to a brief survey of the experimental results, referring the interested reader to the specialized literature (Agterberg and Yang, 2001; Geginewart, 1996; Murthy and Shankar, 1995; Samokhin, 1997; Shimahara, 1998b; Shimahara et al., 1996; Symington, 1999; Yang, 2001).

C. Heavy fermion superconductors

The first experimental investigations on the LOFF phase used heavy-fermion compounds such as CeRu_2 (Huxley, 1993), UPd_2Al_3 (Gibson, 1993) and UBe_{13} (Thomas, 1996). For all these materials the conditions for the formation of the LOFF state are met. For example CeRu_2 is in a metallurgically clean state; moreover it exhibits extreme type II behavior, because the Ginzburg-Landau parameter, which discriminates between the two type of superconductors

(Saint-James et al., 1969), has the value $\kappa = 16$. As another example, the compound UPd_2Al_3 used by (Gloos, 1993) is characterized by a rather large value of the parameter κ in (6.9) i.e. $\kappa = 2.4$, while also being a very clean superconductor. To quote another result, in the analysis of a high quality single crystal of UBe_{13} (Thomas, 1996), the very high value $H_{c2}(0) \sim 140$ KOe was reached. All these experimental results are however inconclusive. In a critical analysis of the experiment of (Gloos, 1993), (Norman, 1993) shows that the computed Gorkov upper critical field does not correspond to the experimental results reported there; for further analysis of the compound UPd_2Al_3 see (Yin and Maki, 1993) and (Schmianski, 1994). In the case of $CeRu_2$, (Tenya, 1999) shows that the observed effects can be explained by flux pinning mechanisms involving disorder. (Mödlér, 1996) makes a comparative study of high quality single crystals of UPd_2Al_3 and $CeRu_2$ in the mixed state. The order parameter exhibits a periodic array of nodal planes perpendicular to the Abrikosov vortex lines. In the mixed state the pinning force is very weak; however the authors find, for $H > 10$ KOe and $T < 0.9T_c$, a first order transition to a state characterized by strong pinning, which might be interpreted as the formation of a LOFF state. The mechanism by which Abrikosov vortex lines in type II superconductors are pinned to the vortex cores is similar to the one that pins vortex lines to non-superfluid neutrons in a rotating superfluid within neutron stars. It will be explained in more detail in Subsection VI.H in connection to a possible role of the QCD LOFF state in the physics of pulsars.

D. Two-dimensional, quasi-two-dimensional and organic superconductors

As we already mentioned, the paramagnetic effect can dominate if the superconducting bulk has a layered structure and the magnetic field acts parallel to it, because in this case the orbital upper critical field can be extremely high and the breaking due to the spin interaction is most significant. The importance for two-dimensionality (2D) to favor the LOFF state was first observed in (Bulaevskii, 1973) and (Bulaevskii, 1974) where both the orbital and the spin effect were taken into account and the upper critical field $H_{c2}(T)$ was calculated; in (Buzdin and Kulic, 1984) the analysis was carried out near the tricritical point. For the same reason also quasi-one-dimensional (Q1D) compounds were discussed (Buzdin and Polonski, 1987; Buzdin and Tugushev, 1983; Dupuis, 1995; Dupuis et al., 1993), even though the results of (Shimahara, 1998a) indicate that the 2D structures are favored in comparison the 1D ones.

These results were generalized to arbitrary temperature and d-wave superconductivity in (Shimahara and Rainer, 1997). The main result of this paper is that the critical field curve $H_{c2}(T)$ is non monotonic and consists of different pieces corresponding to different Landau levels, characterized by $n > 0$. On the contrary, the Ginzburg-Landau theory would predict the pair wave function to be in the lowest energy Landau level, with $n = 0$ at H_{c2} . The paper (Shimahara, 1998a) studies the most favored structure for a 2D LOFF crystal with a cylindrical Fermi surface. First, the author finds that in general the 2D structures are favored over the 1D ones; second, it finds that the favored crystalline structure changes with T . For s-wave the results are as follows: at high temperature the antipodal pair condensate

$$(r) / 2 \cos q \quad r \quad (6.12)$$

is favored. This was the result found by (Larkin and Ovchinnikov, 1964) in 3D at $T = 0$. Decreasing the temperature other structures become favored: first the triangle, then the square and finally, at low temperatures, the hexagon. For d-wave pairing at high temperature again (6.12) is favored, while at small temperature the square dominates; on the other hand at intermediate temperatures the phase transition should be first order. The result at $T = 0$ has been confirmed by (Wong and Maki, 2002), see Eq. (6.10). As shown in (Lebed', 1986), the quasi-2D superconductors can be treated as essentially 2D and therefore the results of (Shimahara, 1998a) should hold also for quasi-2D compounds provided the external field is sufficiently strong and is kept parallel to the superconducting layer.

(Klein et al., 2000) consider a layered superconductor in a magnetic field of arbitrary orientation with respect to the conducting plane. The calculation is based on the quasi-classical Eilenberger equations (Eilenberger, 1968), (Alexander et al., 1985) and allows to elucidate the structure of the stable states below H_{2c} minimizing the free energy. The stable states are neither pure LOFF states nor pure Abrikosov vortex states, but are two-dimensional periodic structures or quasi-one-dimensional structures where LOFF domains are separated by vortex chains. (Barzykin and Gorkov, 2002) address 2D surface superconductivity in presence of intense magnetic fields parallel to the surface. The spin-orbit interaction at the surface changes the properties of the LOFF state; the authors find that strong spin-orbit interactions significantly broadens the range of parameters where the LOFF phase can exist and produces periodic superconducting stripes running along the field direction on the surface.

Organic superconductors are good candidates for the formation of the LOFF state for the reasons mentioned above: i) They have narrow electron bands and therefore they are in principle clean type II superconductors; ii) due to their low dimensionality the orbital pair-breaking effect is suppressed for magnetic fields parallel to the layers they form. For these reasons they have been discussed by several authors, e.g. (Burkhardt and Rainer, 1994; Dupuis, 1995; Dupuis et al., 1993; Gorkov and Lebed', 1987; Lebed', 1986; Shimahara, 1994, 1997). It is interesting to note that

in general to detect the transition from the homogeneous BCS phase to the LOFF phase thermodynamic signatures are chosen. This however can give ambiguous results since the signatures can be produced by phase transitions of different nature. Therefore Ref. (Yang and Agterberg, 2000) proposes the use of the Josephson effect. According to this analysis, at the Josephson junction between two superconductors, one in the BCS and the other in the LOFF phase, the Josephson current is suppressed.

As discussed in (Shimahara and Rainer, 1997), the upturn of the upper critical field $dH_c/dT^2 > 0$ is a common feature in the LOFF state in quasi-2D systems and is due a Fermi surface effect. Investigations on the sensitivity of the LOFF state to the shape of the Fermi surface are in (Aoi et al., 1974; Shimahara, 1994, 1997). This upturn and a first order transition below the critical field have been observed in the organic compound $-(BEDT-TTF)_2Cu(NCS)_2$. This quasi-two-dimensional (Q2D) organic superconductor is examined by a number of authors (Houzet and Buzdin, 2000a; Ishiguro, 2000; Nam et al., 1999; Singleton et al., 2001, 2000; Symington et al., 2001) and, for a similar compound, (Goddard et al., 2002). These studies indicate that some evidence of the formation of the LOFF state has been reached. For example (Singleton et al., 2000) studied resistance and magnetic behavior of single crystals of this superconductor in magnetic fields up to 33 T and at temperatures between 0.5 K and 11 K. When the magnetic field lies precisely in the Q2D planes of the material, they find evidence for a phase transition from the superconducting mixed state into a LOFF state, manifested as a change in the rigidity of the vortex system. (Manno and Klein, 2000) compare the theoretical anisotropic upper critical field H_c of a quasi-two-dimensional d-wave superconductor with recent H_{c2} data for $-(BEDT-TTF)_2Cu(NCS)_2$ and find agreement both with regard to the angular and the temperature dependence of H_c . According to these authors this supports the suggestion that the LOFF phase exists in this material for exactly plane-parallel orientation of the magnetic field.

In (Uji, 2001) field induced superconductivity was reported in an organic superconductor $(BETS)_2FeCl_4$ ($BETS = \text{bis(ethylenedithio)tetraselenafulvalene}$). A possible mechanism to create field induced superconductivity is the Peter-Jaccarino effect (Jaccarino and Peter, 1962). However the upwards convex nature of the lower critical field as a function of the temperature casts doubts on this interpretation. Therefore some authors, e.g. (Balicas et al., 2001), have proposed that these results can be interpreted as evidence of the formation of the LOFF state. These results were reviewed in (Houzet et al., 2002) and (Shimahara, 2002). In particular in the latter paper, an experimental phase diagram of the field-induced superconductivity in this organic compound was theoretically reproduced by a combination of the LOFF state and the Jaccarino-Peter mechanism. (Tanatar et al., 2002) discusses whether LOFF state has been observed via thermal conductivity (κ) in quasi-two-dimensional organic superconductor $-(BETS)_2GaCl_4$. For clean samples the behavior of (κ) is similar to the one expected by a second order phase transition and is consistent with the formation of a LOFF phase.

E. Future developments

The superconducting LOFF phase might be realized even if the difference in chemical potentials of two species were not generated by a magnetic field acting on electron spins. Apart from nuclear physics and pulsars, to be discussed below, another context might be offered by ultracold quantum degenerate Fermi gas of atoms comprising two hyperfine states. The experimental investigations of ultracold gases were first dedicated to the study of the Bose-Einstein condensation (Anderson, 1995; Bradley et al., 1997; Davis, 1995; Fried, 1998); subsequently these techniques have been extended also to magnetically trapped ultracold alkali Fermi gases or to gases with coexisting Bose-Einstein condensate and Fermi gas (Modugno et al., 2002; Roati et al., 2002; Schreck et al., 2001). In particular two state mixtures of ultracold gases have been employed, with ^{40}K vapors (DeMarco and Jin, 1999; DeMarco et al., 2001), or 6Li (Garanade, 2002; O'Hara, 2001), or a mixture of 6Li and 7Li (Mewes et al., 1999). Future developments could lead to the observation of superconductivity and Cooper fermion pairs condensation in these systems. As discussed in (Combescot, 2000) it is quite likely that the two hyperfine states would have different atomic populations, since at the moment there are no known fast relaxation mechanisms to equalize the two atomic populations. Therefore superconductivity for two-state ultracold Fermi gases is likely to be of the LOFF type. The author of Ref. (Combescot, 2000) has performed a theoretical study of 6Li under the above mentioned conditions; he considers not only s wave interactions, but also an anisotropic term induced by density fluctuation exchange and shows that the range where the LOFF phase is realized increases with the increasing role of the anisotropic term. This is an interesting theoretical development, which adds new interest to the experimental investigations of ultracold atomic Fermi gases. It remains to be seen, however, if such possibility is actually realized in Nature.

F. LOFF phase in nuclear physics

Neutron-proton pair correlations and the possibility of $n-p$ Cooper pair condensation are presently studied in several different contexts, from heavy ion collisions to astrophysics. They have been investigated, using the BCS theory, in finite nuclear matter (Alm et al., 1993, 1990, 1996; Baldo et al., 1992; Sedrakian et al., 1997; Vonderfecht et al., 1991), and by mean-field effective interactions in finite nuclei. In several cases nuclear matter is highly asymmetric, with proton concentration at most 30-40% in supernova matter and 10% in neutron stars. These asymmetries are detrimental to nucleon superconductivity; on the other hand, for weakly asymmetric states, fermion condensation is indeed possible. For example, weakly isospin asymmetric nuclear matter favors the formation of Cooper pairs in the 3S_1 - 3D_1 channel, due to the presence of a tensor force; gaps are of the order of 10 MeV. Condensation in this channel might be relevant for low density bulk matter such as dilute nuclear matter in supernovas. On the other hand there is no evidence of large gap isospin singlet pairing in ordinary nuclei, which might be explained by the presence of spin orbit interaction (Goodman, 1999; Martinez-Pinedo et al., 1999). The authors (Sedrakian and Lombardo, 2000) study the dependence of the gap as a function of both the isospin asymmetry $n_p = (n_n - n_p)/n$ and the temperature, using realistic nuclear interactions. For small asymmetries the gap develops a maximum at a certain intermediate temperature; for large asymmetries the superconducting phase exists only at finite temperature, because the smearing effect of the temperature on the Fermi surfaces favors condensation. At higher values of n_p (> 0.11 in their model) pairing is no longer possible.

Also in the context of isospin asymmetric nuclear matter it is possible to have a transition from the BCS state to a LOFF phase instead of the normal state (Isayev, 2002; Sedrakian, 2001; Sedrakian et al., 1997). In Ref. (Sedrakian, 2001) the possibility of spatially inhomogeneous condensate in asymmetric nuclear matter is studied. Condensation is possible in different channels. The isospin triplet channels are favored for large enough asymmetries; more exactly the channel 1S_0 dominates at low densities and the channel 3P_2 - 3F_2 (or 1P_2) at high densities. For weak asymmetries the dominant channels are the isospin singlets 3S_1 - 3D_1 (low densities) and 3D_2 (high density). The author considers the case of low density; as the isospin singlet 3S_1 - 3D_1 has a strength much larger than the isospin triplet 1S_0 , he neglects the latter. The interaction is modelled by the Paris nucleon-nucleon potential. The gap equations are solved numerically and have non trivial solutions for non vanishing total momentum of the pair P . The LOFF phase is favored for $n_p > 0.25$ and $P = 0.3p_F$, independent of n_p . For $n_p > 0.37$ pairing exists only in presence of non-vanishing P . The maximal values of n_p and P compatible with the LOFF state are 0.41 and $0.3p_F$ respectively (the actual values are indicative, as a refinement of the treatment of the nuclear interaction may change them by a factor as large as 3). The results are obtained at $T = 3$ MeV. From the BCS to the LOFF phase the phase transition is first order, while one passes from the LOFF to the normal state by a second order phase transition. No attempt is made to determine the most favorite crystalline structure.

Under hypotheses similar to those of the previous paper (Isayev, 2002) studies the effect of coupling between the isospin singlet and isospin triplet, since at low densities pairing between these two channels may be important (Akhiezer et al., 1999). Besides, the author goes beyond the approximation of "bare" nucleon interaction, by using the Fermi-liquid phenomenological approach (Akhiezer et al., 1994). By these changes one finds interesting peculiarities at $T = 0$. First, the triplet-singlet channel turns out to be energetically favored; second, the phase transition from the LOFF to the normal state can be of first order, depending on the nature of the nucleon interaction. While still model dependent, these investigations of the LOFF phase in nuclear interactions are interesting as they offer, in principle, a different way to the LOFF phase. To be closer to phenomenology one should consider however more complicated structures such as, for example, hyperon rich matter. Alternatively the modulation of the order parameter might be caused by Pauli paramagnetism due to strong magnetic fields in highly magnetized neutron stars (magnetars). In this case one could have a splitting in the Fermi surfaces of a nucleon pair in the $I = 1, L = 0$ channel (Sedrakian, 2001).

G. Why color LOFF superconductivity could exist in pulsars

In this Subsection and in the next one we will be interested in some numerical estimates of the values of the parameters needed for the LOFF phase in pulsars to occur. In general, color superconductivity in quark matter might be realized in compact stars. This expectation follows from the following two facts.

First of all the BCS critical temperature is given by

$$T_c = 0.57 T_{BCS} \quad (6.13)$$

and in QCD T_{BCS} is expected to range between 20 to 100 MeV. This estimate arises from weak coupling calculations (Beane and Bedaque, 2000; Beane et al., 2001; Brown et al., 2000a,b,c; Evans et al., 2000; Hong et al., 2000; Hsu and Schwetz, 2000; Pisarski and Rischke, 1999a,b, 2000a,b; Rajagopal and Shuster, 2000; Schafer, 2000; Schafer and Wilczek, 1999c; Shovkovy and Wijewardhana, 1999; Son, 1999) which are valid only at asymptotically high chemical

potentials 10^8 MeV (Rajagopal and Shuster, 2000), and from models with parameters adjusted to reproduce the physics at zero densities (Alford, 2000; Alford et al., 1998, 1999b; Berges and Rajagopal, 1999; Carter and Diakonov, 1999; Evans et al., 1999a,b; Rajagopal, 1999; Rapp et al., 1998, 2000; Schafer, 2001; Schafer and Wilczek, 1999b; Wilczek, 2000). None of these calculations is valid at chemical potentials around 400 MeV, which correspond roughly to the density of the inner core of a neutron star, as we shall see below. However in all these cases one gets values of the gaps of the order quoted before.

The second fact has to do with the thermal history of a pulsar. The general belief is that compact stars such as pulsars are formed in the core of a supernova explosion. The temperature at the interior of the supernova is about 10^{11} K, corresponding to 10 MeV ($1 \text{ MeV} = 1.1065 \cdot 10^0 \text{ K}$). The star cools very rapidly by neutrino emission with the temperature going down to 10^9 - 10^{10} K in about one day. The neutrino emission is then dominating the cooling for one thousand years. In this period the temperature reaches about 10^6 K. After this period the star cools down due to X-ray and photon emission and in a few million years reaches a surface temperature around 10^5 K. Therefore, for the greatest part of its existence a neutron star has a temperature lower than the critical temperature, with the possibility of forming color superconducting condensates. It follows that also in this context a compact star can be considered at zero temperature because its temperature is much smaller than the typical BCS energy gap, $T_{n;s} = T_{BCS} \approx 10^6 - 10^7$.

We have seen previously that QCD favors the formation of BCS condensates in idealized cases, e.g. two or three massless flavors of quarks. However in realistic cases the three quarks have different Fermi momenta due to the mass difference. It is interesting to have an idea of the order of magnitude of the scales involved in the description of a neutron star with a quark core. We begin with a very crude example of a free gas of three flavor quarks, taking up and down massless and the strange one with mass M_s (Alford et al., 2000). Requiring that the weak interactions are in equilibrium it is easy to determine the chemical potentials and the Fermi momenta for the quarks. We find

$$\begin{aligned} u &= \frac{2}{3} \mu_e; \quad p_F^u = u; \\ d &= +\frac{1}{3} \mu_e; \quad p_F^d = d; \\ s &= +\frac{1}{3} \mu_e; \quad p_F^s = \sqrt{\frac{2}{3} M_s^2}; \end{aligned} \quad (6.14)$$

where μ_e is average chemical potential

$$\mu_e = \frac{1}{3} (\mu_u + \mu_d + \mu_s) \quad (6.15)$$

and μ_e the chemical potential of the electrons. Notice that

$$\sum_{i=u,d,s} N_i + N_e = N_q = eQ; \quad (6.16)$$

where

$$N_q = \sum_{i=u,d,s} N_i; \quad Q = \frac{2}{3} N_u - \frac{1}{3} (N_d + N_s) = N_e; \quad (6.17)$$

The chemical potential for the electrons is fixed by requiring electrical neutrality, corresponding to the following condition for the grand potential at zero temperature

$$Q = \frac{\partial \Omega}{\partial \mu_e} = 0; \quad (6.18)$$

is obtained from Eq. (2.60) (omitting the volume factor)

$$\Omega = \frac{1}{2} \sum_{i=u,d,s} \int_0^{p_F^i} p^2 (E_i(p) - \mu_i) dp; \quad (6.19)$$

In our case we get

$$\Omega = \frac{3}{2} \sum_{i=u,d,s} \int_0^{p_F^i} p^2 (E_i(p) - \mu_i) dp + \frac{1}{2} \int_0^{p_F^e} p^2 (p - \mu_e) dp; \quad (6.20)$$

where

$$E_{u,d}(p) = p; \quad E_s(p) = \sqrt{p^2 + M_s^2}; \quad (6.21)$$

Although the integral is feasible its expression is algebraically involved and it is easier to do all calculations numerically. In particular the result for the chemical potential of the electrons for different values of μ as a function of M_s is given in Fig. 24.

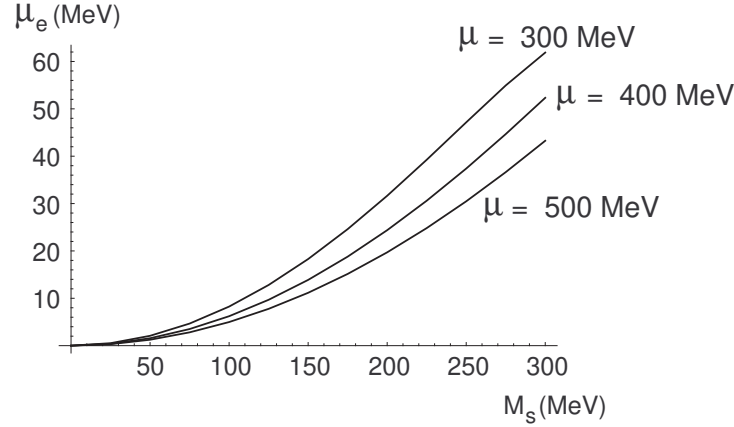


FIG. 24 The chemical potential of the electrons vs. M_s for three values of the average chemical potential.

We can get an analytical expression by performing an expansion up to the order M_s^4 . One gets

$$\mu_e = \frac{M_s^2}{4} \quad (6.22)$$

and

$$\frac{3}{4} M_s^4 + \frac{3}{4} M_s^2 \mu^2 - \frac{7}{32} \frac{12 \log(M_s=2)}{2} M_s^4; \quad (6.23)$$

The baryon density is obtained as

$$B = \frac{1}{3} \frac{\rho}{\rho} = \frac{1}{3} \sum_{i=u,d,s} (p_F^i)^3; \quad (6.24)$$

The plot of the ratio of the baryon density to the nuclear baryon density is given in Fig. 25. The nuclear baryon density has been assumed as the inverse of the volume of a sphere of radius about 1.2 fm. Within the same approximation as before one finds

$$B = \frac{3}{2} \left(1 - \frac{1}{2} \frac{M_s^2}{\mu^2} \right); \quad (6.25)$$

We note that densities in the core are of the order of 10^{15} g/cm^3 , corresponding to a chemical potential of the order of 400 MeV, as shown in Fig. 25.

In particular let us discuss the range of values around 400 MeV of the average chemical potential, with a strange mass of the order 200-300 MeV (the strange mass here is not the current mass but an effective density dependent mass). With $M_s = 300 \text{ MeV}$ one finds $\mu_e = 53 \text{ MeV}$ (56 MeV from the approximate equation) with Fermi momenta

$$p_F^u = 365 \text{ MeV}; \quad p_F^d = 418 \text{ MeV}; \quad p_F^s = 290 \text{ MeV}; \quad (6.26)$$

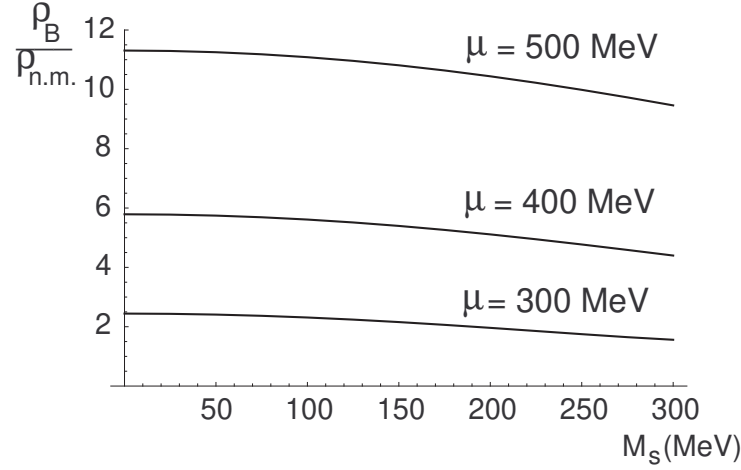


FIG. 25 The ratio of the baryon density of the free quark gas to the nuclear baryon density vs. M_s , for three values of the average chemical potential.

and a baryon density about 4.4 times the nuclear matter density. With $M_s = 200$ MeV the result is $\mu_e = 24$ MeV (25 MeV from the approximate equation) and

$$p_F^u = 384 \text{ MeV}; \quad p_F^d = 408 \text{ MeV}; \quad p_F^s = 357 \text{ MeV}; \quad (6.27)$$

and a baryon density about 5.1 times the nuclear matter density. To go to baryon densities relevant to the central core of the star, i.e. densities from 6 to 8 times the nuclear matter density, one needs to go to higher values of μ and lower values of M_s where the difference among of the Fermi momenta is lower. This can be seen from Fig. 26, or using our approximate expression for μ_e :

$$p_F^u = \frac{M_s^2}{6}; \quad p_F^d = \frac{M_s^2}{12}; \quad p_F^s = \frac{5M_s^2}{12}; \quad (6.28)$$

with

$$p_F^d = p_F^u = p_F^s = \frac{M_s^2}{4}; \quad (6.29)$$

The previous results are rather general, but in order to discuss the possible astrophysical applications we need to fix a value for μ_0 . Notice that we can trade the coupling constant G (see Eq. (4.55)) for μ_0 since G is fixed once we give the cutoff Λ . On the other hand, the equation for the chiral gap (Rajagopal and Wilczek, 2001) gives a relation between the NJL cutoff $\Lambda = \Lambda_c + \Delta$, the coupling G and the constituent quark mass. By taking the constituent mass around 300–400 MeV and fixing Δ , one has still a parameter to play around and it is possible to get values of μ_0 from about 20 MeV up to about 100 MeV. In the present case, since the typical value of μ inside the LOFF window is $0.7 \mu_0$ and

$$\mu = \frac{1}{2}(\mu_d + \mu_u) = \frac{1}{2}\mu_e; \quad (6.30)$$

we can reproduce approximately the situation illustrated at the beginning of this Subsection with $M_s = 300$ MeV by choosing $\mu_0 = 40$ MeV. With this choice the LOFF grand potential at $\mu = \mu_1$ is of the order 10^{-7} GeV^4 which, as we shall see in Section VI H, is of the right order of magnitude to give rise to the glitch phenomena (Alford et al., 2000). Notice also that the LOFF condensate evaluated at μ_1

$$\Delta_{\text{LOFF}}(\mu_1) \approx 0.25 \mu_0 = 10 \text{ MeV} \quad (6.31)$$

is much larger than a typical temperature of neutron stars, of the order of keV's.

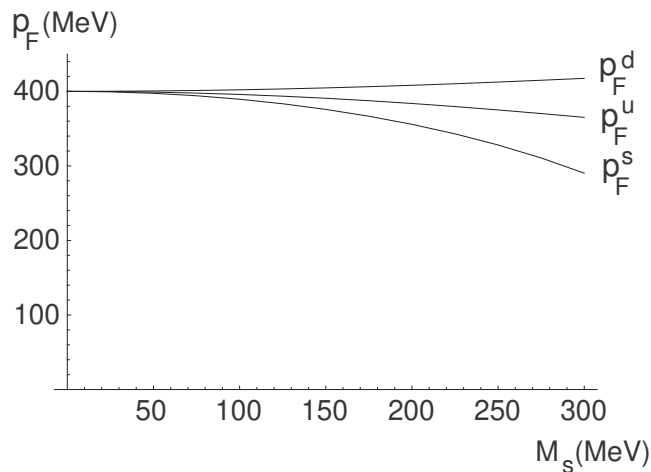


FIG. 26 The Fermi momenta of the three quarks vs. M_s .

H. Astrophysical implications of the QCD LOFF phase

While a great experimental effort is devoted to the search of the LOFF phase in condensed matter, so far nothing similar happens for the crystalline phase of QCD. The reason is that it is difficult to create the experimental conditions of high density and low temperature for hadronic matter. The crystalline superconducting phase of quarks may however result relevant for astrophysical dense systems, in particular in the explanation of pulsar glitches. Pulsars are rapidly rotating stellar objects, characterized by the presence of strong magnetic fields and by an almost continuous conversion of rotational energy into electromagnetic radiation. The rotation periods can vary in the range 10^{-3} sec up to a few seconds; these periods increase slowly and never decrease except for occasional glitches, i.e. sudden increases of the rotational frequencies, when the pulsar spins up with a variation in frequency of the order of $\Delta \nu = 10^6$ or smaller. Glitches are a typical phenomenon of the pulsars, since probably all the pulsars experience them.

Pulsars are commonly identified with neutron stars; these compact stars are characterized by a complex structure comprising a core, an intermediate region with superfluid neutrons and a metallic crust. With a chemical potential of the order of 400 MeV, as we have seen, the conditions for color superconductivity in the CFL or the LOFF versions might be reached in the core. Before examining this possibility, let us however describe the standard explanation of glitches, in the form originated by the papers (Alpar et al., 1984a; Anderson and Itoh, 1973). This model is based on the idea that the sudden jumps of ν are due to the movements outwards of rotational vortices in the neutron superfluid and their interaction with the crust. Crucial ingredients of the model are therefore the existence of a superfluid and a crystal (the metallic crust). This is one of the main reasons that allows the identification of pulsars with neutron stars, as only neutron stars are supposed to have a metallic crust. The LOFF state can be relevant in this context because, if there is a LOFF phase inside the pulsar, the superfluid might interact with the LOFF crystal instead of the crust, thus providing an alternative or complementary mechanism for the glitches. Thus far, there is no developed model for the pinning of the superfluid vortices to the QCD LOFF crystals within compact stars. Therefore we limit our survey to an introduction to the subject, along the lines of (Alford, 2000; Alford et al., 2001b; Nardulli, 2002c).

Let us consider a compact star whose metallic crust rotates with angular velocity Ω . The superfluid inside the star should not rotate because, in absence of friction, the crust cannot communicate its rotation to the superfluid component. The velocity of the superfluid is $\mathbf{v}_s = \frac{\hbar}{m} \nabla \phi$ where ϕ is the phase of the superfluid condensate wave function. The consequence of this formula would be $\nabla \cdot \mathbf{v}_s = 0$. This would imply the absence of rotation in the superfluid, which however does not correspond to the state of minimal energy (for a discussion see (Landau et al., 1980)). The correct condition is

$$\nabla \cdot \mathbf{v}_s = 2\pi n \quad ; \quad (6.32)$$

where \hbar is the quantum of vorticity: $\hbar = \frac{h}{m}$. For Eq. (6.32) to hold the curve ϕ must wind a singular point; the integer n is the winding number which counts the number of times the curve goes around the singular point; the most energetically favorable condition is realized by $n = 1$. If ϕ is in a plane the condition (6.32) holds for any plane and the locus of the singular points is a vortex line (v.l.). In absence of rotation there are no v.l.'s; the minimal angular

velocity v_{min} for the formation of the first vortex line is

$$v_{crit} = \frac{h}{mR^2} \ln \frac{R}{a} ; \quad (6.33)$$

Here we are assuming a cylindrical configuration with radius R ; a is a cutoff of the order of the interatomic distances. By increasing a also the number N of vortex lines per unit area in the superfluid increases according to the formula:

$$N = \frac{m}{h} \quad (6.34)$$

and one gets, instead of (6.32),

$$\oint_C \mathbf{v} \cdot d\mathbf{l} = N A^2 ; \quad (6.35)$$

where A is the area encircled by C . Eventually the v.l.'s tend to fill all the space. As a numerical example one can estimate N for the pulsar in the Crab nebula. Here $m = 2m_N$ (the condensate is formed by neutral bosons: pairs of neutrons) and $\omega = \omega_{pulsar}$ gives $N \approx 1.9 \cdot 10^6 \text{ cm}^{-2}$ with an average distance between vortex lines $d = N^{-1/2} \approx 10^{-2} \text{ cm}$. If the vortex line is a straight line, \mathbf{v}_s is perpendicular both to the vortex line and to the radius joining the singular point and the point at which we compute \mathbf{v}_s . At a distance r from the singular point one has

$$v_s = \frac{n}{r} ; \quad (6.36)$$

as can be immediately seen from (6.32). More generally:

$$\mathbf{v}_s = \frac{1}{2} \frac{\nabla \times \mathbf{R}}{R^3} ; \quad (6.37)$$

where \mathbf{R} is the distance vector from the vortex line to the point at which we compute the superfluid velocity.

During the rotation the vortex lines follow the rotational motion of the vessel, which is clear because they are pinned at the boundary of the superfluid; in particular, for rotations around an axis, the vortex lines are, by symmetry, straight lines parallel to the rotation axis. Their motion imitates the motion of the liquid as a whole and, as a consequence, also for the superfluid one can use the hydrodynamical formula

$$\mathbf{v} = \frac{1}{2} \nabla \times \mathbf{v}_s ; \quad (6.38)$$

which in principle would be valid only for the normal component.

Let now $n(r)$ be the number of vortices per unit area at a distance r from the rotation axis; if $\mathbf{v} = \mathbf{v}_s$ is the superfluid velocity, one gets

$$\oint_C \mathbf{v} \cdot d\mathbf{l} = \int_0^{Z_r} \int_0^{2\pi} \mathbf{r} \cdot \mathbf{v} = 2 \int_0^{Z_r} \int_0^{2\pi} r^2 n(r^0) dr^0 ; \quad (6.39)$$

We put $k = 2\pi \hbar = h/2m_n$ and write (6.39) as follows:

$$2\pi r^2 n(r) = k \int_0^{Z_r} 2\pi r^2 n(r^0) dr^0 ; \quad (6.40)$$

which implies

$$k n(r) = 2\pi n(r) + r \frac{\partial n}{\partial r} ; \quad (6.41)$$

Since the total number of v.l.'s is conserved, one has

$$\frac{\partial n}{\partial t} + \mathbf{v}_r \cdot \nabla n = 0 ; \quad (6.42)$$

where \mathbf{v}_r is the radial component of the superfluid velocity. We write (6.40) as

$$2\pi r^2 n(r) = k \int_0^{Z_r} dS \quad (6.43)$$

and take the time derivative, using (6.42) to get

$$2 r^2 \frac{\partial}{\partial t} = k \int_0^Z r dS r \quad (r \neq 0) : \quad (6.44)$$

Using the Gauss theorem one gets $2 r^2 \frac{\partial}{\partial t} = k 2 r v_r$, i.e.

$$\frac{\partial}{\partial t} = \frac{k v_r}{r} = 2 \dot{\omega}(r) + r \frac{\partial}{\partial r} \frac{v_r}{r} : \quad (6.45)$$

Eq. (6.45) shows that the only possibility for the superfluid to change its angular velocity ($\neq 0$) is by means of a radial motion, i.e. $v_r \neq 0$.

Let us now consider a rotating superfluid in contact with rotating normal matter on which an external torque is acting (Alpar et al., 1984a). We denote by I_c and ω_c the moment of inertia and angular velocity of the normal components that, in a neutron star, includes the crust and possibly other normal components. The equation of motion of the normal component is

$$I_c \dot{\omega}_c(t) = M_{ext} + M_{int} : \quad (6.46)$$

Besides the external torque M_{ext} , basically related to the spin down of the pulsar (or the steady accretion in binary pulsars), we have included the internal torque M_{int} due to the interaction with the superfluid:

$$M_{int} = \int dI_p - (r; t) \quad (6.47)$$

where dI_p is the infinitesimal moment of inertia of the superfluid component. Eqs. (6.45-6.47) are the equations of motion for the angular velocities ω_c and ω_s (superfluid and crust). The two velocities are coupled not only through M_{int} , but also by v_r , because we will show below that v_r depends on the difference $\omega_c - \omega_s$. We note again that fundamental for this model is the existence of radial motion, for, if $v_r = 0$, then $\omega_c = \text{const.}$ and only ω_s changes, due to the external torque alone.

In the neutron star, superfluid neutrons (in Cooper pairs) coexist with nuclei of the crust. Also in the crust there are superfluid neutrons, but they are characterized by a different (and smaller) ξ . Computing the difference in the free energies between the two phases one obtains the difference of pressures and, consequently, the force per unit length of vortex line. Let b be the average distance between the nuclei; b is also the average distance between two consecutive pinning centers. Let us assume

$$2 \xi_0 < b ; \quad (6.48)$$

where ξ_0 is the superconducting coherence length, which also gives the dimension of the vortex core, since ξ_0 is of the order of the spatial extension of the Cooper pair. The maximum pinning force is obtained when the vortex passes through one layer of the lattice; therefore the maximum force per unit length of vortex line is

$$f_p \sim \frac{E_p}{b} ; \quad (6.49)$$

where

$$E_p = F_s - F_c / \xi_s^2 ; \quad (6.50)$$

where F_s and F_c are the free energies of the superfluid neutrons and the nucleons in the crust; ξ_s is the gap for superfluid neutrons and one can neglect ξ_c , the gap of superfluid neutrons in the crust since $\xi_c \ll \xi_s$. Eq. (6.50) implies that neutrons tend to remain in the volume V of the vortex core because they experience a force repelling them from the superconducting phase (if neutron rich nuclei are present, the repulsion will be less important). Typical values for the pinning energy per nucleus E_p at densities $3 \cdot 10^3 - 1.2 \cdot 10^4 \text{ g/cm}^3$ are

$$E_p = 1 - 3 \text{ MeV} ; \quad (6.51)$$

while $b = 25 - 50 \text{ fm}$ and $\xi_0 = 4 - 20 \text{ fm}$ give

$$f_p = 40 - 1200 \text{ MeV}^3 ; \quad (6.52)$$

On the basis of these considerations let us now sketch a possible mechanism for the formation of glitches (Apar, 1977; Apar et al., 1984a,b; Anderson and Itoh, 1973) (for further references see below). We consider the rotating neutron star with superfluid neutrons in its interior and a metallic crust, which is a simplified model, but adequate to our purposes. As stressed already, we distinguish between the superfluid velocity \mathbf{v}_s and the crust velocity \mathbf{v}_c . Let us suppose that they are initially equal, which is a consequence of the pinning. Due to the spinning down of the star, \mathbf{v}_c decreases; as long the vortex cores are pinned to the crust lattice, the neutron superfluid cannot spin down, because the radial motion is forbidden. There is therefore a relative velocity of the superfluid with respect to the pinned vortex core because $\mathbf{v}_s > \mathbf{v}_c$:

$$\mathbf{v} = (\mathbf{v}_s - \mathbf{v}_c) \wedge \mathbf{r} : \quad (6.53)$$

The interaction between the normal matter in the core of the v.l. and the rest of normal matter (nuclei in the lattice, electrons, etc.) produces a Magnus force per unit length given by

$$\mathbf{f} = k \wedge \mathbf{v} ; \quad (6.54)$$

where the direction of \mathbf{k} coincides with the rotation axis and its modulus is equal to the quantum of vorticity. \mathbf{f} is the force exerted on the vortex line; as it cannot be larger than f_p there is a maximum difference of angular velocity that the system can maintain:

$$\dot{\Omega}_{cr} = (\dot{\Omega}_c)_{max} = \frac{f_p}{k r} = \frac{E_p}{k b} : \quad (6.55)$$

If $\dot{\Omega} < \dot{\Omega}_{cr}$ the vortices remain pinned at the lattice sites instead of moving with the superfluid as they generally do inside it (see discussion above). On the contrary, if $\dot{\Omega} > \dot{\Omega}_{cr}$, the hydrodynamical forces arising from the mismatch between the two angular velocities ultimately break the crust and produce the conditions for the glitch. A possible way to get it is by the observation following Eq. (6.45). If a bunch of vortex lines are unpinned and move outwards then eq. (6.45) implies that the angular velocity (and the angular momentum) of the superfluid decreases, and, therefore, the angular momentum of the crust increases, which is revealed from outside as a spin up of the star, i.e. a glitch. A numerical analysis would imply solving the set of Eqs. (6.45–6.47), but this is outside the scope of the present review⁵. Let us instead discuss the possible role of the LOFF phase in this context. The QCD LOFF phase provides a lattice structure independently of the crust. Therefore it meets one of the two requirements of the model for glitches in pulsars we have outlined above, the other being the presence of a superfluid. On the other hand the only existing calculations for the inhomogeneous phase in color superconductivity have been performed for the case of two flavors, which however, in the homogeneous case, does not present superfluidity, since there are no broken global symmetries. Superfluidity is on the other hand manifested by the CFL phase of QCD. Therefore a realistic application to QCD superfluid has to wait until a calculation of the LOFF phase with three flavors will be completed. For the time being one can give some order of magnitude estimates (Alford et al., 2001b). Let us assume the following choice of the parameters: $\mu_{2SC} = 40 \text{ MeV}$, $\mu_{LOFF} = 8 \text{ MeV}$, corresponding to the Fulde-Ferrel state; since $q = 1/2$ and $\mu_{2SC} = 0.7 \mu_{LOFF}$, one would get for the average distance between nodal planes $b = (2\pi/q) \approx 9 \text{ fm}$ and for the superconducting coherence length $\xi_0 = 6 \text{ fm}$. From (3.28), with $\mu = \mu_1$ and an extra factor of 4 to take into account the two flavors and the two colors, we get the free energy per volume unit as follows⁶: $\mathcal{F}_{LOFF} = 8 \cdot (10 \text{ MeV})^4$ and therefore, from (6.50), the pinning energy of the vortex line is

$$E_p = \mathcal{F}_{LOFF} j b^3 = 6 \text{ MeV} : \quad (6.56)$$

To get the pinning force we cannot use (6.49) since (6.48) does not hold in this case. For an order of magnitude estimate one can use

$$f_p \sim \frac{E_p}{b^2} ; \quad (6.57)$$

giving a pinning force per unit length of the vortex of the order of

$$f_p \sim 3 \cdot 10^3 \text{ MeV}^3 : \quad (6.58)$$

⁵ Models differ in the mechanism by which angular momentum is released; instead of performing outward movements for example v.l.'s might break the crust or rearrange it. For reviews see (Apar, 1995; Pines and Apar, 1985) and, more recently, (Apar et al., 1993; Epstein and Baym, 1992; Link and Epstein, 1996; Ruderman, 1991; Ruderman et al., 1998).

⁶ Using the exact expression instead of (3.28), that is valid only in the weak coupling limit, one would get $\mathcal{F}_{LOFF} = 5 \cdot (10 \text{ MeV})^4$.

Comparing these numerical values with Eqs. (6.51) and (6.52) one can see that these order of magnitude estimates give figures similar and therefore some of the glitches in neutron stars may be generated well inside the star by vortices related to the LOFF phase of QCD.

As we already stated these conclusions are tentative because the analysis of the QCD LOFF phase needs extension to the three flavor case; moreover the true ground state is likely to be different from the Fulde-Ferrel one plane wave structure. Nevertheless they are encouraging and leave open the possibility that neutron stars might give another laboratory where to study the inhomogeneous superconducting phase. It can be useful to stress that even in quark stars, in the QCD superconducting LOFF phase, one would get a crystal structure given by a lattice characterized by a geometric array where the gap parameter varies periodically. This would overcome the objection that pulsars cannot be strange stars. This objection is based on the following observation: If strange matter there exists, quark stars should be rather common; however, in absence of metallic crusts, strange stars can hardly develop vortices, at least by the model we have described here. On the contrary, if the color superconductivity is able to produce a crystalline structure it could also give rise to glitches and the argument in favor of the existence of strange stars would be reinforced.

VII. CONCLUSIONS

Inhomogeneous crystalline superconductivity was predicted forty years ago by Larkin, Ovchinnikov, Fulde and Ferrell, but realistic conditions for its experimental investigations became available only a few years ago. In condensed matter the existence of the LOFF phase, with its characteristic space modulation of the energy gap, still awaits complete confirmation. This is due to the fact that it is indeed a subtle effect. It arises when the Fermi surfaces of the two species participating in the Cooper pairing are different. However for large separation pairing is not possible at all and superconductivity disappears altogether. In condensed matter the separation of the Fermi surfaces is obtained by a Zeeman splitting due to an exchange interaction due to a magnetic field. However the needed field strength is such to destroy superconductivity due to diamagnetic effects. As we discussed in the paper, the way to avoid the problem was to use unconventional superconductors such as organic compounds. These materials have in fact a layered structure and therefore, if the magnetic field is parallel to the layers, the orbital effects can be controlled.

New opportunities have recently arisen to detect the LOFF phase in atomic physics (ultracold atomic gases), nuclear physics and especially quark matter. This last development is a consequence of the recent excitement generated by the study of QCD at high density and small temperature. Inhomogeneous crystalline superconductivity in this context could be generated by the difference in quark chemical potentials induced by weak interactions in the inner core of pulsars. Their main phenomenological effect might therefore be to provide a mechanism for the explanation of glitches in pulsars. If pulsars are neutron stars with a core made up by color superconducting matter, this mechanism would be complementary to the standard models of glitches. If pulsars are strange stars, then the crystalline structure of the condensate would provide the possibility for pinning the superfluid vortices and eventually creating the glitches.

This paper was mainly aimed to the presentation of a unified formalism to describe the LOFF phase both in condensed and hadronic matter. The simplest way in our opinion to describe superconductivity effects, including the LOFF state, is by the effective lagrangian approach. Since they are based on the general mathematical ground of the Renormalization Group, effective lagrangians allow the conditions for this unification. The existence of a common mathematical basis should allow experts of one side to fully appreciate and take advantage of the progresses made in the other. We would be gratified if this paper turned out to be useful to this end.

Acknowledgments

One of us (G.N.) would like to thank CERN Theory Division for the kind hospitality offered during the completion of this paper. We would like to thank R. Gatto for his invaluable help in common work and for reading the manuscript and E. Fabiano, and M. Mannarelli for the very pleasant scientific collaboration. We also wish to thank K. Rajagopal for a number of useful discussions on color superconductivity and the LOFF phase. Our thanks are finally due to M. Alford, J. Bowers, M. Cimiale, R. Combescot and H. Shimahara for useful correspondence on the present review.

APPENDIX A : Calculation of J and K

We give here an outline of the calculation of the integrals J and K appearing in the GL expansion at $T = 0$. Using the definition of J, Eq. (3.5), and K, eq. (3.6), we have

$$\begin{aligned} J &= J(q_1; q_2; q_3; q_4) = + \frac{ig}{2} \int_{-1}^1 \frac{d\omega}{4} \int_{-1}^1 d\omega_1 \frac{dE}{2} \sum_{i=1}^4 Y^4 f_i(E; \omega; \omega_1; q) \\ &= + \frac{ig}{2} \int_{-1}^1 \frac{d\omega}{4} \int_{-1}^1 d\omega_1 \frac{dE}{2} \sum_{i=1}^4 Y^2 \frac{1}{E + i \operatorname{sign} E + \omega + 2\omega_1 k} \\ &\quad \frac{1}{E + i \operatorname{sign} E + 2\omega_1 k} ; \end{aligned} \quad (A1)$$

$$\begin{aligned} K &= K(q_1; q_2; q_3; q_4; q_5; q_6) = \frac{ig}{2} \int_{-1}^1 \frac{d\omega}{4} \int_{-1}^1 d\omega_1 \frac{dE}{2} \sum_{i=1}^6 Y^6 f_i(E; \omega; \omega_1; q) \\ &= \frac{ig}{2} \int_{-1}^1 \frac{d\omega}{4} \int_{-1}^1 d\omega_1 \frac{dE}{2} \sum_{i=1}^6 Y^3 \frac{1}{E + i \operatorname{sign} E + \omega + 2\omega_1 k} \\ &\quad \frac{1}{E + i \operatorname{sign} E + 2\omega_1 k} ; \end{aligned} \quad (A2)$$

where we have defined

$$\begin{aligned} k_1 &= 0; \quad k_2 = q_1 - q_2; \quad k_3 = q_1 - q_2 + q_3 - q_4; \\ \omega_1 &= q_1; \quad \omega_2 = q_1 - q_2 + q_3; \quad \omega_3 = q_1 - q_2 + q_3 - q_4 + q_5; \end{aligned} \quad (A3)$$

with the conditions $q_1 - q_2 + q_3 - q_4 = 0$ and $q_1 - q_2 + q_3 - q_4 + q_5 - q_6 = 0$ for J and K respectively. We introduce the Feynman variables x_j, y_j ($j = 1, 2$ for J and $j = 1, 2, 3$ for K) to form the vectors $k = \sum_i x_i k_i$ and $\omega = \sum_i y_i \omega_i$; after rotation of the energy integration contour $E \rightarrow i p_4$ we get:

$$\begin{aligned} \int_{-1}^1 \frac{dE}{2} \sum_{i=1}^4 \frac{Y^4}{E + \omega + 2\omega_1 k} &= \int_{-1}^1 \frac{dp_4}{2} \frac{(1 - p_4 x_k)}{[p_4 + \omega + 2\omega_1 k]^2} dx_n; \\ \int_{-1}^1 \frac{dE}{2} \sum_{i=1}^6 \frac{Y^6}{E + \omega + 2\omega_1 k} &= \int_{-1}^1 \frac{dp_4}{2} \frac{(1 - p_4 y_k)}{[p_4 + \omega + 2\omega_1 k]^2} dy_n; \end{aligned} \quad (A4)$$

next we perform the integration by the residues method and the angular integration; for J the result is

$$J = \frac{ig}{8} \int_{-1}^1 dp_4 (p_4) \int_{-1}^1 \sum_{n=1}^4 Y^2 dx_n dy_n \frac{(1 - p_4 x_k) (1 - p_4 y_k)}{[(ip_4)^2 + v_F^2 k^2 + y_j^2]^2}; \quad (A5)$$

After the energy integration we remain with

$$J = \frac{g}{8} \int_{-1}^1 \sum_{n=1}^4 Y^2 dx_n dy_n \int_{-1}^1 \sum_{k=1}^4 x_k \int_{-1}^1 \sum_{k=1}^4 y_k \frac{1}{[v_F^2 k^2 + y_j^2]^2}; \quad (A6)$$

This expression is general; we can specialize it to the various crystal structures, as explained in the text.

For K we get, instead of (A5), the result

$$\begin{aligned} K &= \frac{3ig}{8} \int_{-1}^1 dp_4 (p_4) \int_{-1}^1 \sum_{n=1}^6 Y^3 dx_n dy_n \int_{-1}^1 \sum_{k=1}^4 x_k \int_{-1}^1 \sum_{k=1}^4 y_k \\ &\quad \frac{1}{[(ip_4)^2 + v_F^2 k^2 + y_j^2]^4}; \end{aligned} \quad (A7)$$

which, after energy integration, becomes

$$K = \frac{g}{16} \int_{-1}^1 \sum_{n=1}^6 Y^3 dx_n dy_n \int_{-1}^1 \sum_{k=1}^4 x_k \int_{-1}^1 \sum_{k=1}^4 y_k \frac{1}{[v_F^2 k^2 + y_j^2]^3}; \quad (A8)$$

APPENDIX B: Expansion of Ω around the tricritical point

Let us consider the expansion of $\Omega(q)$ in $Q = qv_F$, at finite T and μ , which can be obtained from Eq. (3.4) after introducing the Matsubara frequencies:

$$\Omega(q) = \frac{1}{2}gT \sum_{n=-1}^Z \frac{d\omega}{4} \sum_{n=-1}^Z \frac{1}{(i\omega_n^2 + \omega^2 - \epsilon_F)(i\omega_n^2 + \omega^2)}; \quad (B1)$$

Expanding the first denominator in the momentum q we find

$$\Omega(q) = \frac{1}{2}gT \sum_{n=-1}^Z \frac{d\omega}{4} \sum_{n=-1}^Z \frac{1}{i\omega_n^2 + \omega^2} \sum_{m=0}^Z \frac{(2\omega - \epsilon_F)^{2m}}{(i\omega_n^2 + \omega^2)^{m+1}}; \quad (B2)$$

where, as in Eq. (2.70),

$$\omega_n = \omega_n + i\eta; \quad (B3)$$

Notice that we have inverted the sum over the Matsubara frequencies with the integration over ω . In this way, as we did for the homogeneous case, we are converting the divergence in ω into a divergence in the series, which can be treated as before by introducing a cutoff in the sum. Performing the angular integration and the integration over ω with the help of the following integral

$$\sum_{n=-1}^Z \frac{1}{i\omega_n^2 + \omega^2} \frac{1}{(i\omega_n^2 + \omega^2)^{m+1}} = (-1)^m \frac{1}{2^{2m} \omega_n^{2m+1}}; \quad (B4)$$

we get eventually

$$\Omega(q) = \frac{1}{2}gT \sum_{n=-1}^Z \sum_{m=0}^Z \frac{(-1)^m}{2^{2m+1}} \frac{Q^{2m}}{\omega_n^{2m+1}}; \quad (B5)$$

By using the definition of the first term in the grand potential as $\Omega(q)$ multiplied by $2=g$ we recover easily the expression (3.42) for $\tilde{\Omega}$. In analogous way, to get $\tilde{\Omega}$ and $\tilde{\Omega}$ one proceeds expanding J (see Eq. (3.5) and K (see Eq. (3.6)).

References

- Abrikosov, A. A., 1957, Zh. Exptl. teor. Fiz. 32, 1442.
- Abrikosov, A. A., L. P. Gor'kov, and I. E. Dzyaloshinski, 1963, Methods of Quantum Field Theory in Statistical Physics (Dover, New York).
- Agasian, N. O., B. O. Kerbikov, and V. I. Shevchenko, 1999, Phys. Rept. 320, 131.
- Agterberg, D. F., and K. Yang, 2001, J. Phys.: Condens. Matter 13, 9259.
- Akhiezer, A. I., A. A. Isayev, S. V. Peletnitsky, and A. A. Yatsenko, 1999, Phys. Lett. B 451, 430.
- Akhiezer, A. I., V. V. Krasilnikov, S. V. Peletnitsky, and A. A. Yatsenko, 1994, Phys. Rep. 245, 1.
- Alexander, J. A. X., T. P. Orlando, D. Rainer, and P. M. Tedrow, 1985, Phys. Rev. B 31, 5811.
- Alexander, S., and J. M. C. Tague, 1978, Phys. Rev. Lett. 41, 702.
- Alford, M. G., 2000, eprint hep-ph/0003185.
- Alford, M. G., 2001, Ann. Rev. Nucl. Part. Sci. 51, 131.
- Alford, M. G., J. Berges, and K. Rajagopal, 1999a, Nucl. Phys. B 558, 219.
- Alford, M. G., J. Berges, and K. Rajagopal, 2000, Nucl. Phys. B 571, 269.
- Alford, M. G., J. A. Bowers, J. M. Cheyne, and G. A. Cowan, 2003, Phys. Rev. D 67, 054018.
- Alford, M. G., J. A. Bowers, and K. Rajagopal, 2001a, J. Phys. G 27, 541.
- Alford, M. G., J. A. Bowers, and K. Rajagopal, 2001b, Phys. Rev. D 63, 074016.
- Alford, M. G., K. Rajagopal, and F. W. Ilczek, 1998, Phys. Lett. B 422, 247.
- Alford, M. G., K. Rajagopal, and F. W. Ilczek, 1999b, Nucl. Phys. B 537, 443.
- Alm, T., B. L. Friman, G. Roepke, and H. Schulz, 1993, Nucl. Phys. A 551, 45.
- Alm, T., G. Roepke, and M. Schmidt, 1990, Z. Phys. A 337, 355.
- Alm, T., G. Roepke, A. Sedrakian, and F. W. I. eber, 1996, Nucl. Phys. A 406, 491.
- Alpar, M. A., 1977, Astrophys. J. 213, 527.
- Alpar, M. A., 1995, in M. A. Alpar et al. eds., The Lives of Neutron Stars (Kluwer), p. 185.

- Alpar, M. A., P. Anderson, D. Pines, and J. Shaham, 1984a, *Astrophys. J.* 276, 325.
- Alpar, M. A., P. Anderson, D. Pines, and J. Shaham, 1984b, *Astrophys. J.* 278, 791.
- Alpar, M. A., H. F. Chau, K. S. Cheng, and D. Pines, 1993, *Astrophys. J.* 409, 345.
- Anderson, M. H. et al., 1995, *Science* 269, 198.
- Anderson, P., and N. Itoh, 1973, *Nature* 256, 25.
- Anderson, P. W., 1959, *J. Phys. Chem. Solids* 11, 26.
- Aoi, K., W. D. Dietrich, and P. Fulde, 1974, *Z. Physik B* 267, 223.
- Aslamazov, L. G., 1969, *Sov. Phys. JETP* 28, 773.
- Bailin, D., and A. Love, 1984, *Phys. Rept.* 107, 325.
- Baldo, M., I. Bombaci, and U. Lombardo, 1992, *Phys. Lett. B* 283, 8.
- Balicas, L., J. Brooks, K. Storr, S. Uchi, M. Tokumoto, H. Tanaka, H. Kobayashi, A. Kobayashi, V. Barzykin, and L. P. Gor'kov, 2001, *Phys. Rev. Lett.* 87, 067002.
- Bardeen, J., L. N. Cooper, and J. R. Schrieffer, 1957, *Phys. Rev.* 106, 162.
- Barrois, B. C., 1977, *Nucl. Phys. B* 129, 390.
- Barzykin, V., and L. P. Gor'kov, 2002, *Phys. Rev. Lett.* 89, 22702.
- Beane, S. R., and P. F. Bedaque, 2000, *Phys. Rev. D* 62, 117502.
- Beane, S. R., P. F. Bedaque, and M. J. Savage, 2000, *Phys. Lett. B* 483, 131.
- Beane, S. R., P. F. Bedaque, and M. J. Savage, 2001, *Nucl. Phys. A* 688, 931.
- Bedaque, P. F., 2002, *Nucl. Phys. A* 697, 569.
- Benfatto, G., and G. Gallavotti, 1990, *Phys. Rev. B* 42, 9967.
- Berges, J., and K. Rajagopal, 1999, *Nucl. Phys. B* 538, 215.
- Bernhard, C. et al., 1999, *Phys. Rev. B* 59, 14099.
- Bowers, J. A., J. Kundu, K. Rajagopal, and E. Shuster, 2001, *Phys. Rev. D* 64, 014024.
- Bowers, J. A., and K. Rajagopal, 2002, *Phys. Rev. D* 66, 065002.
- Bradley, C. C., C. A. Sackett, and R. G. Hulet, 1997, *Phys. Rev. Lett.* 78, 985.
- Brown, W. E., J. T. Liu, and H.-C. Ren, 2000a, *Phys. Rev. D* 62, 054013.
- Brown, W. E., J. T. Liu, and H.-C. Ren, 2000b, *Phys. Rev. D* 61, 114012.
- Brown, W. E., J. T. Liu, and H.-C. Ren, 2000c, *Phys. Rev. D* 62, 054016.
- Bulaevskii, L. N., 1973, *Sov. Phys. JETP* 37, 1133.
- Bulaevskii, L. N., 1974, *Sov. Phys. JETP* 38, 634.
- Burkhardt, H., and D. Rainer, 1994, *Ann. Physik* 3, 181.
- Buzdin, A. I., and Kachkachi, 1997, *Phys. Lett. A* 225, 341.
- Buzdin, A. I., and M. L. Kubic, 1984, *J. Low Temp. Phys.* 54, 203.
- Buzdin, A. I., and S. V. Polonski, 1987, *Zh. Exp. teor. Fiz.* 93, 747.
- Buzdin, A. I., and V. V. Tugushev, 1983, *Zh. Exp. teor. Fiz.* 85, 735.
- Carter, G. W., and D. Diakonov, 1999, *Phys. Rev. D* 60, 016004.
- Casalbuoni, R., 2001, *AIP Conf. Proc.* 602, 358.
- Casalbuoni, R., F. DeFazio, R. Gatto, G. Nardulli, and M. Ruggieri, 2002a, *Phys. Lett. B* 547, 229.
- Casalbuoni, R., Z.-y. Duan, and F. Sannino, 2000, *Phys. Rev. D* 62, 094004.
- Casalbuoni, R., E. Fabiano, R. Gatto, M. Mannarelli, and G. Nardulli, 2002b, *Phys. Rev. D* 66, 094006.
- Casalbuoni, R., and R. Gatto, 1999, *Phys. Lett. B* 464, 111.
- Casalbuoni, R., R. Gatto, M. Mannarelli, and G. Nardulli, 2001a, *Phys. Lett. B* 511, 218.
- Casalbuoni, R., R. Gatto, M. Mannarelli, and G. Nardulli, 2002c, *Phys. Rev. D* 66, 014006.
- Casalbuoni, R., R. Gatto, M. Mannarelli, and G. Nardulli, 2002d, *Phys. Lett. B* 524, 144.
- Casalbuoni, R., R. Gatto, and G. Nardulli, 2001b, *Phys. Lett. B* 498, 179.
- Casalbuoni, R., R. Gatto, and G. Nardulli, 2002e, *Phys. Lett. B* 543, 139.
- Casalbuoni, R., R. Gatto, G. Nardulli, and M. Ruggieri, 2003, *eprint hep-ph/0302077*.
- Casalbuoni, R., et al., 1997, *Phys. Rept.* 281, 145.
- Chandrasekhar, B. S., 1962, *App. Phys. Lett.* 1, 7.
- Clogston, A. M., 1962, *Phys. Rev. Lett.* 9, 266.
- Collins, J. C., and M. J. Perry, 1975, *Phys. Rev. Lett.* 34, 1353.
- Combesoot, R., 2000, *eprint cond-mat/0007191*.
- Combesoot, R., and C. Mora, 2002, *eprint cond-mat/0203031*.
- Cooper, L. N., 1956, *Phys. Rev.* 104, 1189.
- Davis, K. B. et al., 1995, *Phys. Rev. Lett.* 75, 3969.
- Decroux, M., and J. Fischer, 1982, in M. B. Maple and J. Fischer eds., *Superconductivity in Ternary Compounds, Part II* (Springer, Heidelberg), p. 57.
- DeMarco, B., and D. S. Jin, 1999, *Science* 285, 1703.
- DeMarco, B., S. B. Papp, and D. S. Jin, 2001, *Phys. Rev. Lett.* 86, 5409.
- Deryagin, D. V., D. Y. Grigoriev, and V. A. Rubakov, 1992, *Int. J. Mod. Phys. A* 7, 659.
- Dupuis, N., 1995, *Phys. Rev. B* 51, 9074.
- Dupuis, N., G. Montambaux, and C. A. R. Sade Melo, 1993, *Phys. Rev. Lett.* 70, 2613.
- Dyugaev, A. M., I. D. Vagner, and P. Wyder, 2001, *eprint cond-mat/0112286*.
- Eichten, E., and B. Hill, 1990, *Phys. Lett. B* 234, 511.

- Eilenberger, G., 1968, *Z. Physik* 214, 195.
- Epstein, R. I., and G. Baym, 1992, *Astrophys. J.* 387, 276.
- Evans, N., J. Homuzdiar, S. D. H. Hsu, and M. Schwetz, 2000, *Nucl. Phys. B* 581, 391.
- Evans, N., S. D. H. Hsu, and M. Schwetz, 1999a, *Nucl. Phys. B* 551, 275.
- Evans, N., S. D. H. Hsu, and M. Schwetz, 1999b, *Phys. Lett. B* 449, 281.
- Frautschi, S. C., 1978, presented at Workshop on Hadronic Matter at Extreme Energy Density, Erice, Italy, Oct 13-21, 1978.
- Fried, D. G. et al., 1998, *Phys. Rev. Lett.* 81, 3811.
- Fulde, P., and R. A. Ferrell, 1964, *Phys. Rev.* 135, A 550.
- Gegebart, P. et al., 1996, *Ann. Physik* 5, 307.
- Georgi, H., 1990, *Phys. Lett. B* 240, 447.
- Giannakis, I., J. T. Liu, and H.-C. Ren, 2002, *Phys. Rev. D* 66, 031501.
- Ginzburg, L., and L. D. Landau, 1950, *Zh. Exsp. teor. Fiz.* 20, 1064.
- Ginzburg, V. L., 1957, *Sov. Phys. JETP* 4, 153.
- Glauber, K. et al., 1993, *Phys. Rev. Lett.* 70, 501.
- Goddard, P., S. Tozer, J. Singleton, A. Ardaavan, A. Abate, and M. Kumoo, 2002, *J. Phys. Condens. Matter* 14, L495.
- Goddard, A. L., 1999, *Phys. Rev. C* 60, 014311.
- Gorkov, L. P., 1959, *Zh. Exsp. teor. Fiz.* 36, 1918.
- Gorkov, L. P., 1960, *Sov. Phys. JETP* 10, 593.
- Gorkov, L. P., and A. G. Lebed', 1987, *Europhys. Lett.* 4, 941.
- Granade, S. R. et al., 2002, *Phys. Rev. Lett.* 88, 120405.
- Gross, D., and F. Wilczek, 1973, *Phys. Rev. Lett.* 30, 1343.
- Grunberg, L. W., and L. Gunther, 1966, *Phys. Rev. Lett.* 16, 996.
- Hadžiev, V. G. et al., 1999, *Phys. Status Solidi B* 211, R5.
- Hong, D. K., 2000a, *Nucl. Phys. B* 582, 451.
- Hong, D. K., 2000b, *Phys. Lett. B* 473, 118.
- Hong, D. K., 2001, *Acta Phys. Polon. B* 32, 1253.
- Hong, D. K., V. A. Miransky, I. A. Shovkovy, and L. C. R. Wijewardhana, 2000, *Phys. Rev. D* 61, 056001.
- Houzet, M., and A. Buzdin, 2000a, *Europhys. Lett.* 50, 375.
- Houzet, M., and A. I. Buzdin, 2000b, *Europhys. Lett.* 50, 375.
- Houzet, M., A. I. Buzdin, I. Bulavskii, and M. Maley, 2002, *Phys. Rev. Lett.* 88, 227001.
- Houzet, M., Y. Merdesoif, O. Coste, and A. I. Buzdin, 1999, *Physica C* 316, 89.
- Hsu, S. D. H., 2000, eprint hep-ph/0003140.
- Hsu, S. D. H., and M. Schwetz, 2000, *Nucl. Phys. B* 572, 211.
- Huxley, A. D. et al., 1993, *J. Phys.: Cond. Matter* 5, 7709.
- Isayev, A. A., 2002, *Phys. Rev. C* 65, 031302.
- Isgur, N., and M. B. Wise, 1989, *Phys. Lett. B* 232, 113.
- Isgur, N., and M. B. Wise, 1990, *Phys. Lett. B* 237, 527.
- Ishiguro, T., 2000, *J. Supercond.* 13, 817.
- Jaccarino, V., and M. Peter, 1962, *Phys. Rev. Lett.* 9, 290.
- Kamerlingh Onnes, H., 1911, *Leiden Comm.* 120b, 122b, 124c.
- Klein, U., D. Rainer, and H. Shimahara, 2000, *J. Low Temp. Phys.* 118, 91.
- Krey, U., 1973, *Int. J. Magn.* 4, 153.
- Kundu, J., and K. Rajagopal, 2002, *Phys. Rev. D* 65, 094022.
- Landau, L., and E. M. Lifshitz, 1996, *Statistical Physics, Part I* (Butterworth, Heinemann).
- Landau, L., E. M. Lifshitz, and L. P. Pitaevskii, 1980, *Statistical Physics, Part II* (Oxford: Pergamon).
- Larkin, A. J., and Y. N. Ovchinnikov, 1964, *Zh. Exsp. teor. Fiz.* 47, 1136.
- Le Bellac, M., 1996, *Thermal Field Theory* (Cambridge University Press, Cambridge, England).
- Lebed', A. G., 1986, *JETP Lett.* 44, 114.
- Leibovich, A. K., K. Rajagopal, and E. Shuster, 2001, *Phys. Rev. D* 64, 094005.
- Link, B., and R. I. Epstein, 1996, *Astrophys. J.* 457, 844.
- London, F., and H. London, 1935, *Proc. Roy. Soc. A* 149, 71.
- Machida, K., and H. Nakanishi, 1989, *Phys. Rev. B* 30, 122.
- Maki, K., 1964, *Physics* 1, 127.
- Maki, K., and H. W. On, 1996, *Czech. J. Phys.* 46, 1035.
- Manab, S., and U. Klein, 2000, *J. Phys. Condens. Matter* 28, L471.
- Manohar, A. V., and M. B. Wise, 2000, *Cambridge Monogr. Part. Phys. Nucl. Phys. Cosmol.* 10, 1.
- Martinez-Pinedo, G., K. Langanke, and P. Vogel, 1999, *Nucl. Phys. A* 651, 379.
- Matsuo, S., S. Higashitani, Y. Nagato, and K. Nagai, 1998, *J. Phys. Soc. Japan* 67, 280.
- Meissner, W., and R. Ochsensfeld, 1933, *Naturwissenschaften* 21, 787.
- Mewes, M. O., G. Ferrari, F. Schreck, A. Sinatra, and C. Salomon, 1999, *Phys. Rev. A* 61, 011403.
- Möller, R. et al., 1996, *Phys. Rev. Lett.* 76, 1292.
- Modugno, G., G. Roati, F. Riboli, F. Ferlaino, F. J. B. Rech, and M. Inguscio, 2002, *Science* 297, 2240.
- Murthy, G., and R. Shankar, 1995, *J. Phys. Condens. Matter* 7, 9155.
- Nam, M.-S., J. Symington, J. A. Singleton, S. J. Blundell, A. Ardaavan, M. Kumoo, and P. Day, 1999, *J. Phys. Condens. Matter*

- 11, L477.
- Nambu, Y., 1960, Phys. Rev. 117, 648.
- Nambu, Y., and G. Jona-Lasinio, 1961a, Phys. Rev. 122, 345.
- Nambu, Y., and G. Jona-Lasinio, 1961b, Phys. Rev. 124, 246.
- Nardulli, G., 2002a, Riv. Nuovo Cim. 25N 3, 1.
- Nardulli, G., 2002b, eConf C 010815, 104.
- Nardulli, G., 2002c, in Quark-gluon plasma and heavy ion collisions (World Scientific), eprint hep-ph/0206065.
- Neubert, M., 1994, Phys. Rept. 245, 259.
- Nomura, M., 1993, Phys. Rev. Lett. 71, 3391.
- O'Hara, K. M., et al., 2001, Phys. Rev. Lett. 85, 2092.
- Park, B.-Y., M. Rho, A. W. Iwazba, and I. Zahed, 2000, Phys. Rev. D 62, 034015.
- Pickett, W. E., R. Weht, and A. B. Shick, 1999, Phys. Rev. Lett. 83, 3713.
- Pines, D., and A. A. Ippar, 1985, Nature 316, 27.
- Pisarski, R. D., and D. H. Rischke, 1999a, Phys. Rev. Lett. 83, 37.
- Pisarski, R. D., and D. H. Rischke, 1999b, Phys. Rev. D 60, 094013.
- Pisarski, R. D., and D. H. Rischke, 2000a, Phys. Rev. D 61, 074017.
- Pisarski, R. D., and D. H. Rischke, 2000b, Phys. Rev. D 61, 051501.
- Polchinski, J., 1993, in Recent directions in particle theory: from superstrings and black holes to the standard model (TASI - 92) (World Scientific), eprint hep-th/9210046.
- Politzer, H. D., 1973, Phys. Rev. Lett. 30, 1346.
- Pringle, D. J. et al., 1999, Phys. Rev. B 59, R11679.
- Rajagopal, K., 1999, Nucl. Phys. A 661, 150.
- Rajagopal, K., 2001, AIP Conf. Proc. 602, 339.
- Rajagopal, K., and E. Shuster, 2000, Phys. Rev. D 62, 085007.
- Rajagopal, K., and F. W. Ilczek, 2001, in At the frontier of particle physics, vol. 3 (World Scientific), eprint hep-ph/0011333.
- Rapp, R., T. Schafer, E. V. Shuryak, and M. Velkovsky, 1998, Phys. Rev. Lett. 81, 53.
- Rapp, R., T. Schafer, E. V. Shuryak, and M. Velkovsky, 2000, Annals Phys. 280, 35.
- Rapp, R., E. V. Shuryak, and I. Zahed, 2001, Phys. Rev. D 63, 034008.
- Rauchschwalbe, U. et al., 1982, Phys. Rev. Lett. 49, 1448.
- Rischke, D. H., D. T. Son, and M. A. Stephanov, 2001, Phys. Rev. Lett. 87, 062001.
- Roati, G., F. Riboli, G. Modugno, and M. Inguscio, 2002, Phys. Rev. Lett. 89, 140403.
- Ruderman, M., 1991, Astrophys. J. 382, 587.
- Ruderman, M., T. Zhu, and K. Chen, 1998, Astrophys. J. 492, 267.
- Saint-James, D., G. Samma, and E. J. Thomas, 1969, Type II Superconductivity (Pergamon Press, Oxford).
- Samokhin, K. V., 1997, Physica C 274, 156.
- Samma, G., 1963, J. Phys. Chem. Solids 24, 1029.
- Schafer, T., 2000, Nucl. Phys. B 575, 269.
- Schafer, T., 2001, Int. J. Mod. Phys. B 15, 1474.
- Schafer, T., and F. W. Ilczek, 1999a, Phys. Rev. Lett. 82, 3956.
- Schafer, T., and F. W. Ilczek, 1999b, Phys. Lett. B 450, 325.
- Schafer, T., and F. W. Ilczek, 1999c, Phys. Rev. D 60, 074014.
- Schafer, T., and F. W. Ilczek, 1999d, Phys. Rev. D 60, 114033.
- Schmies, H. et al., 1994, Physica B 199, 125.
- Schreck, F., L. K. Haykovich, K. L. Corwin, G. Ferrari, T. Bourdel, and J. Cubizolles, 2001, Phys. Rev. Lett. 87, 080403.
- Sedrakian, A., 2001, Phys. Rev. C 63, 025801.
- Sedrakian, A., T. Alam, and U. Lombardo, 1997, Phys. Rev. C 55, R582.
- Sedrakian, A., and U. Lombardo, 2000, Phys. Rev. Lett. 84, 602.
- Shankar, R., 1994, Rev. Mod. Phys. 66, 129.
- Shimahara, H., 1994, Phys. Rev. B 50, 12760.
- Shimahara, H., 1997, J. Phys. Soc. Japan 66, 541.
- Shimahara, H., 1998a, J. Phys. Soc. Japan 67, 736.
- Shimahara, H., 1998b, J. Phys. Soc. Japan 67, 1872.
- Shimahara, H., 2002, J. Phys. Soc. Japan. 71, 1644.
- Shimahara, H., S. Matsuo, and K. Nagai, 1996, Phys. Rev. B 53, 12284.
- Shimahara, H., and D. Rainer, 1997, J. Phys. Soc. Japan 66, 3591.
- Shovkovy, I. A., and L. C. R. Wijewardhana, 1999, Phys. Lett. B 470, 189.
- Shuster, E., and D. T. Son, 2000, Nucl. Phys. B 573, 434.
- Singleton, J., N. Harrison, C. H. Mielke, J. Schlueter, and A. M. Kiani, 2001, J. Phys-condensm at 13, L899.
- Singleton, J., J. A. Symington, M.-S. Nam, A. Ardavan, M. Kumoo, and P. Day, 2000, J. Phys. Condens. Matter 12, L641.
- Son, D. T., 1999, Phys. Rev. D 59, 094019.
- Son, D. T., and M. A. Stephanov, 2001, Phys. Rev. Lett. 86, 592.
- Splitter, K., D. T. Son, and M. A. Stephanov, 2001, Phys. Rev. D 64, 016003.
- Symington, J. A., J. Singleton, M.-S. Nam, A. Ardavan, M. Kumoo, and P. Day, 2001, Physica B 294-295, 418.
- Symington, J. A. et al., 1999, Phys. Rev. Lett. 83, 3713.

- Takada, S., 1970, *Prog. Theor. Phys.* 43, 27.
- Takada, S., and T. Izuyama, 1969, *Prog. Theor. Phys.* 41, 635.
- Tallon, J. et al., 1999, *IEEE Trans. Appl. Supercond.* 9, 1696.
- Tanatar, M. A., T. Ishiguro, H. Tanaka, and H. Kobayashi, 2002, *Phys. Rev. B* 66, 134503.
- Tenya, K. et al., 1999, *Physica B* 259-261, 692.
- Thomas, F. et al., 1996, *J. Low Temp. Phys.* 102, 117.
- Uji, S. et al., 2001, *Nature* 410, 908.
- Vonderfecht, B. E., C. G. Gearhart, W. H. Dickho, A. Polls, and A. Ramos, 1991, *Phys. Lett. B* 253, 1.
- Werthamer, N. R., H. Helfand, and P. C. Hohenberg, 1966, *Phys. Rev.* 147, 295.
- Wilczek, F., 2000, *Nucl. Phys. A* 663, 257.
- Won, H., and K. Maki, 2002, *Physica B* 322, 315.
- Yang, K., 2001, *Phys. Rev. B* 63, 140511.
- Yang, K., and D. F. Agterberg, 2000, *Phys. Rev. Lett.* 84, 4970.
- Yin, G., and K. Maki, 1993, *Phys. Rev. B* 48, 650.